A MODIFIED SEQUENTIAL GRID LAYOUT TO INCREASE PRODUCTION RATES IN DEEP LEVEL HARD ROCK MINES

YOLANDE JOOSTE

Presented as fulfilment for the degree

MSc (Applied Science)

IN THE FACULTY OF ENGINEERING, BUILT ENVIRONMENT AND INFORMATION TECHNOLOGY

DEPARTMENT OF MINING ENGINEERING

UNIVERSITY OF PRETORIA

ABSTRACT

A MODIFIED SEQUENTIAL GRID LAYOUT TO INCREASE PRODUCTION RATES IN DEEP HARD ROCK MINES

Supervisor: Prof. D.F. Malan

Department: Mining Engineering

University: University of Pretoria

Degree: MSc (Applied Science)

Scattered mining was practised on Kusasalethu Mine (previously Elandsrand Gold Mine) prior to 1998, but as mining proceeded deeper, it was no longer a feasible option. The scattered mining method would have resulted in unacceptably high stress levels and energy release rates on the active mining faces. Longwall mining was considered as it was practiced on neighbouring mines. This would have ensured that energy and stress levels remained within acceptable limits and avoided the formation of remnants at depth. Kusasalethu Mine required a more flexible mining method owing to the highly variable grade, the presence of multiple faults and dykes and the high production rate required. A mining method was therefore developed that consisted of dip stabilizing pillars for regional support as well as bracket pillars to support geological structures. This was called the Sequential Grid mining method. Sequential Grid mining addressed two main problems, namely, negotiating the adverse geology and the erratic grade of the VCR orebody. However, a recent drop in production resulted in the need for alternatives and improvements to the original mining layout. This involved modifications to the design in order to increase production rates without any compromise to safety.

An investigation to modify for the Sequential Grid mining method was therefore conducted by the author in order to determine the consequences for layout stability. A few alternatives were investigated to determine the best possible solution for the Sequential Grid design. As a result, the modified Multi-raise mining method was introduced to address the problems that were experienced with the original design.

This study compared the original mining method and the Multi-raise mining with regards to layout stability.

Investigation of the seismic data showed no significant differences between the original Sequential Grid mining and the proposed Multi-raise mining. The numerical modelling of the mining layouts showed slightly higher interim Energy Release Rates (ERR) and Average Pillar Stress (APS) levels during the extraction process. The final values for these parameters are nevertheless similar to the original Sequential Grid mining method. It is therefore concluded that the Multi-raise mining method will not have adverse effects on the mine stability.

It is concluded that changes to the original Sequential Grid mine design are possible without influencing the seismic hazard. In addition the anticipated interim increases in ERR and APS levels could be kept within acceptable levels through slight decreases to the extraction ratio.

The concept of an average value for the stress distribution in a remaining portion of solid rock (pillars) surrounded by underground mining excavations is used as the rock engineering design parameter called average pillar stress (APS). Although averages are generally simple to calculate given the availability of appropriate data, average values for the stress distributed with pillars is somewhat more complex especially when working in the realm of numerical methods. The calculation of APS by MINSIM 2000 has been investigated and compared with work done by Napier and Malan in 2011 which illustrated the difficulties that arise in the determination of this parameter. A step by step method in MINSIM 2000 is proposed to ensure that the calculation of APS is done appropriately.

The study also investigated the use of the Modelled magnitude method to analyse future seismic trends. The study illustrated that the expected seismic trends will be very similar for the Multi-raise method compared to the original Sequential Grid mining method.

ACKNOWLEDGEMENTS

I wish to express my appreciation to the following organisations and persons who made this study possible:

a. Harmony Gold

b. Professor Francois Malan, my supervisor, for his guidance and support.

c. Kevin Riemer

d. Kevin Brentley

TABLE OF CONTENT

LIST OF TABLES

LIST OF FIGURES

Chapter 1

HISTORY OF DEEP LEVEL GOLD MINING IN SOUTH AFRICA

1.1. INTRODUCTION

The increase in mining depth in the South Africa mining industry during the last few decades, especially in the gold mining industry, resulted in a severe rockburst problem (Klokow, Riemer and Ferreira, 2003). One of the main strategies employed by the gold mining industry to address the seismic problem was to incorporate stability pillars into the mine design.

Strike stabilizing pillars was introduced in the 1960's (Ortlepp and Spottiswoode, 1982) after theoretical studies indicated that the energy release rates can be reduced by decreasing volumetric closure in stopes (Salamon and Cook, 1966). They stated that: "*As mining extends to greater depth, the frequency and severity of rockbursts is likely to increase. It appears that a substantial reduction in the rockburst hazard can be achieved only by radical changes in the present stoping method"*. They illustrated the value of leaving reef stability pillars as a means to minimise rockbursts by controlling the volumetric closure and the resulting energy released rates.

The introduction of stability pillars proved to be successful in reducing volumetric closure as shown by Hagan (1987), Diering (1987) as well as Lenhardt and Hagan (1990). This nevertheless resulted in other problems, mostly associated with the pillars. Research was therefore required to obtain an optimal design layout which will eliminate these problems, as well as reduce the rockburst hazard.

1.2. HISTORY OF GOLD MINING IN SOUTH AFRICA

South Africa has the largest known gold reserves in the world with an estimated 40 000 tons, which is approximately 40-50 % of the global gold reserves (Wogan, 2009). The Witwatersrand basin extend for 280 kilometres from Klerksdorp in the west to Bethal in the east and the gold bearing reefs is found up to 4 kilometres deep in places. The reef was discovered by an Australian prospector, George Harrison in 1886 on the farm, "Langlaagte". This later became the western outskirts of Johannesburg. The immediate area was proclaimed a public digging area by President Kruger later that year, sparking South Africa's most important gold rush.

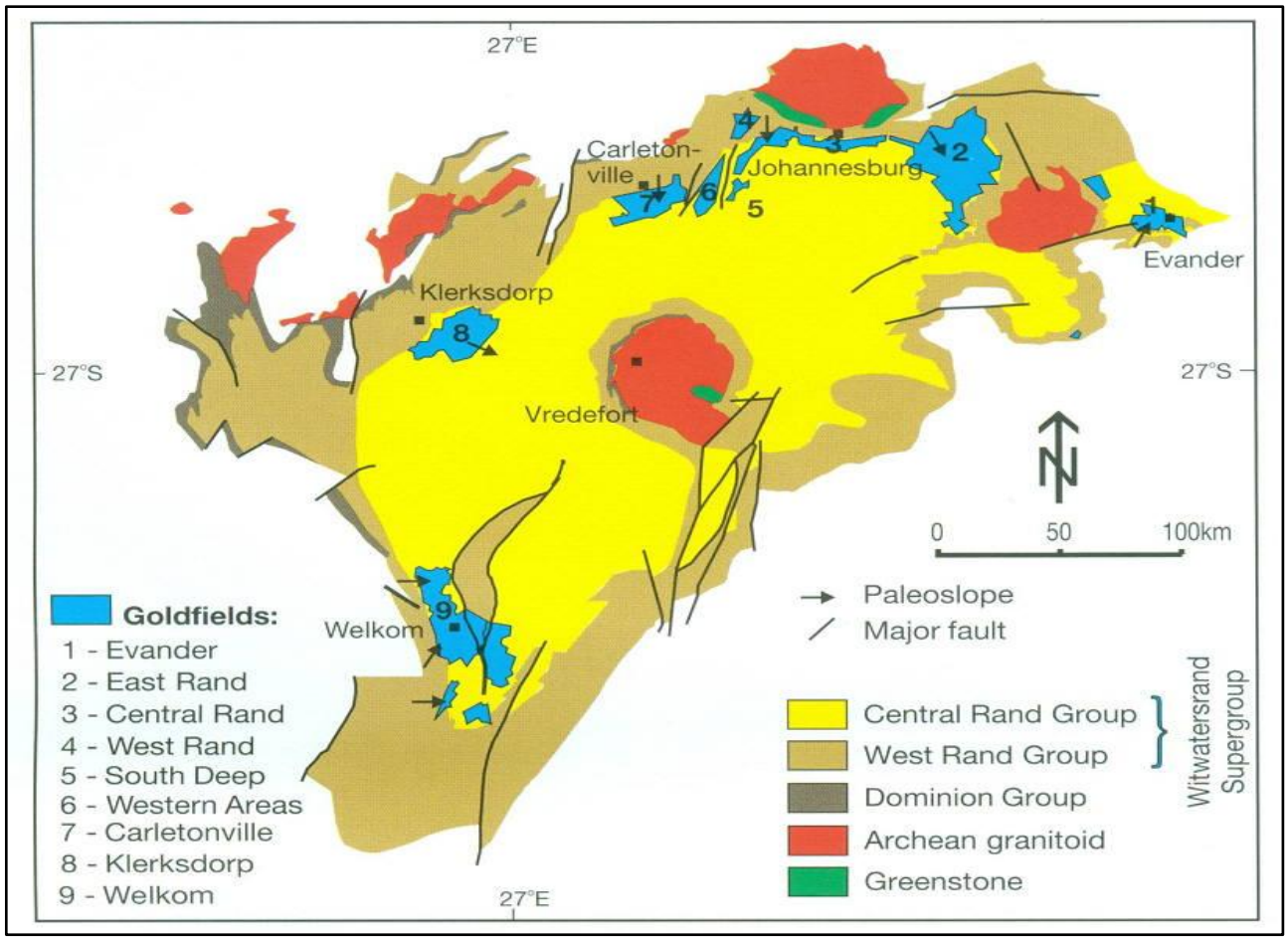

Figure 1: Surface and subsurface distribution of the Witwatersrand Super Group, Dominion Group and Mesoarchaean granite–greenstone basement domes (after Frimmel, 2005)

The earliest mining occurred along and adjacent to the outcrop. An early death of the fledging goldfields loomed in the late 1880's when it became evident that the gold reef was not oxidised below 35 m and chemical methods were required to extract the gold from the crushed reef. Luckily the problem was solved and this started the long and fascinating history of deep level gold mining in the Witwatersrand goldfields.

Today, many of the older mines have little reef left or are already closed, but the area still produces a significant amount of the total world supply of gold and remains an important part of the South African economy.

1.3. EVOLUTION OF THE DEEP MINING LAYOUTS

In the early decades of the 20th century, decline shafts were used to gain access to the gold bearing reef. Scattered mining with mine pole or mat pack supports, often supplemented with pillars and sand fill, was used with considerable success for shallow mining areas. Rockbursting, caused by remnants at deeper level, became a serious problem during the 1940's.

Longwall stoping was started at ERPM Mine with the main objective being to reduce the incidence related to mining induced seismicity. Hill (1942) illustrated that more than 90% of the seismicity that occurred on ERPM could be linked to the "isolated pillars" left behind by the scattered mine design. He illustrated that these pillars could be largely avoided by implementing the "longwall" mining method. This was implemented at Crown Mines and ERPM in 1940.

The longwall layouts seemed to be largely successful, except for large damaging seismic events that still occurred on geological structures. This became worse as the mining depths increased.

A few years later, additional stability pillars where left as the advantages of these pillars were highlighted by Cook et al (1966). Studies conducted by Deliac and Gay (1984) and MacGarr and Wiebols (1977) illustrated that the occurrence of rockbursts were minimal in

the mining areas protected by the stability pillars compared to areas where no pillars were used. Salamon and Wagner (1979) argued that large seismic events are likely to occur very infrequently and that the level of seismicity in areas protected by stability pillars will be much lower than normal longwall faces without pillar protection.

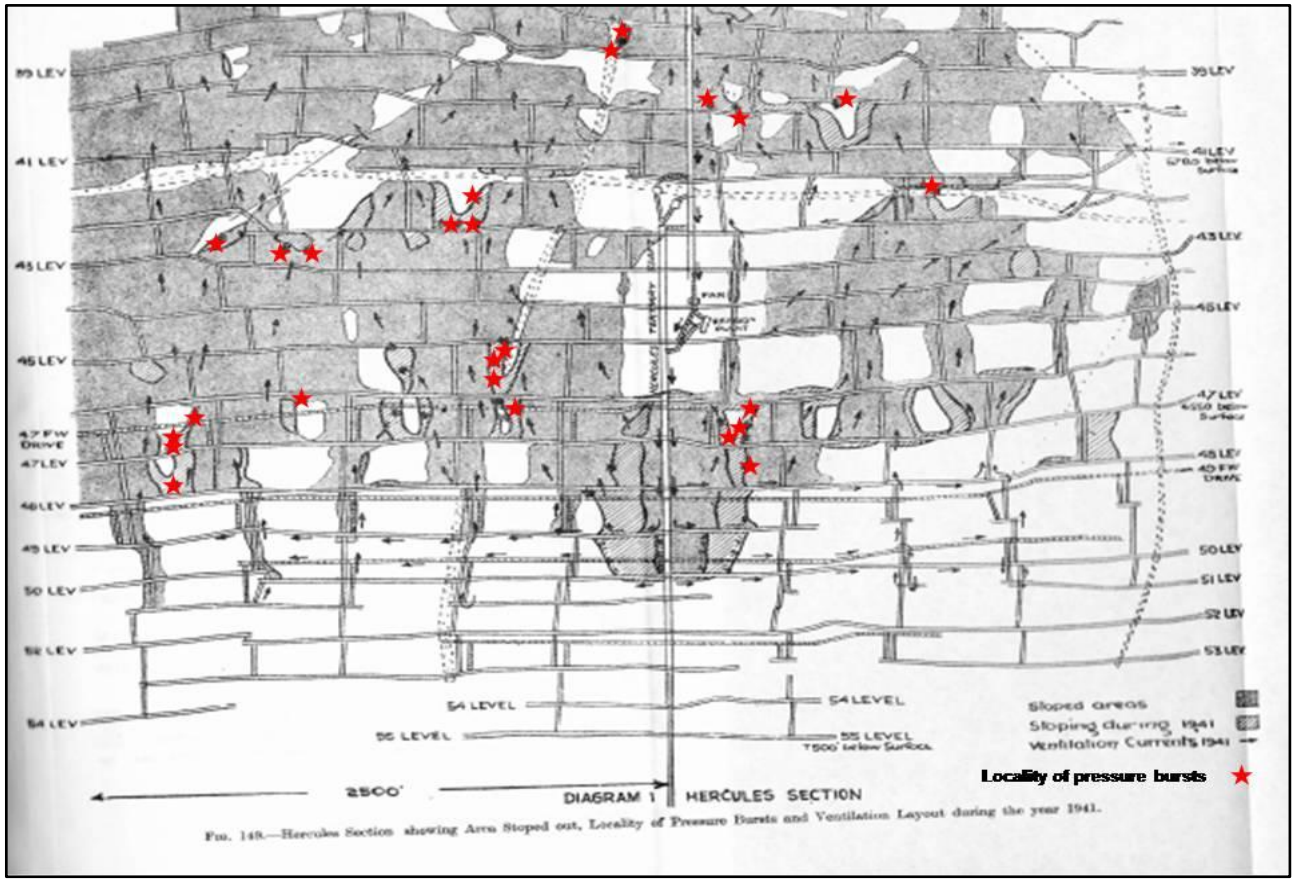

Figure 2: ERPM mine, Hercules section showing area stoped out and the locality of pressure bursts. This was prior to the adoption of the longwall layouts at the mine (after Spottiswoode, 1983)

The success of the stability pillars at ERPM Mine's Hercules section lead to the adoption of stabilizing pillars at the Blyvooruitzicht Mine during the late 1970's below 16 level (Spottiswoode and Ortlepp, 1983). Above 16 level, the mine utilized scattered mining methods with raises at 200 m intervals. The many remnants, which resulted from this layout, were generally extracted with little trouble, except where geological structures were present. For the deeper parts of the mine, the longwall layout as shown in Figure 3 was the main strategy to minimize the rockburst problem. This was used fairly successful except for a few rare occasions when large rockbursts resulted in extensive damage.

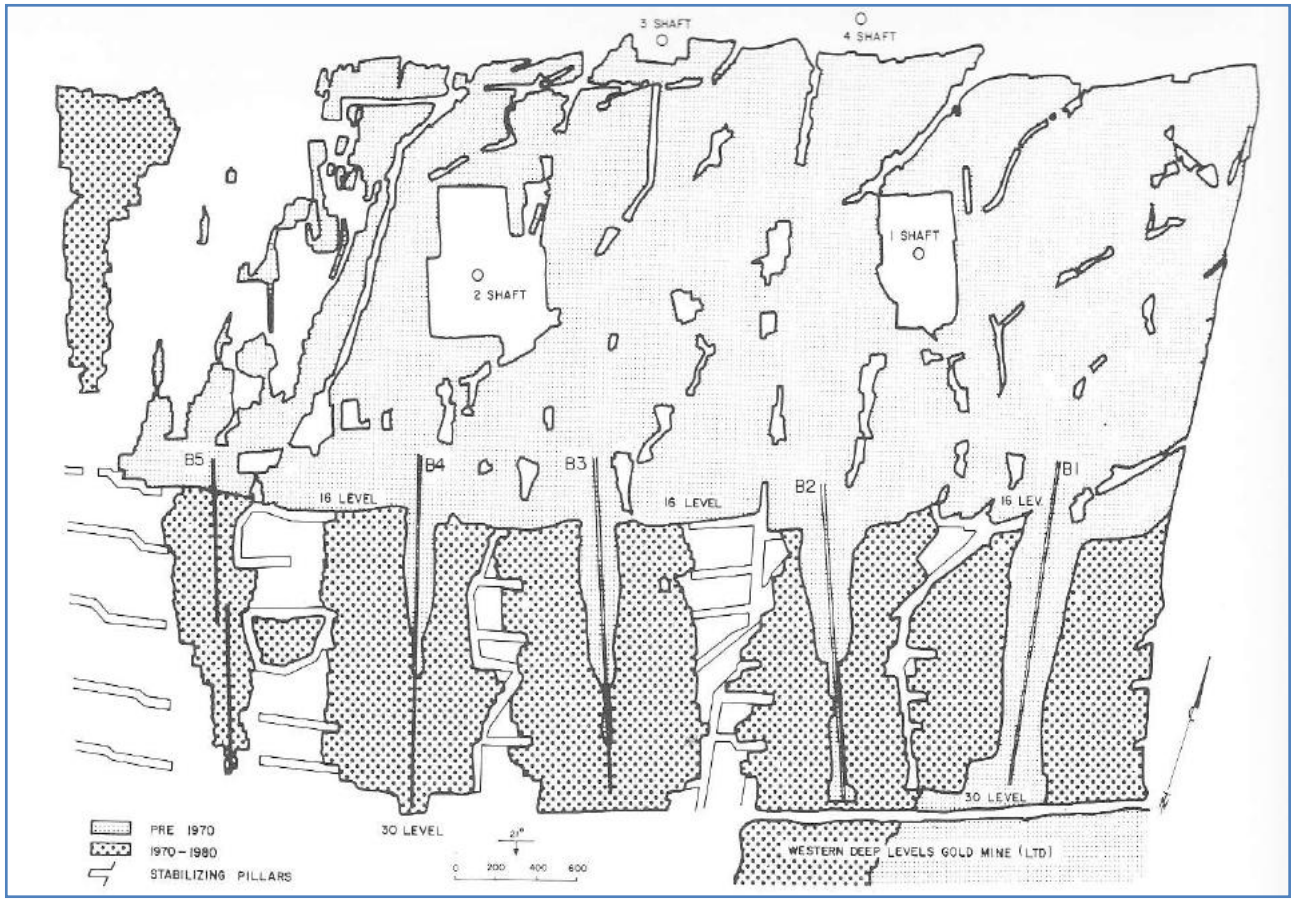

Figure 3: Plan of Blyvooruitzicht Mine, showing remnants above 16 level and the longwalls and stabilizing pillars below 16 level (after Spottiswoode, 1982)

The accident statistics shown in Figure 4 indicates the probable effect of the stability pillars on the fatality rate. It shows the rockburst fatality rate per 10 000 m^2 stoped since 1971 and the average monthly face advance per quarter for the same period. The decline in the face advance and increase in the casualty rate from 1974 to 1977 are largely due to the longwalls encountering more geology while approaching the final remnant stages. An increase in the face advance is evident again for the late 1970's while the fatality rate decreased again. This initially created the expectation that longwalls and the stability pillars will control the rockburst problem to a large extent.

Unfortunately the rockburst problem in the mining industry did not disappear with the introduction of the modified layouts and the fatality rates owing to rockbursting escalated to unacceptable high levels in the late 70's at Western Deep Levels Mine (Hagan, 1987).

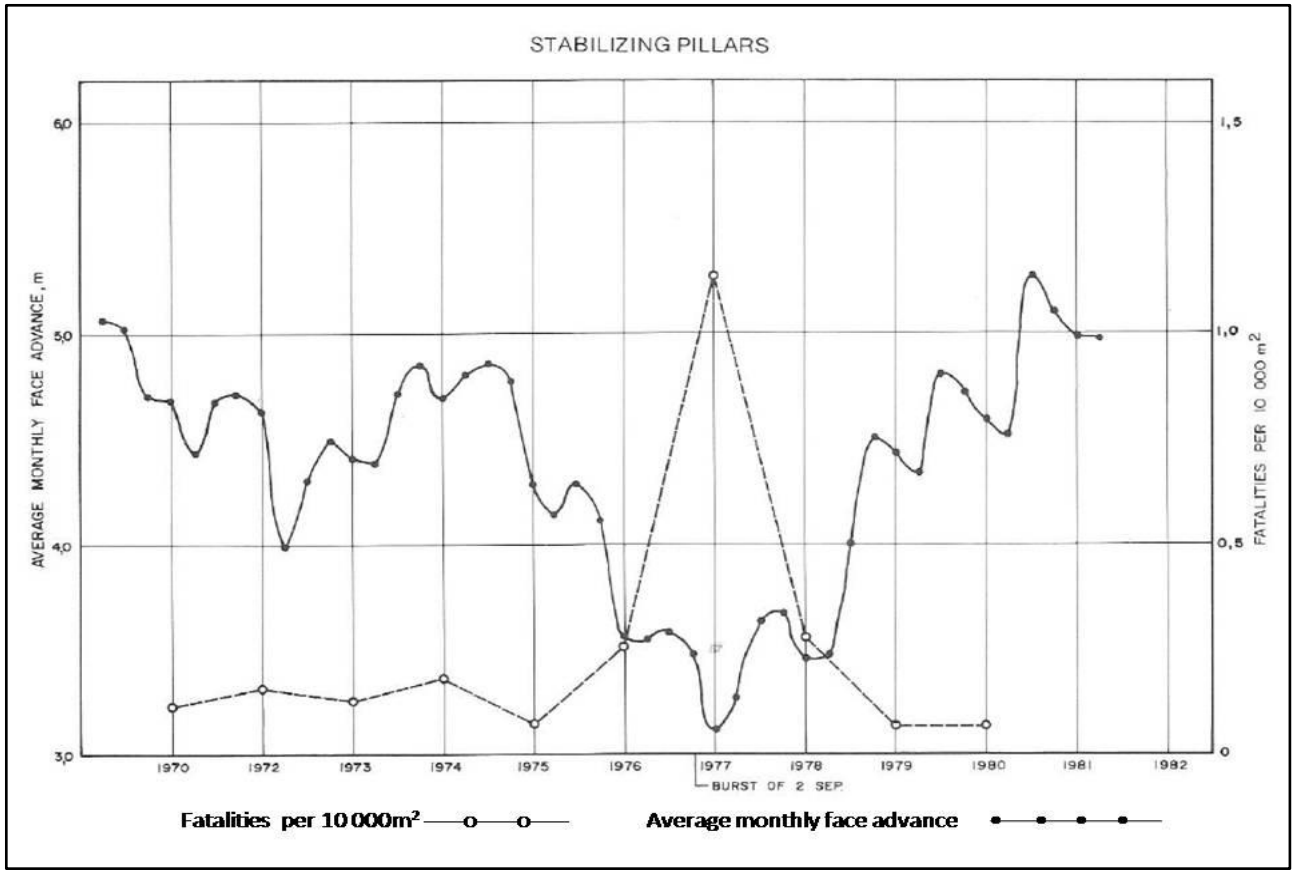

Figure 4: Quarterly average of monthly face advance and annual casualty rate for Blyvooruitzicht Mine from 1970 to 1980 (after Spottiswoode, 1982)

The energy release rate (ERR) concept was introduced in the 1960's and is a measure of energy changes and stress concentrations. The expected correlation with seismicity and mining conditions was illustrated by a number of workers (e.g. see Jager and Ryder, 1999). ERR is not a direct expression of seismic energy release due to mining as most of the energy, more that 97%, is release aseismically in the form of fracturing, crushing and sliding of blocks in the fractured rock mass. ERR takes into account the effects of depth and geometry of adjacent mining and is related to the amount of volumetric closure occurring.

Energy release rates are calculated as follows according to Jager and Ryder (1999):

$$ERR = \frac{1}{2} q_v \left(\frac{\Delta V}{\Delta A}\right) \qquad (1)$$

Where,

ΔA is the incremental area mined;

ΔV is the resulting change in the volumetric convergence in the stope;

q_v is virgin vertical stress;

$q_v \Delta V$ is then the incremental change in the potential energy of the overlying strata.

According to Ryder and Jager (2002), to determine ERR using numerical modelling, it is recommended that the following equation be used:

$$ERR = \frac{1}{2}\sigma^p s^p \qquad (2)$$

where,

s^p is the convergence at the face L prior to any additional mining;

σ^p is the absolute normal stress acting over a small advance prior to mining.

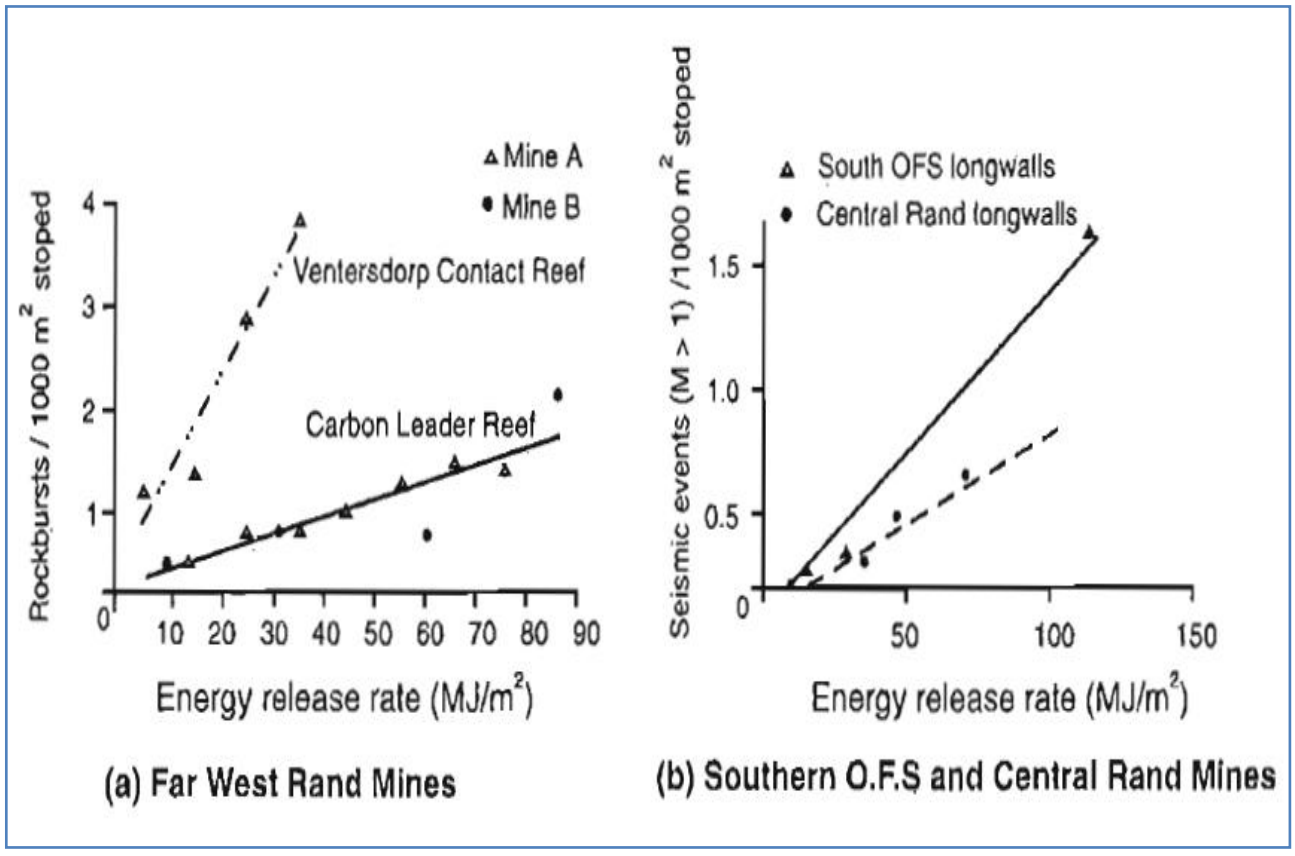

Figure 5: Results of studies in deep longwall mines shows a correlation between ERR and seismicity or incidence of damaging rockburst accidents (after Jager and Ryder, 1999)

ERR may be equivocal in predicting rock fall hazards (see Figure 6 for the typical causes of fatals), but it is quite different when considering the situation with rockbursts.

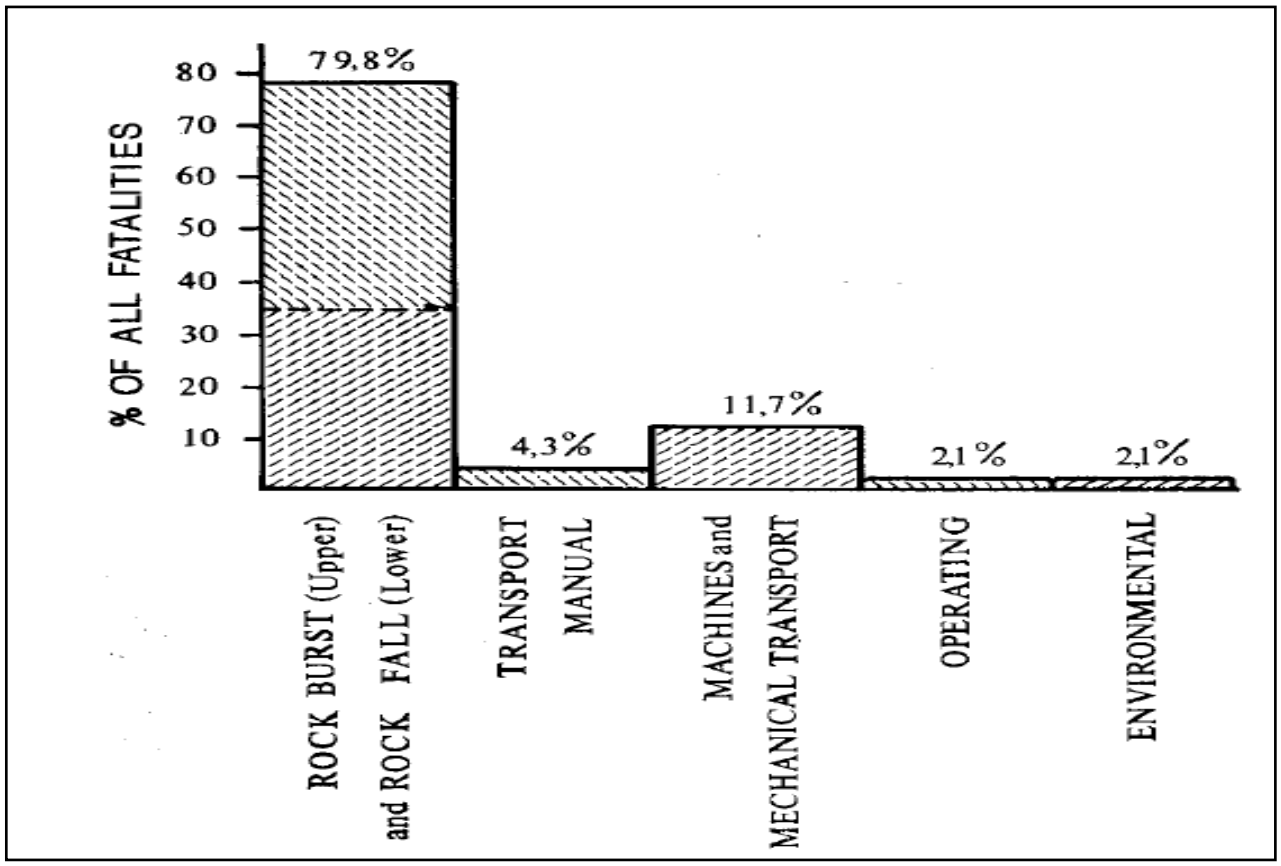

Figure 6: Typical causes of mining related fatalities (after Heunis, 1980)

Various studies conducted in deep longwall mines indicated that the seismic problem experienced on these mines are strongly related to the average energy release rates in the stopes (see Figure 5). Analyses of rockbursts occurrences in the CSIR-Miningtek/SIMRAC database suggested that the risk of rockbursting increases as the level of ERR increases (see Figure 7):

- Joughin (1966) reported the first results relating the rockburst problem experienced at Harmony Gold Mine to energy release rates.
- In 1976, Salamon and Wagner reported similar results as those obtained by Joughin, for the East Rand Proprietary Mines (ERPM).

- At Western Deep Levels, Heunis (1980) conducted a detailed investigation over a period of 4 years, also investigating the effect of different reef types as shown above in Figure 5. His study also showed a strong relationship between energy release rates and rockburst incidences similar to what is seen in Figure 5a according to Jager and Ryder, 1999 (see Figure 7).

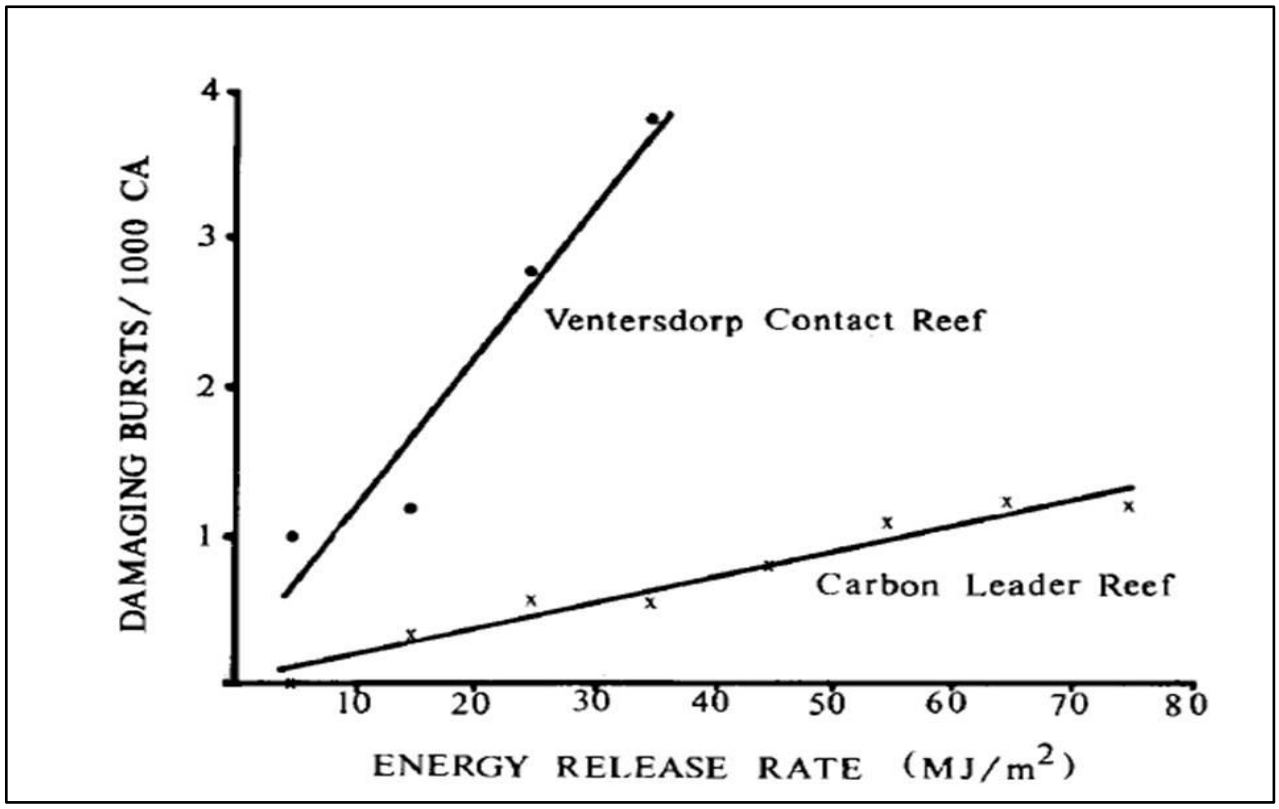

Figure 7: The relationship between damaging rockbursts and energy release rates for two different reef types (after Heunis, 1980)

These studies indicated that to minimize the rockburst hazard, the energy release rates (ERR) needs to be controlled. Energy release rates are proportional to the product of the stress acting on the area of rock prior to extraction and its displacement after extraction. To reduce the ERR, the elastic convergence therefore needs to be minimised and one effective way to do this is by reducing the amount of mining (Tanton, McCarthy and Hagan, 1984).

The positive results obtained at ERPM and Blyvooruitzicht Mines resulted in a systematic pillar design being implemented at Western Deep Levels in 1979 to assist with the

reduction in seismic related accidents (Tanton, McCarthy and Hagan, 1984). At this mine, a series of breast-mining panels made up a so-called “Christmas tree” shape longwall with the total dip length varying between 500 m and 1800 m. The longwalls were mined both east- and westwards. Strike orientated barrier pillars of approximately 35 m in width were left between the major longwalls (spaced 113 m apart) for ventilation and fire control purposes.

The layout attempted to maintain the face stresses as low and as uniform as possible during the extraction of the entire working area. The energy release rate (ERR) criterion was used as an aid in the assessment of average stress levels at the working faces, as well as an indicator of possible seismic incidence in geologically–undisturbed mining situations (Hagan, 1987). Similarly, the excess shear stress (ESS) criterion (Jager and Ryder, 1999) was used to give a semi-quantitative assessment of the effect of stope layouts on the seismic potential and stability of geological structures that trend through the mine.

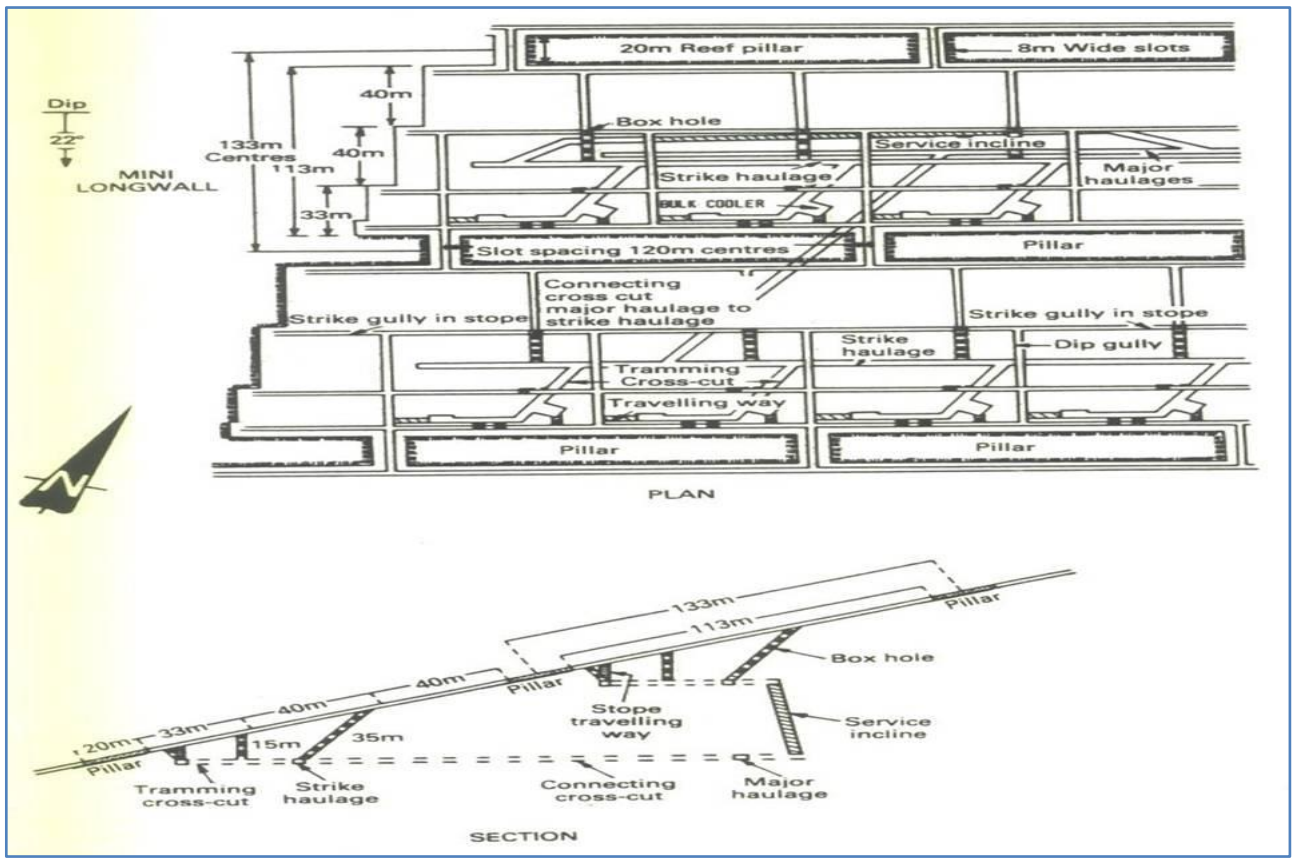

Figure 8: Pillar layout at Western Deep Levels Mine (after Tanton, 1984)

The strike stability pillar concept has various advantages and disadvantages when compared to the scattered mine layout, which was used with great success in the medium depth mines. The disadvantages of the longwalls with strike stability pillars are the following (Russo-Bello and Murphy, 2000):

- Minimal advanced off reef development results in inadequate information regarding geological structures. Planning of the mine is therefore problematic.
- The majority of geological structures are being mined through, which creates a large amount of off-reef mining operations.
- Geological structures with large throws cannot be negotiated and new development is required to access the reef. This increase costs significantly.
- It is development intensive.

The advantages of the longwalls with the strike stability pillars are as follows:

- No remnants or additional pillars will be formed that needs to be mined in the future again.
- The development is protected against high stresses as it is positioned in overstoped ground.
- Faster access to reef is possible and revenue can therefore be generated quicker.
- Mining operations can be concentrated and this makes management and logistics of the mining activities easier.
- Better ventilation control can be achieved. This is always a problem in the scattered mining environment.

In general, the spacing between strike stability pillars is relatively large, since it is determined by the level spacings. It is therefore restricted in terms of controlling the ERR levels. This is not a problem with the dip stabilizing pillar concept as found in the Sequential Grid mine design.

1.4. SEQUENTIAL GRID LAYOUT (KUSASALETHU MINE)

In recent years, deep level mines situated in the West Rand region of the Witwatersrand goldfields adopted layouts that incorporate a systematic system of dip stabilizing pillars. This layout is largely motivated by its flexibility to mine an orebody that is disrupted by the presence of geological structures, situations where the reef grade is erratic and the occurrence of damaging seismic events associated with the geological structures (Klokow, 2003).

The other major contributor to the selection of the Sequential Grid method above the mini-longwall method is the stability of the pillars (dip versus strike pillars). Hagan (1990) showed that strike stability pillars on the Carbon Leader Reef (CLR) were prone to failure.

The dip pillar stability concept was applied by Murie (1980) to a section of Kusasalethu Mine (70 to 73 level) and he found that the energy release rates was reduced by 50% when compared to the scenario where only bracket pillars were used to clamp geological structures.

Applegate (1986) was the first to propose the 30 m wide dip stability pillars spaced 200 m (170 m skin to skin spacings) apart that would result in approximately 85 % extraction. By early 1990, the design was implemented from 76 to 85 level (Applegate and Arnold, 1990). Part of the initial mine design was the incorporation of bracketing geological structures to address the seismic hazard associated with these geological structures.

The main principles of the Applegate proposal were:

- All significant geological structures must be bracketed.
- Dip stabilising pillars should be located in low-grade areas where possible.

Applegate also showed that the ERR levels can be controlled when following a specific sequence of mining. This is achieved by keeping leads and lags to 10 m or less as far as is practically possible. As the overall face configuration is bottom panel leading, the 10 m

lead / lag rule will assist in maintaining the overall face shape required to limit the ERR's associated with the top panels.

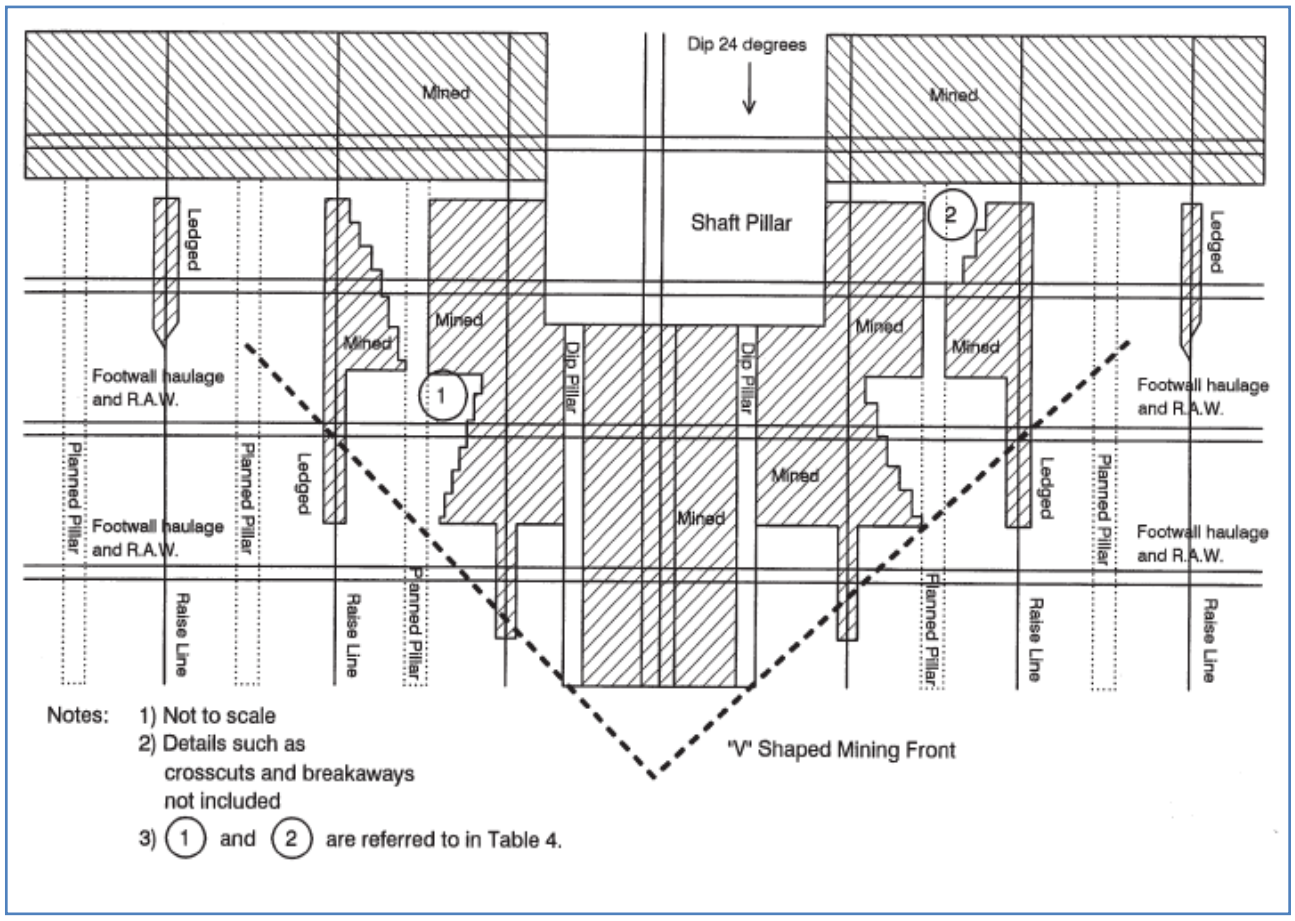

Figure 9: Typical Sequential Grid layout (after Handley, 2000)

The sequence of the Sequential Grid method is described as follows:

- Overall sequence is mining outwards from the shaft on strike, moving from raise line to raise line to the eastern and western boundaries of the mine.
- Deeper levels will be started up later than the shallower sections resulting in a "V" shaped down-dip mining configuration.
- Mining at each raise line proceed first towards the shaft to form the next pillar.
- If the pillar formation is completed, mining commences on the opposite side of the raise line mining away from the shaft towards the next pillar position.

The sequence of the Sequential Grid mining method is shown in Figure 10. It is during the second mining stage that stope spans reach their maximum size, but because the mining proceeds in the direction of the solid, the effect of the large span is minimized. This, together with the use of backfill, will assist with a decrease in closure rates as well as better control of local ground conditions in the working areas.

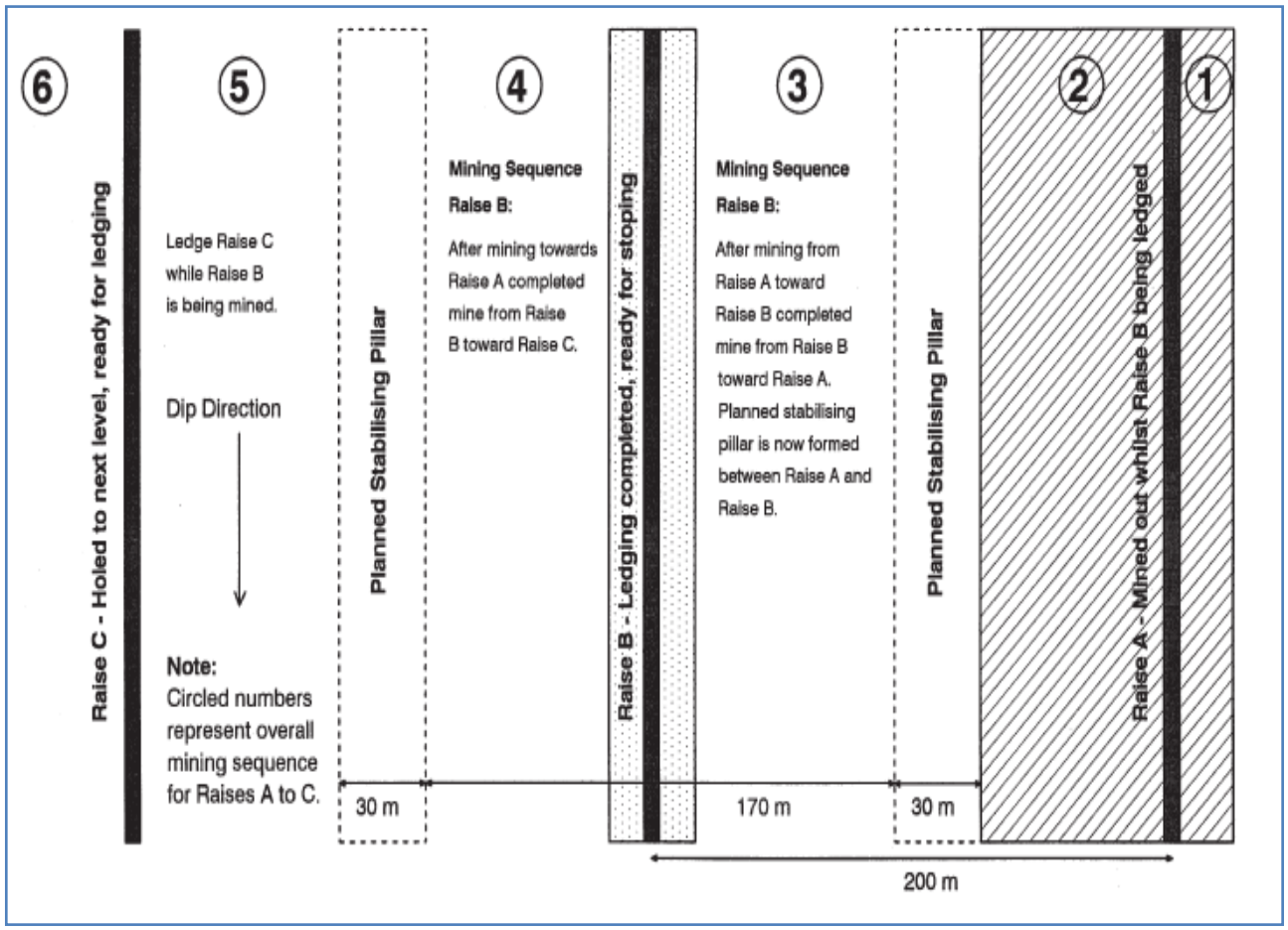

Figure 10: Sequence of Sequential Grid mining method (after Applegate, 1990)

The decision to implement the Sequential Grid mining method for Kusasalethu Mine was based on the following factors (Handley, 2000):

- Less off reef development, thus less capital required for each centare being mined;
- Improved flexibility with respect to mining and planning. This is important for a variable grade ore body;
- Grade recovered is better due to improved selection of mining locations;

- An improvement in the reduction of seismicity due to geological structures that are bracketed;
- Strike stabilizing pillars require ventilation slots which require dangerous mining. This will not be necessary for the Sequential Grid mining as the dip pillars forms natural ventilation areas;
- Strike gullies are more stable as the gullies are not developed parallel to the stabilizing pillars;
- Sequential Grid mining requires that the development remains ahead of the mining. This will ensure that improved geological information is available.

The effectiveness of the Sequential Grid mine layout to combat seismicity was investigated by SIMRAC (1997). The seismic response of the Sequential Grid layout of Kusasalethu Mine was compared with a similar geotechnical environment where traditional longwall mining was practiced (Deelkraal Mine).

The results in Table 1, obtained from the SIMRAC GAP303 report, were reworked by Handley (2000). The table indicates the number of seismic events normalized to the total area mined on the two mines to illustrate the frequency of occurrence of specific magnitude size events. From Table 1 the following can be noted:

- 45 % more mining (in terms of centares) can be done within the Sequential Grid layout compared to the longwall mining before a seismic event with $M_L \geq 0.8$ would occur;
- the difference is quite substantial for seismic events with $M_L \geq 2.0$ as 153 % more mining can be done in the Sequential Grid layout when compared to longwall mining.

This indicates that the potential for a damaging seismic event to occur with the Sequential Grid mining appears to be far lower when compared to longwall mining.

Similar studies were conducted by Essrich (1996) when he compared an area at Kusasalethu Mine with an area at Western Deep Levels Mine. His study showed that the

integration of major geological structures into bracket pillars in the Sequential Grid layout plays an important role in reducing the seismic hazard as mining is not required to intersect the structures. Although the production rates differ significantly for the Essrich study when Tables 1 and 2 are compared, similar trends were obtained.

Table 1: Comparison of seismicity generated by a longwall layout and Sequential Grid mining at Kusasalethu (after SIMRAC GAP 303, 1997)

Parameter	Sequential Grid (SG)	Longwall (LW)	Ratio (SG/LW)
Average mined (centares)	318357	197402	1.61
Average m^2/event with $M_L \geq 0.8$ (total number of events)	428 (783)	296 (667)	1.45
Average m^2/event with $M_L \geq 2.0$ (total number of events)	22740 (14)	8973 (22)	2.53
Magnitude of largest event	3.0	2.9	1.03
Magnitude of second largest event	2.6	2.8	0.93
Effective volume covered by seismic activity (km^3)	1.8	0.5	3.60

Table 2: Comparison of seismicity generated by a longwall and a Sequential Grid stope (after Essrich, 1998)

Parameter	Sequential Grid (SG)	Longwall (LW)	Ratio (SG/LW)
Average mined (centares)	12500	11800	1.06
Average area mined per month(centares)	700	2360	3.37
Average m^2/event with $M_L \geq 1.0$ (total number of events)	431 (29)	223 (53)	1.93
Average m^2/event with $M_L \geq 2.0$ (total number of events)	12500 (1)	2360 (5)	5.30
Magnitude of largest event	3.0	2.9	1.03
Cumulative seismic energy released (MJ)	304	473	0.93

It was concluded from these studies that Sequential Grid mining in the VCR environment is safer than longwall mining with strike stabilising pillars.

Unfortunately a few negative aspects are associated with the Sequential Grid layouts (Handley, 2000):

- The regular mining layout that is required to obtain the grid format can result in the lack of flexibility in mining and planning.
- The sequencing of the panels can result in lower production rates.
- Sequential Grid mining requires a higher up front capital input to establish more mining faces compared to longwall mining. This can result in a negative impact on the rate of return of the mining project.
- Long term potential stability of the dip stability pillars are still unknown, although no known disruptive pillar failure had occurred up to the time the work was published.

These problems need to be resolved before the Sequential Grid layout can be claimed to be the preferred mining method in the deep mining environment.

1.5. MPONENG DIP PILLAR LAYOUT

At Mponeng Mine in the Carletonville area, a different approach to that of longwall mining was also required to reduce the number of rockburst fatalities. A dip pillar concept similar to the Sequential Grid layout, employed at Kusasalethu Mine, was introduced and can be described as scattered mining with controlled mining spans via dip stability pillars (McGill, 2007). The spans were limited to a distance of 180 m and pillar widths of 30 m were used. The method is relatively flexible as the pillars can incorporate geological structures. The general sequencing rules to manage face stresses and mining concentration that resulted in the success of the Sequential Grid layout forms part of this design layout:

- Only single sided mining is allowed.
- The 70 m rule applies where panels are not allowed to mine towards each other within this distance.
- Lead/lags to be kept within 10 m.
- Grid mining is performed so as to mine towards the shaft first and then away from the shaft
- Controlled mining volumes where six crews are the limit per raise line.

Figures 11 and 12 below show the layout as employed by Mponeng Mine. The basic layout of Sequential Grid mining has been applied but too few current/active levels of mining existed to achieve the desired V-shape for the Sequential Grid sequence.

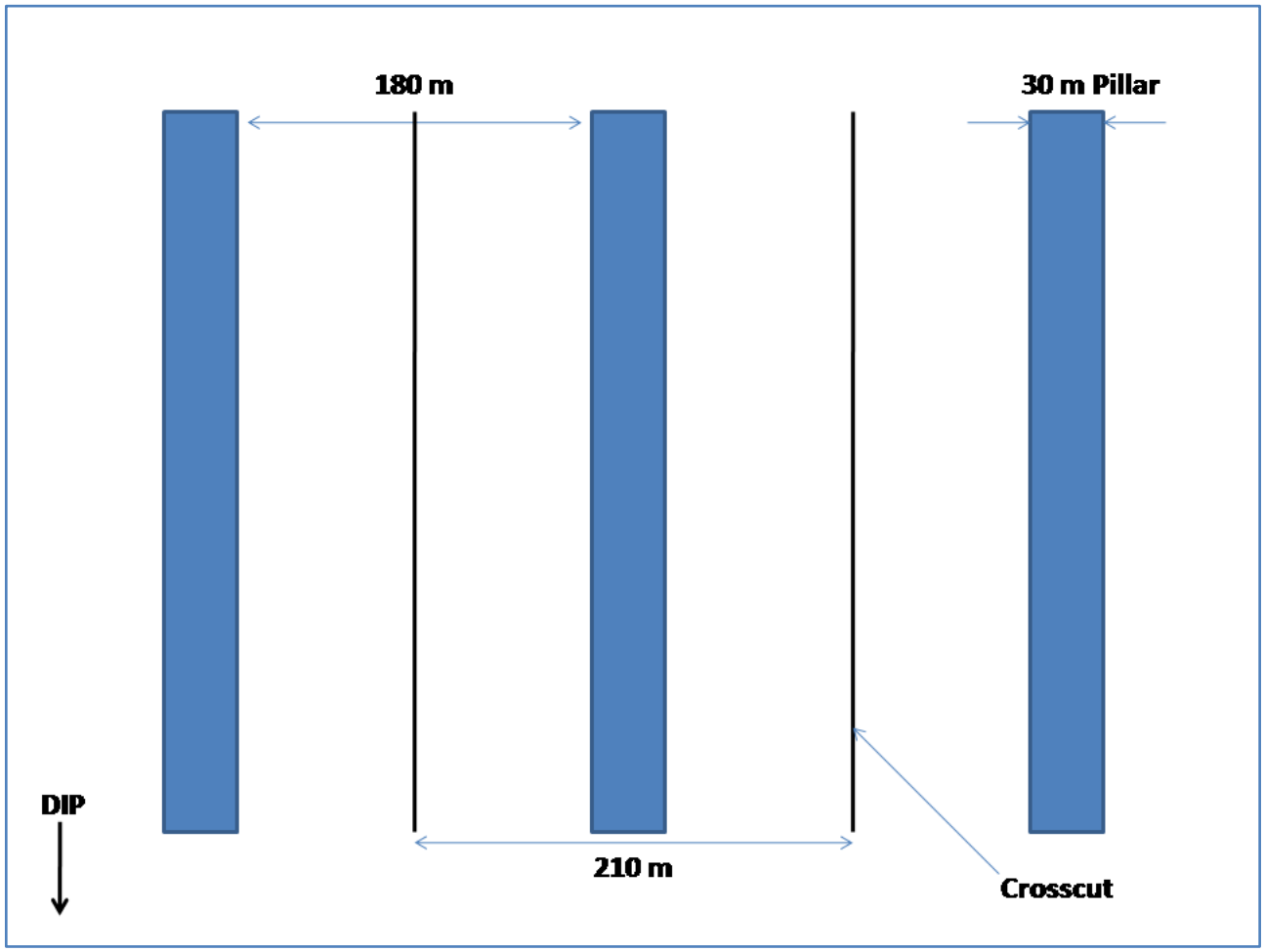

Figure 11: Schematic layout of Mponeng Mine

The success of the layout used at Mponeng Mine was assessed by analysing the seismic data. The assessment was done by comparing seismic events with M_L>0.5 (as it represents the potentially damaging range of events) and it indicated that normalized seismicity levels per 1000 m^2 had decreased 70 % - 75 % (McGill, 2007) for all magnitude ranges, except M_L>3.0 (see Figures 13, 14 and 15).

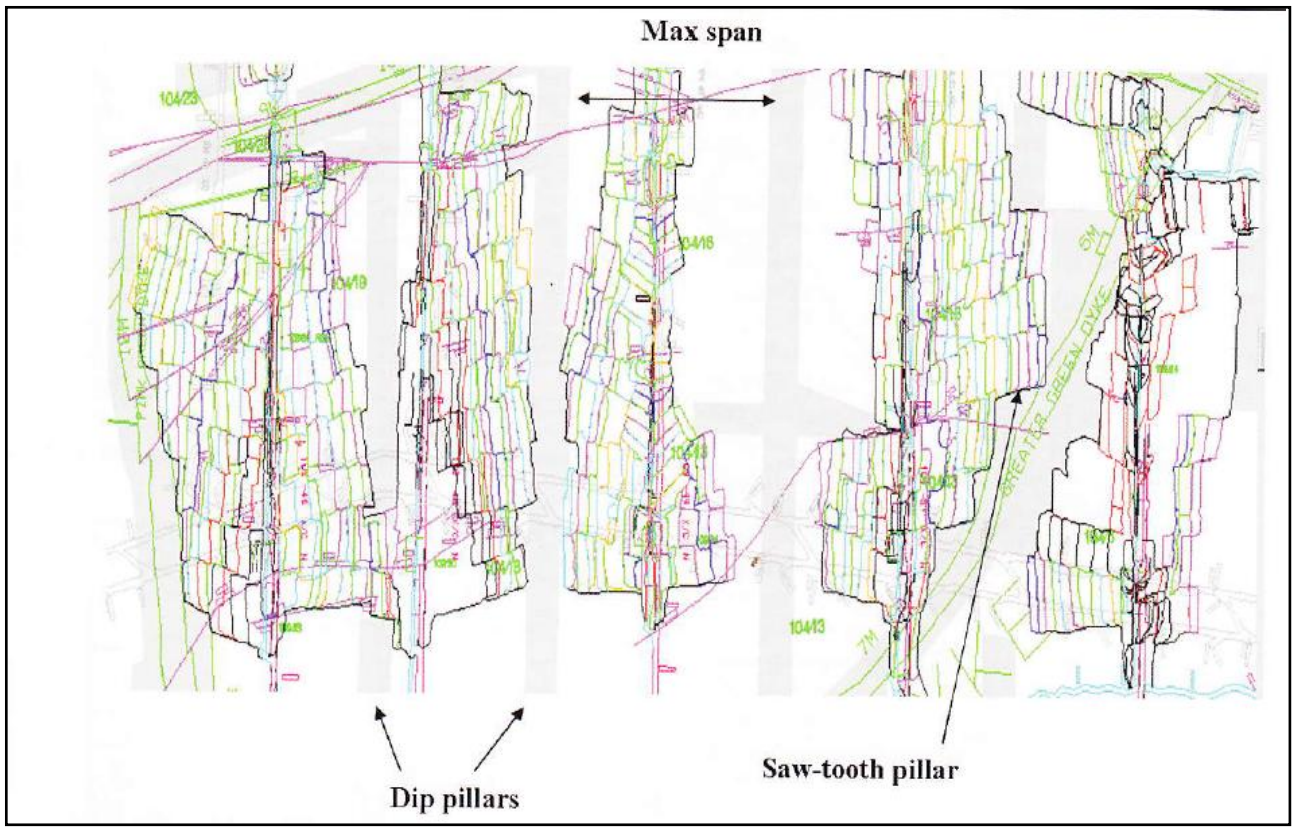

Figure 12: Typical Mponeng Mine grid mining layout (after McGill, 2007)

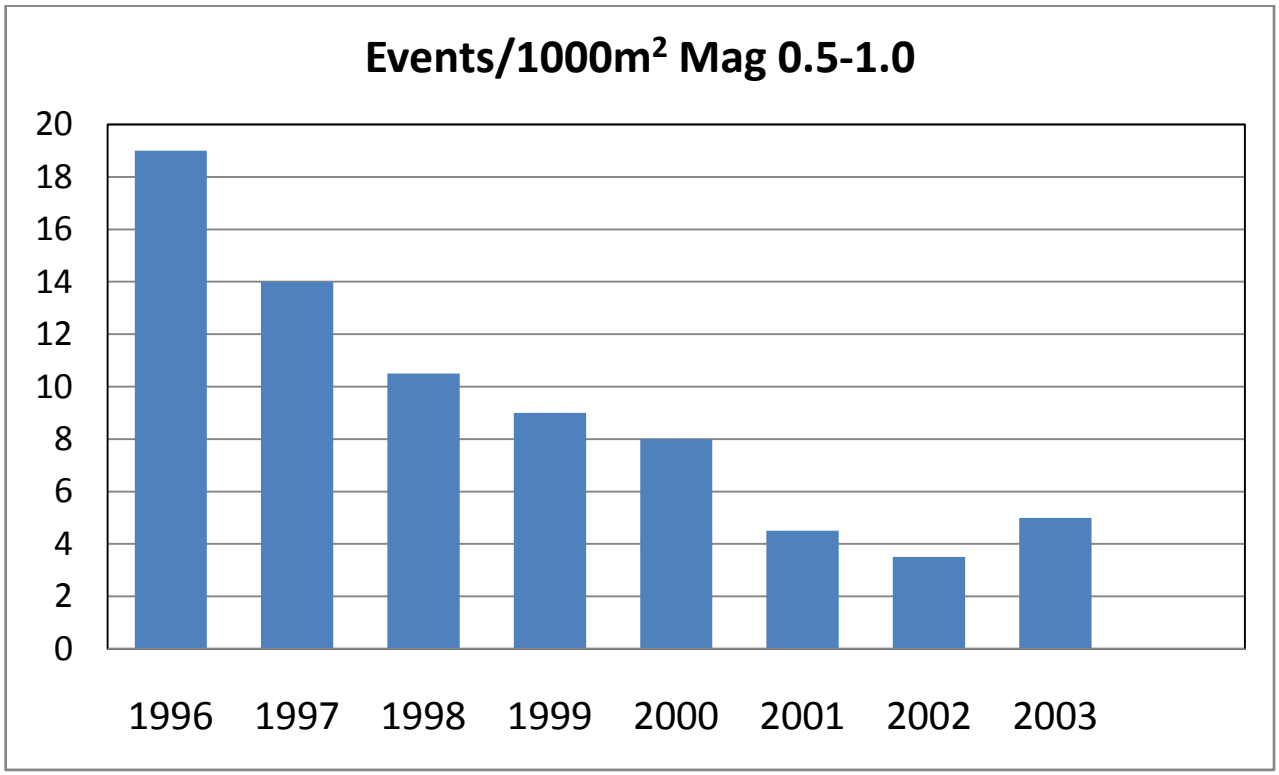

Figure 13: Number of events per 1000 m^2 for M_L between 0.5 and 1.0 (after McGill, 2007)

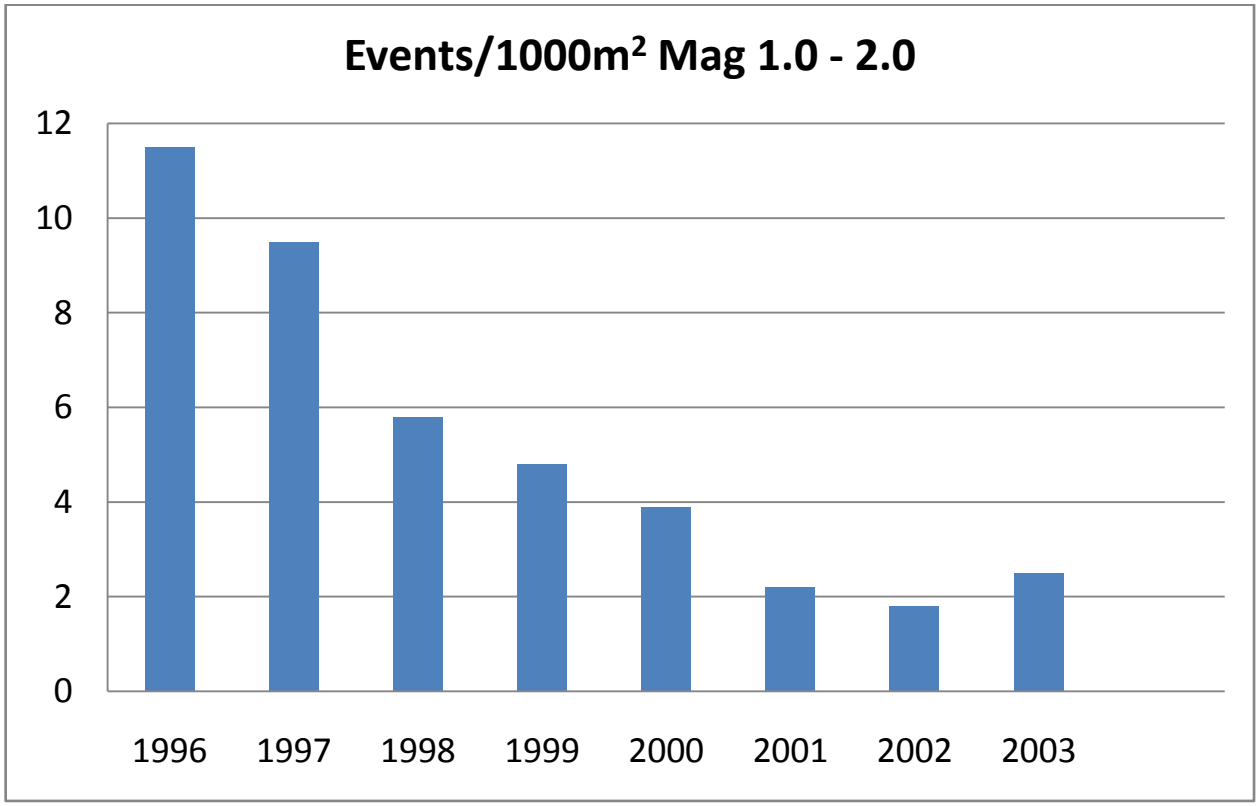

Figure 14: Number of events per 1000 m^2 for M_L between 1.0 and 2.0 (after McGill, 2007)

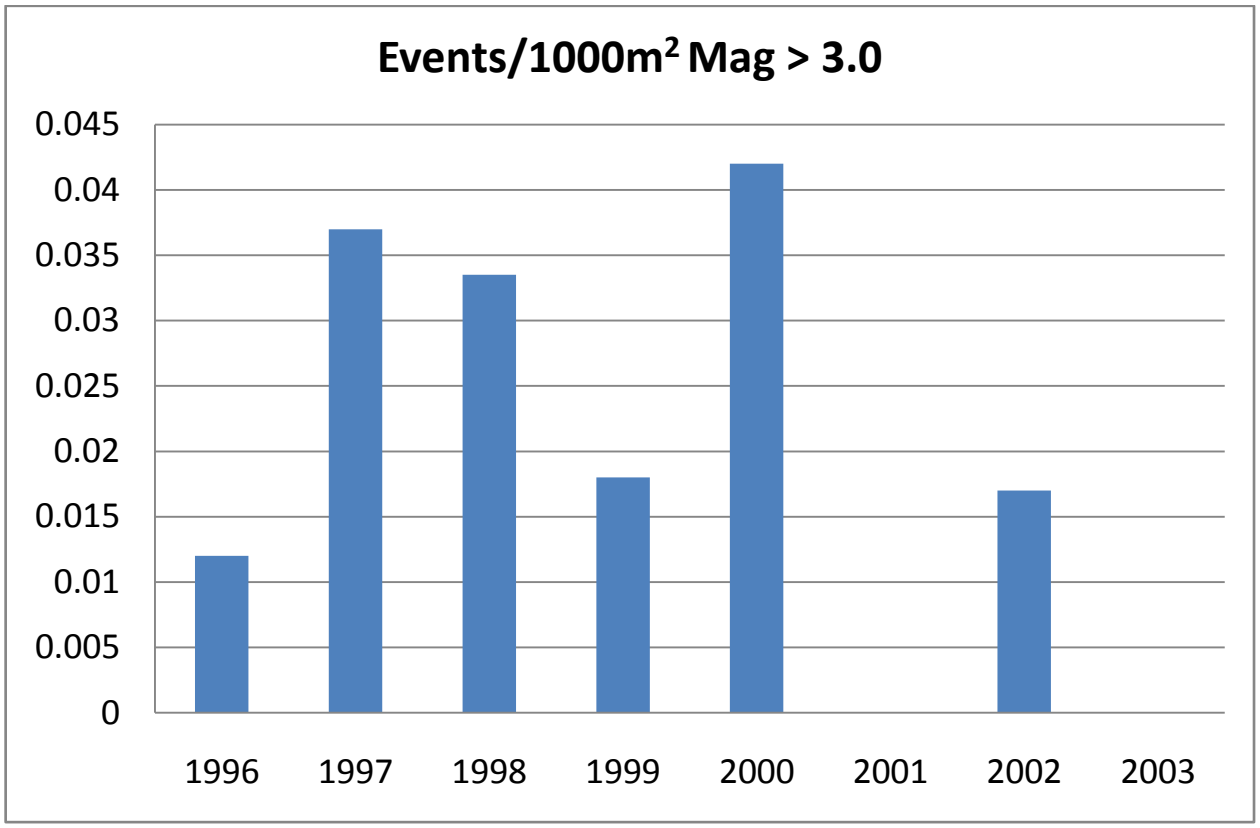

Figure 15: Number of events per 1000 m^2 for M_L>3.0 (after McGill, 2007)

A similar approach was adopted by Goldfields when the mine layout for the No. 5 Shaft Driefontein Gold Mine was designed (Klokow, 2003).The design uses closely spaced dip pillars, some of which clamped fault or dyke structures. The crosscuts to the reef are developed at 180 m intervals with 40 m wide pillars, which results in mining spans of 140 m. The overall sequence is an underhand forming an inverted V-shaped as shown in Figure 16.

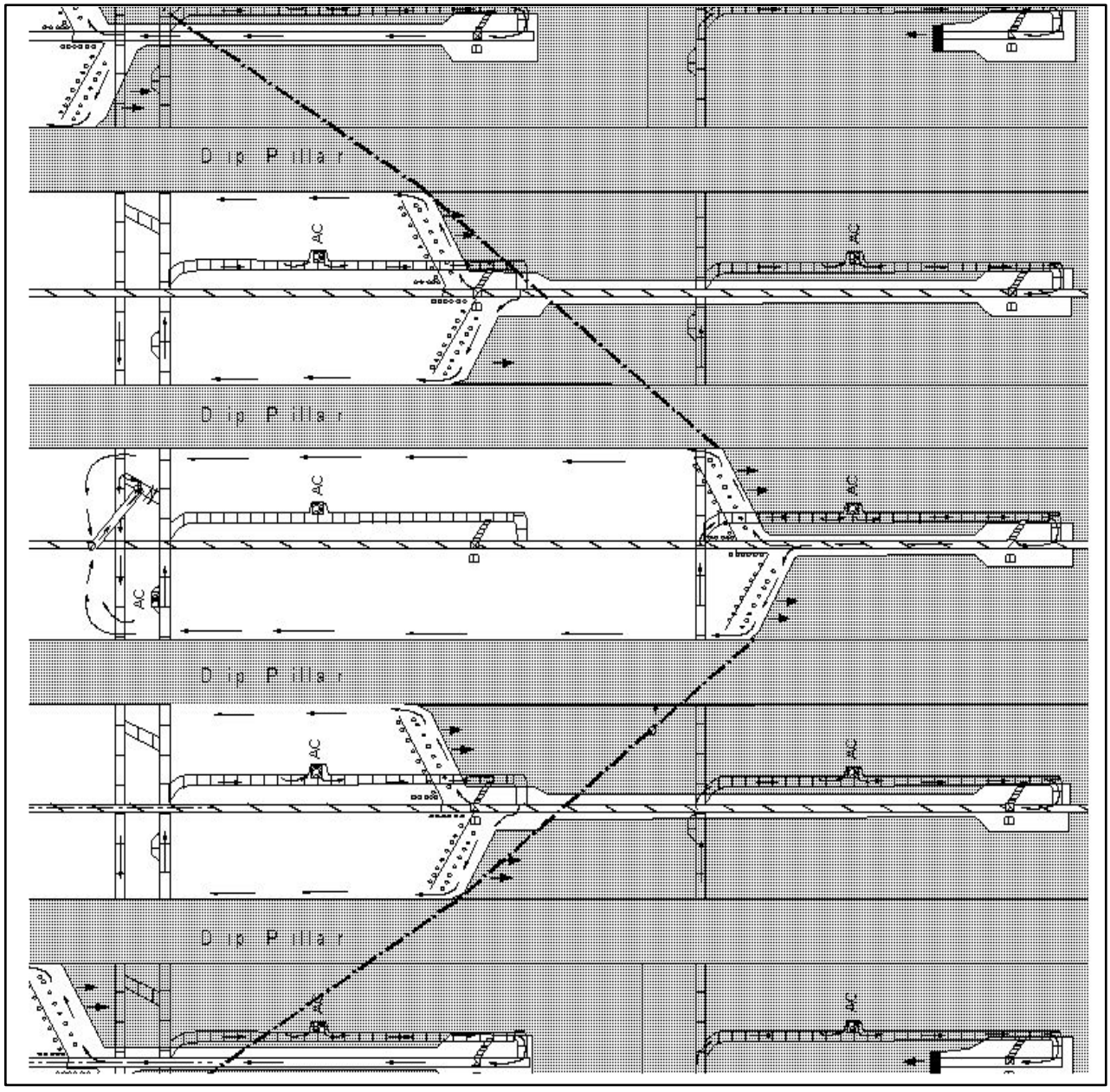

Figure 16: Driefontein No. 5 shaft closely spaced dip pillar layout showing the v-shaped pattern (after Klokow, 2003).

There is a significant time delay between stoping and seismic activities at each of the raise lines studied (Klokow, 2003). In their analyses the gap corresponded to time periods of about twelve months of stoping before the onset of the increased seismic activity. The time delay also related to production levels of about 20000 m^2 per raise line and maximum spans of the order of 100 m and 120 m. This can be significant for the design of stability pillar spacing's in the deep mining environment.

1.6. DEEPMINE RESEARCH PROJECT INTO ULTRA-DEEP MINE LAYOUT ALTERNATIVES

The purpose of the project (Vieira, 2001) was to determine which of the different available mining layouts is the most adequate from an economic and safety perspective. The research work was done as a multi-disciplinary assessment including environmental control, rock engineering, logistics and economics. Four different layouts were identified to be investigated:

- Longwall with strike-orientated stabilising pillars (LSP);
- Sequential Grid mining with dip-orientated stability pillars (SGM);
- Sequential down dip with dip-orientated dip pillars (SDD); and
- Closely spaced dip pillar system (CSDP)

Two of the layouts investigated in the study by Vieira (2001) are similar to layouts analysed in this dissertation. The SGM layout is basically the original Sequential Grid layout as discussed in Section 1.4 (see Figure 17 and 18) and the CSDP system is similar to the layout discussed in Section 5.8 for alternative layouts (see Figure 19).

Some of the results obtained from the research are discussed below:

- The overall macro results from the rock engineering studies indicated that it might be possible to mine safely at ultra depth mining providing that the following conditions are satisfied:

  - Adherence to strict rock engineering guidelines;
  - Constant monitoring of rock mass response;
  - Risk status of working areas are done on a continuous basis
  - Deviations from design guidelines are strictly justified
  - Rock engineering input into mine planning
  - Advance knowledge of geological/geotechnical conditions.

- Micro results indicated that the different methods all pose different hazards, risk and potential problems that need to be addressed individually before final decisions are made about the appropriate design being used.
- The overall conclusions from the multi disciplinary assessment illustrated that it is a complex process to arrive at an optimal mine layout design.
- From the studies, the CSDP emerged as the most advantageous alternative, but it cannot be chosen as the most adequate layout until more detailed investigations are concluded.

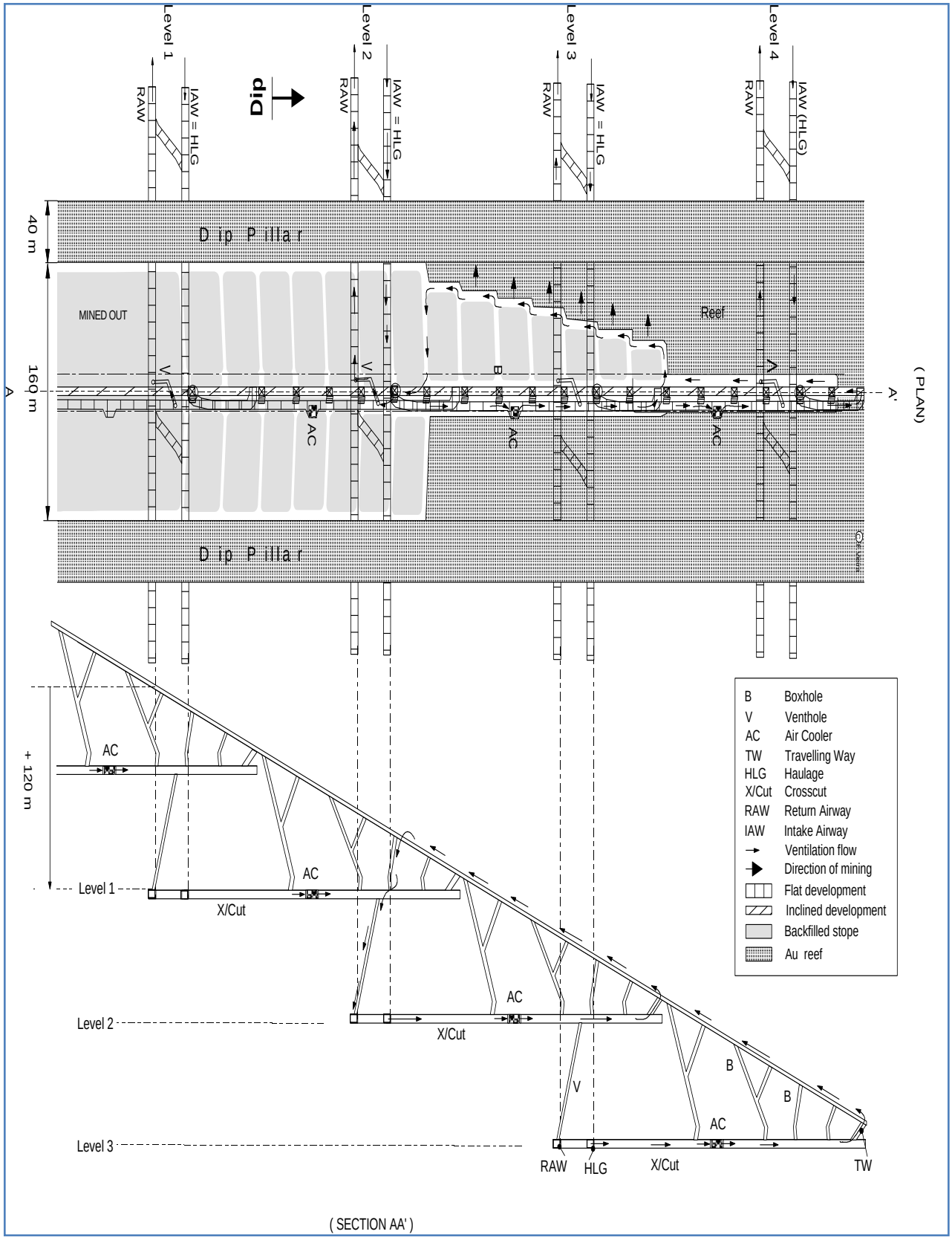

Figure 17: Micro concept of a Sequential Grid mine layout with dip-orientated pillars (after Vieira, 2001)

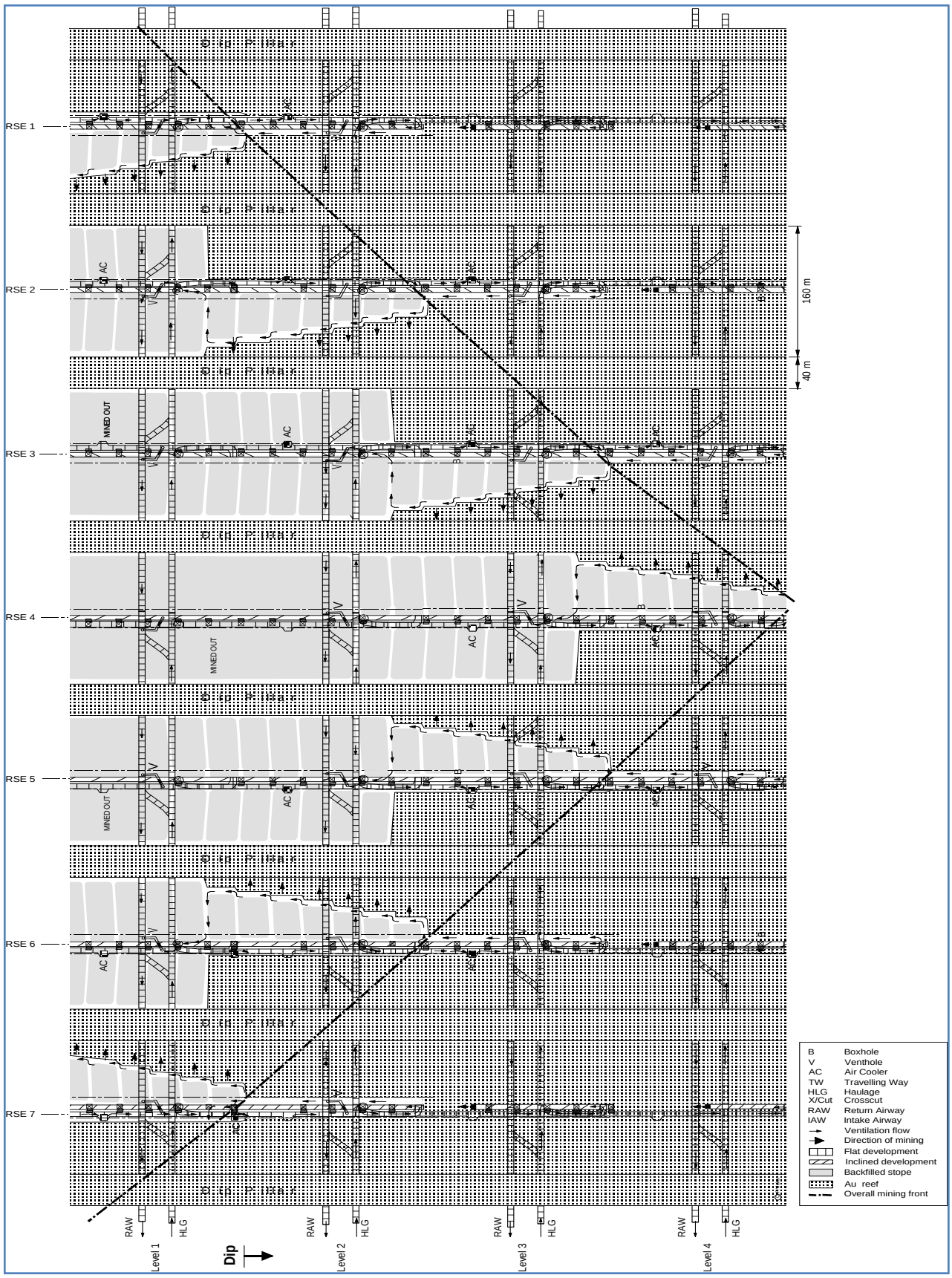

Figure 18: Macro concept of a Sequential Grid mine layout with dip-stabilising pillars (after Vieira, 2001)

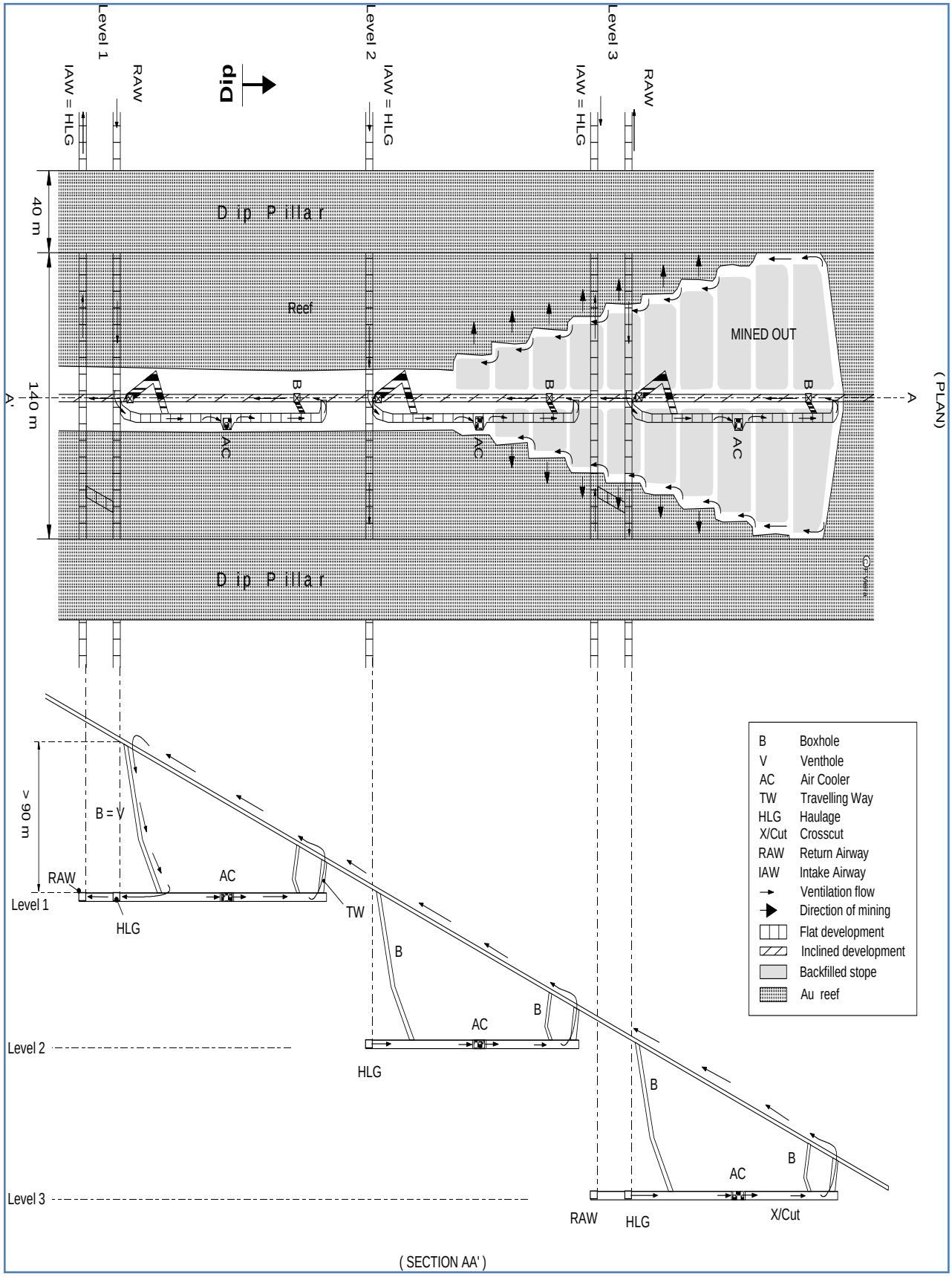

Figure 19: Micro concept of a closely spaced dip pillar mine layout (after Vieira, 2001)

1.7. PROBLEM STATEMENT

Dip stability pillars and a sequential sequence of extraction in deep level hard rock mines seem to be very useful to reduce seismic related incidents. This mining method nevertheless has drawbacks that need to be addressed to ensure that deep level mining will remain safe and financially viable in future. A key problem related to Sequential Grid mining is low production rates. Thus, can the design be altered to increase production rates without increasing the rockburst hazard and keeping deep level mining safe? This problem was investigated in this study with particular reference to the layout at Kusasalethu Mine. The revised method proposed for the mine will be referred to as Multi-raise mining in the remainder of the dissertation.

1.8. METHODOLOGY

To investigate this problem, the following methodology was adopted in this study.

1. An investigation of the different sequenced mining sequences employed by deep level gold mines was conducted.
2. A seismic investigation was conducted to determine if any changes in the seismicity could be identified between the original Sequential Grid mining and the proposed Multi-raise mining.
3. The Modelled Moment method was explored as a tool to investigate future seismic hazard of the proposed Multi-raise mining layout.
4. A numerical modelling study was conducted to investigate differences between the original Sequential Grid and the Multi-raise sequences.
5. Numerical modelling was conducted to investigate alternative methods that will address the shortcoming of the Sequential Grid sequence.
6. Based on the knowledge generated, a revised Sequential Grid method is proposed in this dissertation.

Chapter 2

DESCRIPTION OF CHANGES TO THE SEQUENTIAL GRID DESIGN – MULTI-RAISE MINE DESIGN

2.1. INTRODUCTION

As described in Chapter 1, the Sequential Grid method proved itself as a much better alterative than the longwall mining method employed on many of the deeper mines. The limitations discussed in Chapter 1 nevertheless question whether the method will always be financially viable. A change to the original design was proposed for Kusasalethu Mine where basically multiple raises will be mined simultaneously. This will be referred to as the Multi-raise mining method.

2.2. DESCRIPTION OF MULTI-RAISE MINING METHOD

The Multi-raise mining method differs from the Sequential Grid method mainly by the number of raise lines that are being mined simultaneously on a specific mining level. Sequence stoping is therefore taking place in a number of raise lines simultaneously on the various mining levels.

The major advantage of this method compared to the Sequential Grid method is that the extraction rate of the Multi-raise sequence is higher. This results in a decrease in the extraction time of a specific mining block which again results in the increase of production levels.

Although multiple raises are mined on the same level simultaneously, the basic Sequential Grid rules remain intact where:

- The grid mining is done in such a manner as mining are done towards the shaft first and then away from the shaft.
- Only single sided mining is done
- Deeper levels will be started up later than the shallower sections resulting in a “V” shaped down-dip mining configuration. The “V”- shape will be broader than the “V”– shape for the Sequential Grid configuration due to the fact that more raise lines is started up simultaneously.

Figures 21 and 22 show schematically the difference between the Multi-raise mining sequence and the Sequential Grid sequence. The blue blocks indicate the mining areas that are mined out per mining step while the white blocks represent solid ground. Of importance here is to notice the apparent increase in the extraction rate between the two mining sequences and the “V” – shaped down-dip configuration. It should be noted that the Multi-raise mining method does not necessarily imply an overall faster mining rate, although it can be achieved if more mining crews are utilized.

When the production levels increases for the Multi-raise mining method changes to the seismicity are expected. In the two following chapters the seismic analyses and comparison between the two mining methods are discussed to determine what can be expected in terms of seismicity if the mine design is changed.

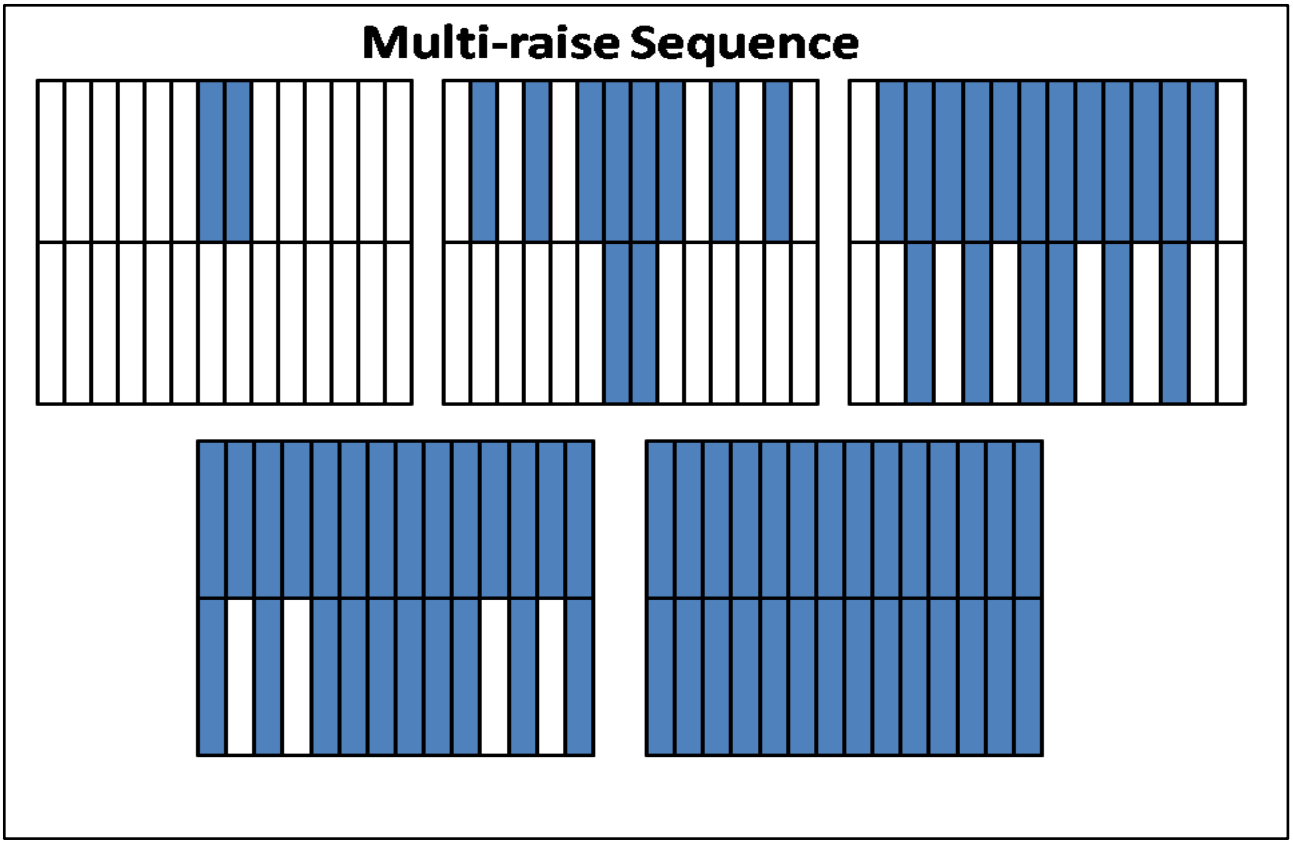

Figure 20: Multi-raise sequence

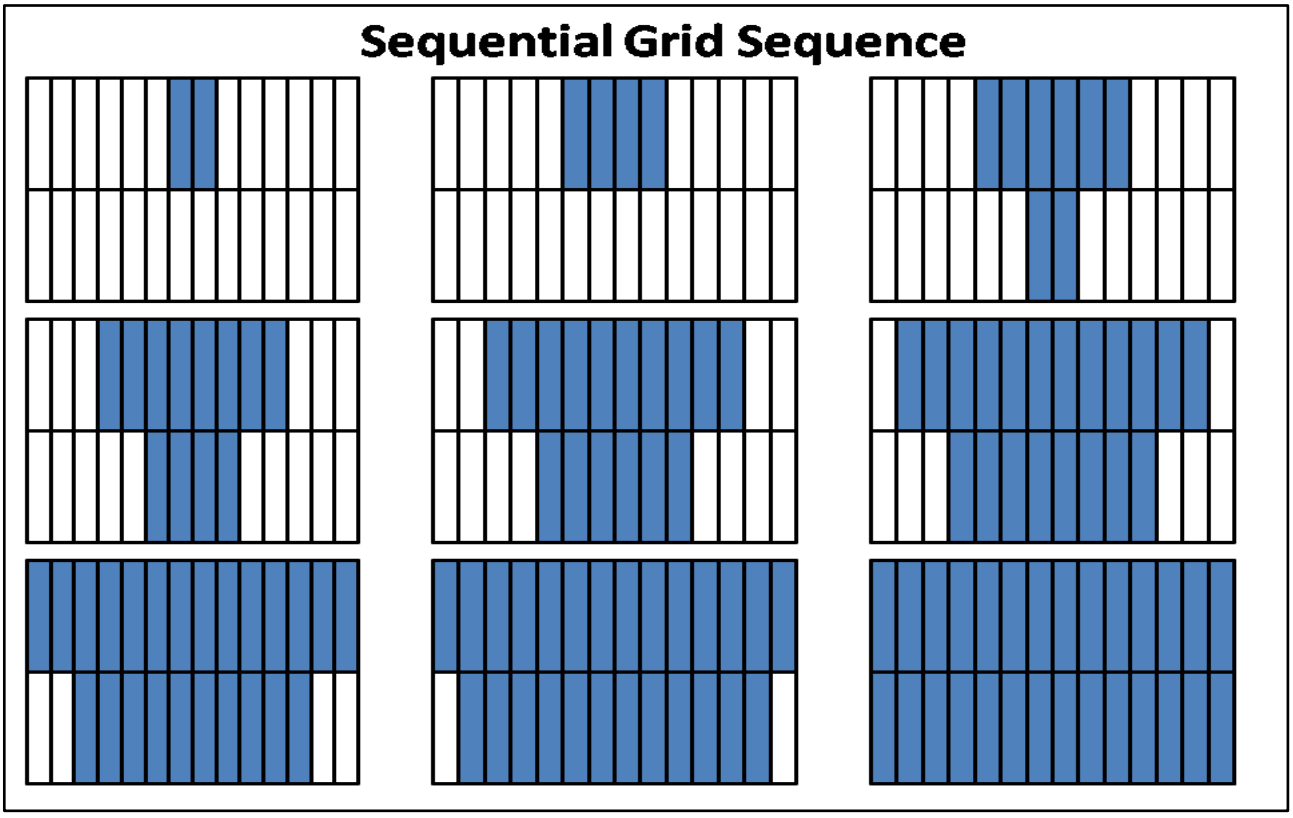

Figure 21: Traditional Sequential Grid sequence

Chapter 3

ANALYSES OF SEISMIC DATA FROM KUSASALETHU MINE

3.1. BACKGROUND

To investigate the seismic response of the Sequential Grid mine design, as postulated by Appelgate in 1991, and compare it with the changes made to this design as described in the previous chapter, it was decided to evaluate the seismicity experienced by the two mining methods employed on Kusasalethu Mine.

Kusasalethu Mine is situated on the far southern section of the West Rand goldfields. It forms part of the central portion of the greater Witwatersrand Basin and mining proceeds on the Ventersdorp Contact Reef (VCR). This is a gold-bearing quartz conglomerate reef band with an east-west strike and it has an average dip of 24° towards the south. It exhibits highly erratic grade characteristics and varies from zero to three meters thick. The thickness of the reef is closely related to the nature of the terrain on which it was laid down. Slope reef tends to be thin and low in gold content while terrace reef tends to be thick with higher grade. In general, the grade is highly variable with unpay zones typically occupying sand-filled channels.

The hangingwall is Ventersdorp Lava, which is characterized by an unaxial compressive strength (UCS) of approximately 300 MPa. Conditions vary considerably across the above mentioned reef type as a result of pilloids, inter pilloid breccias as well as joints associated with slopes and duplicated reef zones. Other contributing factors are the relatively large amount of flat faulting that extends into the hangingwall and the brittle nature of the hangingwall lava. The footwall is competent quartzite, (UCS 180 – 250 MPa) which extends to a depth of approximately 430 m below reef on the eastern boundary and about 550 m below reef on the western boundary. This high strength zone enables

haulages and most of the other related development to be sited deep in the footwall without problems.

Faulting on Kusasalethu Mine is relatively minor when compared to other mines in the Witwatersrand Basin. The main structural trend strikes in a NNE-SSW direction with a minor trend parallel to the strike of the VCR. Dykes and sills intrude the strata; many dykes follow pre-existing fault planes and now display throws previously belonging to the faults. The fault displacements are predominately normal and almost always less than 10 m.

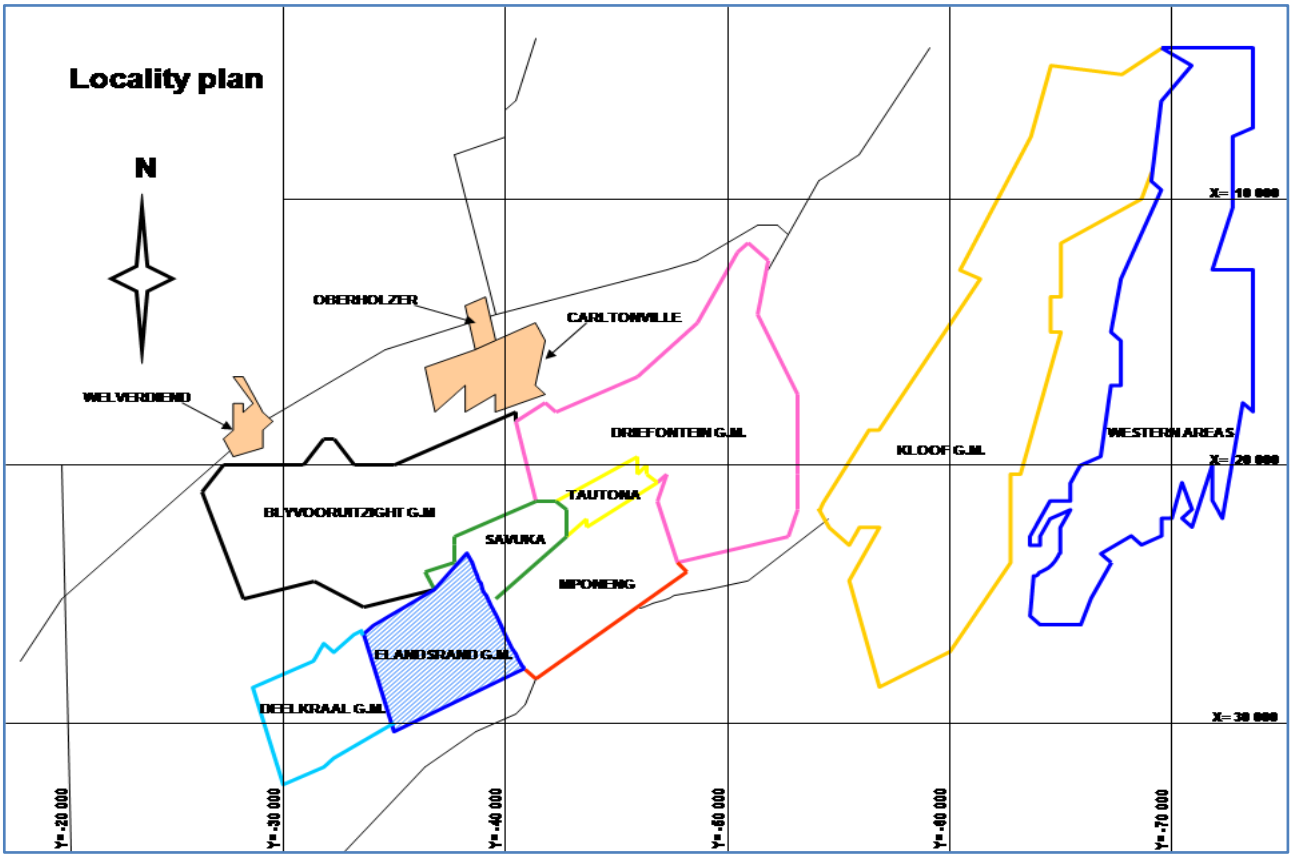

Figure 22: Locality plan of Kusasalethu Mine (formerly Elandsrand Gold Mine)

Figure 24 shows a stratigraphic section looking East through the main and material shaft and the sub shaft.

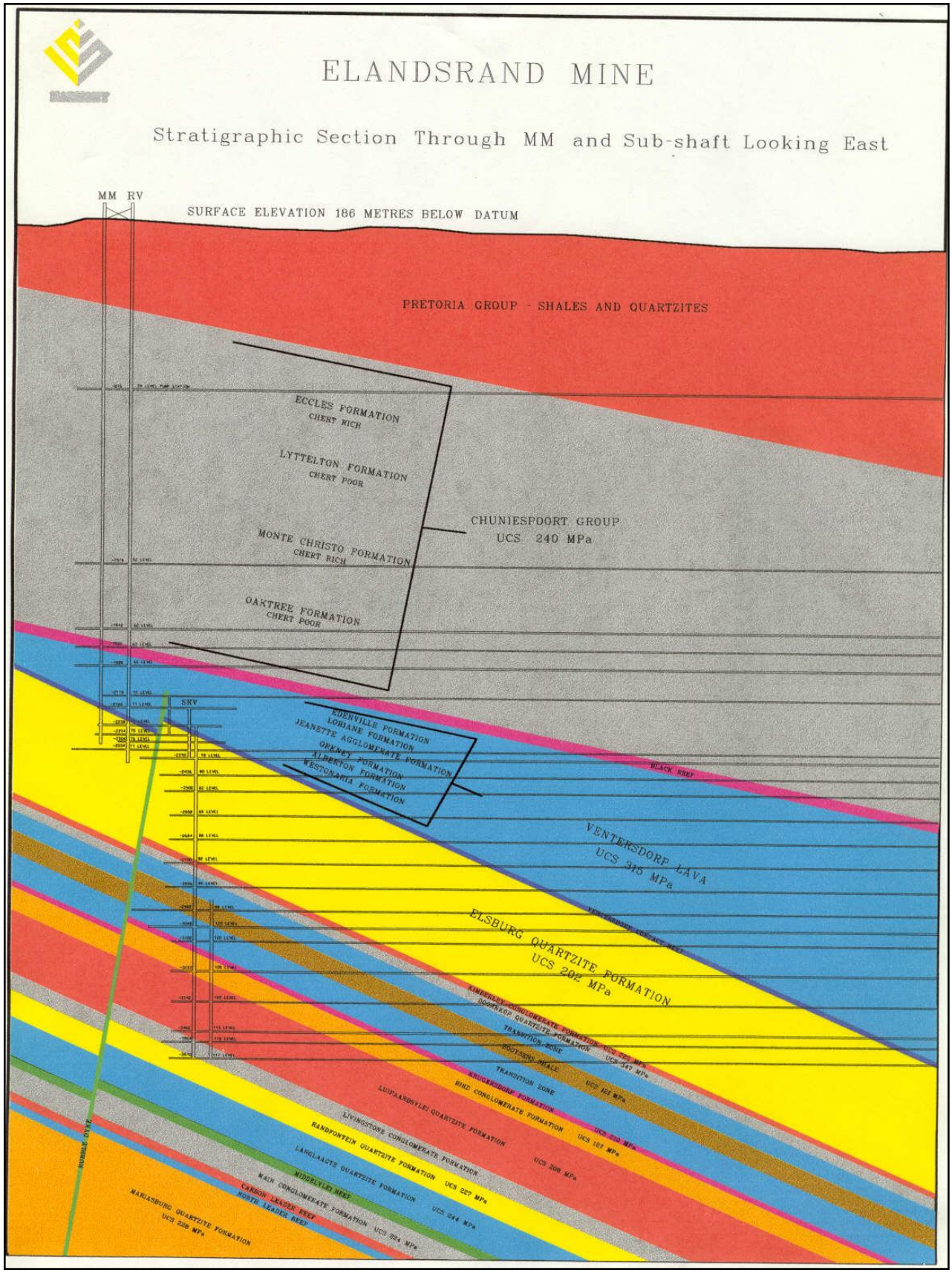

Figure 23: Stratigraphic section through the man and material shafts of Kusasalethu Mine looking east

3.2. HISTORY OF THE SEISMIC NETWORK

Seismicity was recorded at Kusasalethu Mine since 1983 with various different seismic systems. The supervision and administration of the system changed a number of times during the last few decades. It is therefore important to describe the history of the network in some detail and the effect it had on the seismic data.

As early as 1983, the first seismic network in operation at Kusasalethu Mine was a COSMOS system that was developed by Anglo American. The network consisted of 11 seismic stations, one on surface and the remaining 10 seismic stations installed underground between 52 level and 73 level. Communication with a surface minicomputer was achieved using (Perkin Elmar 3220) analogue signals. The locations and magnitudes were calculated on surface.

As mining commenced on the deeper section of the mine, it was associated with a considerable amount of seismicity. This resulted in a number of serious accidents and fatalities. A second system which was developed by the Western Deep Levels Rockburst Prediction Project was installed in 1987. The signals (seismograms) from the six seismic stations were processed underground and then sent to the surface. The location and magnitude of the seismic events were calculated by manually picking arrival times from the waveforms. This system only provided basic information of about the location of the seismicity, but the reasons for the occurrence of the seismicity was not clear.

A decision was made to expand the seismic network and in 1991 an ISSI seismic network became operational. By the end of 1992, a total of 22 seismic stations were operational, each seismic station consisted of a tri-axial geophone and an intelligent seismometer. The expanded seismic network covered approximately 15 km^2 of the mine. Three of the stations were installed on surface and the remaining 19 underground at depths between 52 and 100 levels. The network recorded on average 200 seismic events per day with varying magnitudes.

In 2011 ISSI was sold and the new owners changed the name of the company to IMS (Institute of Mine Seismology). The current IMS seismic network on Kusasalethu Mine consists of 17 operational seismic stations as shown in Figure 25. Expansion of the seismic network is currently underway with the installation of four additional seismic stations between 88 and 105 level.

A large number of seismic events have been recorded since the ISSI network became operational at the end of 1992. The current database extends from 1996 and consists of 837024 seismic events with magnitudes varying between -3.0 and 4.0 M_L. Figure 26 shows the locations of all seismicity with $M_L \geq 3.0$ since 1996. On average, approximately 8000 seismic events are recorded per month.

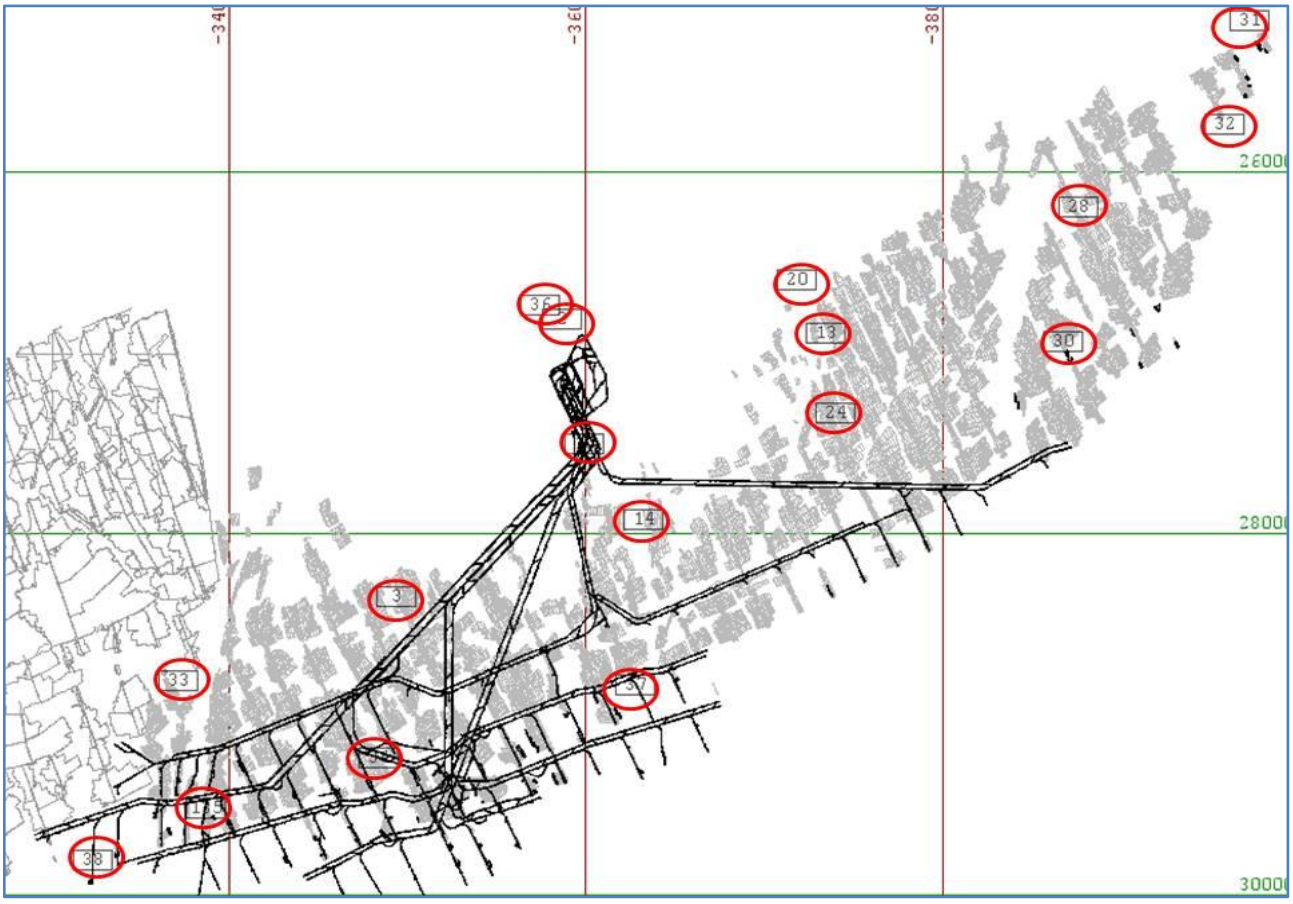

Figure 24: Location of 18 seismic stations at Kusasalethu Mine

Seismicity is an inevitable occurrence when mining activities are occurring deep within the earth's crust. Seismicity induced by mining activities is most often described as rock

failure that results from dynamic changes in the stress state of the intact rock. A seismic event can be described as a sudden inelastic deformation within a give volume of rock (Jager and Ryder, 1999). These sudden inelastic deformations are caused by strain energy that is stored in the rock mass surrounding the excavations.

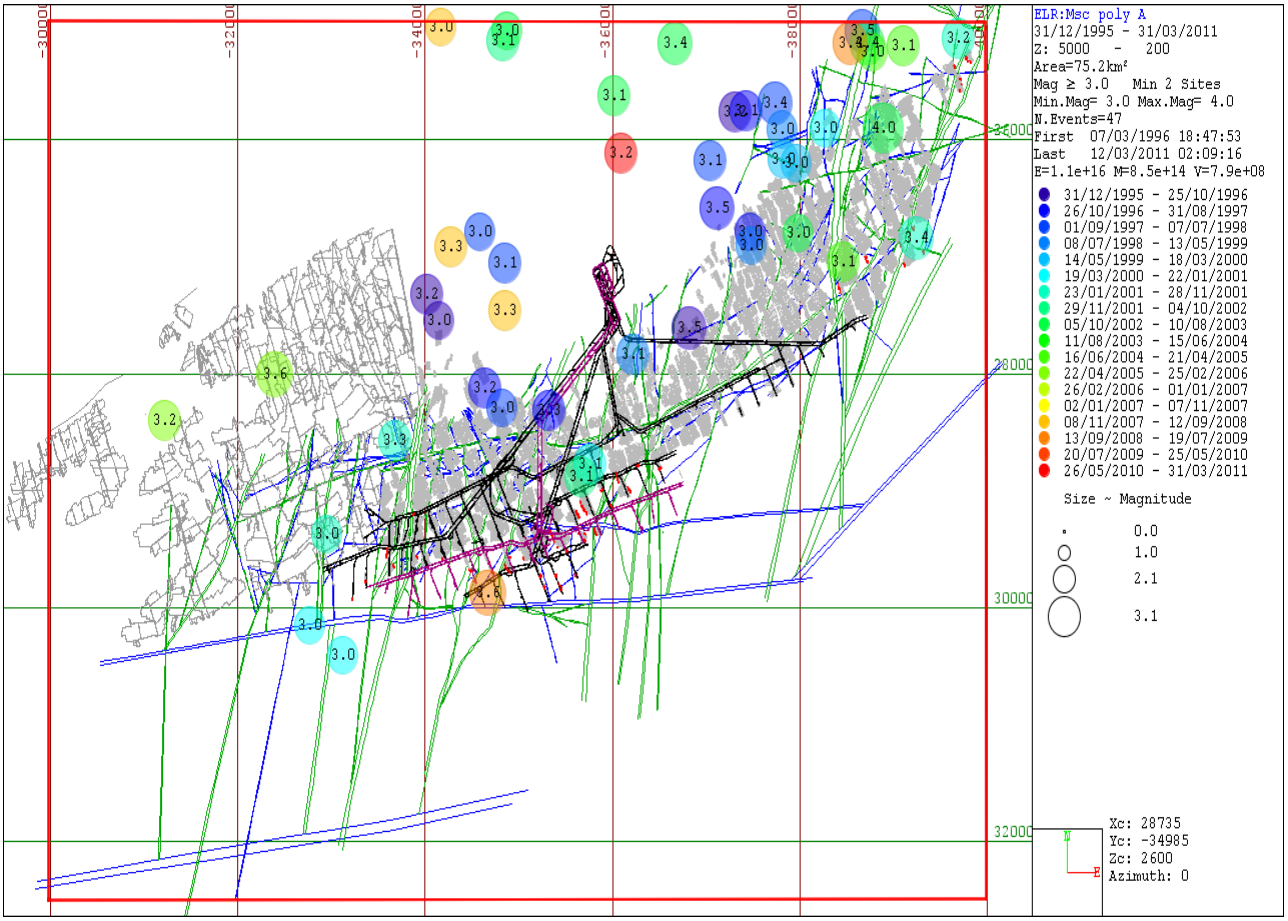

Figure 25: Location of all $M_L \geq 3.0$seismic events since 1996

Mining induced seismicity can be observed worldwide where underground mining is occurring. The most detailed studies on mining induced seismicity were carried out in South Africa where gold mines in the Witwatersrand area are currently stoping up to depths of 3500 km below surface.

Studies (Jordan and Richardson, 2000) have shown that the distribution of mining seismicity is generally bi-modal in nature with two classes of seismic events being identified and generally labelled as Type A and Type B. The bimodal distribution results from these two classes of seismicity being mixed together:

- Type A events are mainly associated with blasting of excavations; they have spectra comparatively enriched in high frequencies, and they usually show an upper magnitude cut-off at M_L ~ 0.5. These seismic events are interpreted to be "fracture-dominated" ruptures of competent rock in front of the active working faces.
- In contrast, Type B events are temporally and spatially distributed throughout the active mining region. These seismic events are interpreted to be associated with faults or other weak geologic structures and are usually associated with magnitudes larger than 0.0.

Figure 27 shows the bimodal distribution for a two year section of the seismic database of Kusasalethu Mine. The red sphere depicts typical Type A seismic events and the yellow spheres the typical Type B events as discussed above.

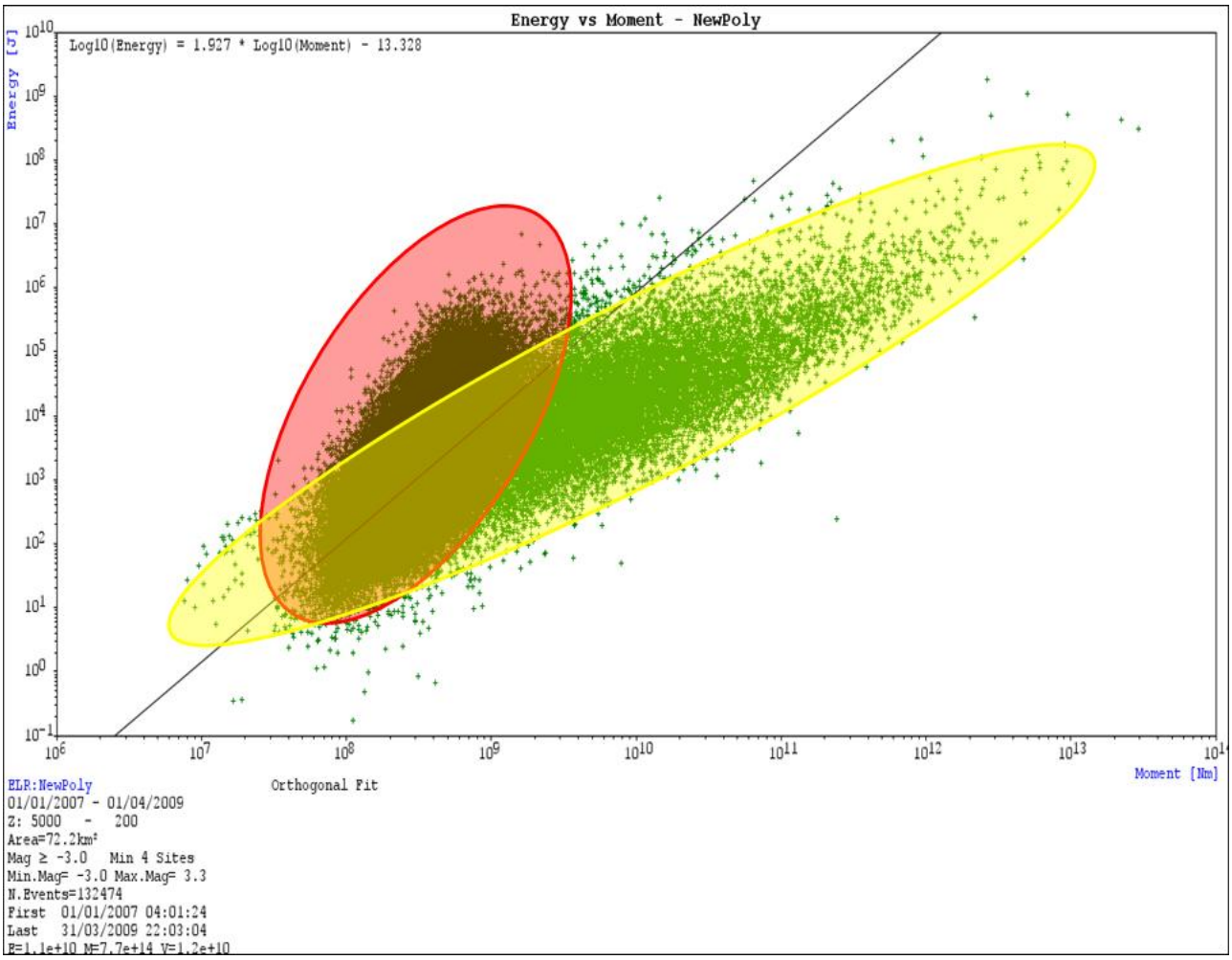

Figure 26: Energy versus moment – Bimodal distribution on Kusasalethu Mine (2 year period)

3.3. SEISMIC HISTORY OF KUSASALETHU MINE

As mentioned in Section 3.2 a large amount of seismic activity has been recorded since the ISSI seismic network became operational at the end of 1992. The annual distribution of all the seismic events with $M_L \geq 0.0$ recorded by the seismic network since 1996 is shown by means of the time series portrayed in Figure 28. A significant decrease in the seismic activity is evident since 2005 which can be directly contributed to the decrease in production from 286062 m^2 during 2003 to 170252 m^2 during 2005.

The diurnal distribution of the potentially damaging events (usually with $M_L \geq 1.0$) for the period November 1994 to April 2011 is shown in Figure 29. An important feature visible from this hourly distribution is the fact that the majority of these seismic events occurred during a 7 hour period (13H00 up to 20H00) which corresponds with the blasting window that predominantly starts after 13H00. A more acceptable and ideal solution would involve a reduction in the length of this time window to say 3 hours, thereby resulting in a decrease in the exposure window of the working crews to seismicity.

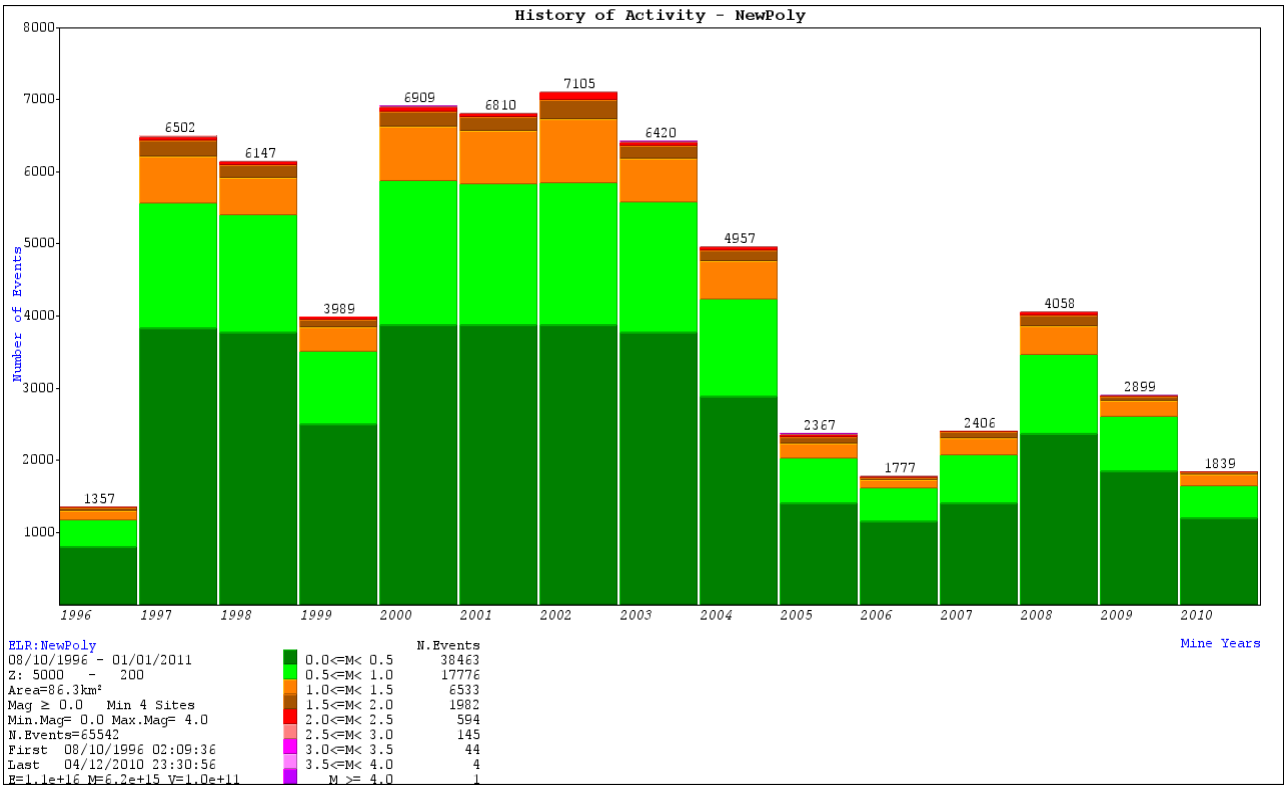

Figure 27: Yearly activity for all seismicity recorded since 1996

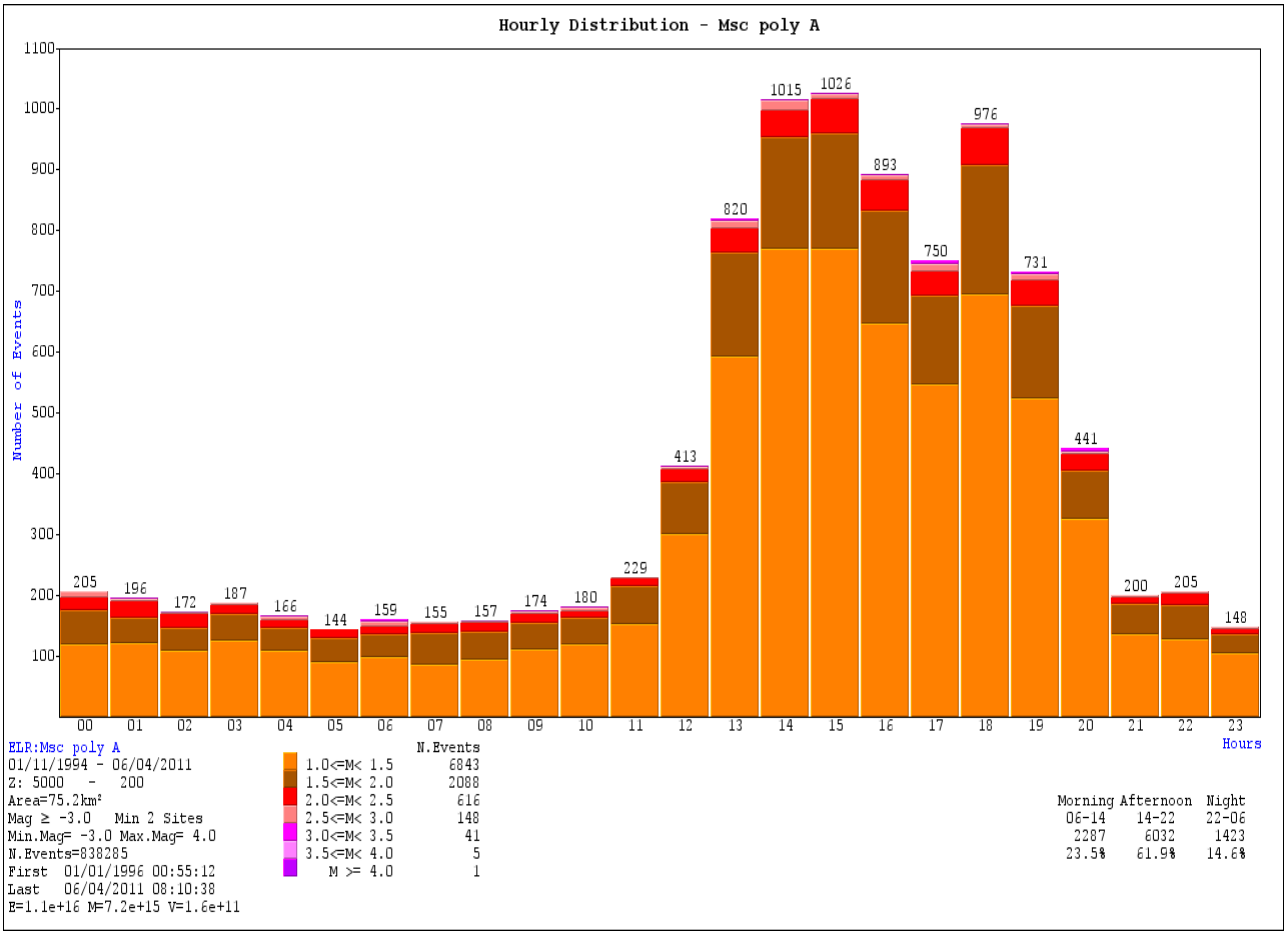

Figure 28: Time distribution (24 hours) from 1996

The magnitude distribution for all seismic events since 1996 is presented in Figure 30 and appears complete up to about 3.7 M_L level. Beyond this the incomplete nature of the distribution generally results from the greater recurrence period of the larger magnitude seismic events. The green distribution is the given magnitude distribution while the blue distribution is a cumulative distribution i.e. greater than any given magnitude.

Only three seismic events with $M_L \geq 3.0$ have occurred since 1996 with the largest having a local magnitude of 4.0 and occurred during April 2003 on the eastern side of the mine where it was located close to the Grass dyke.

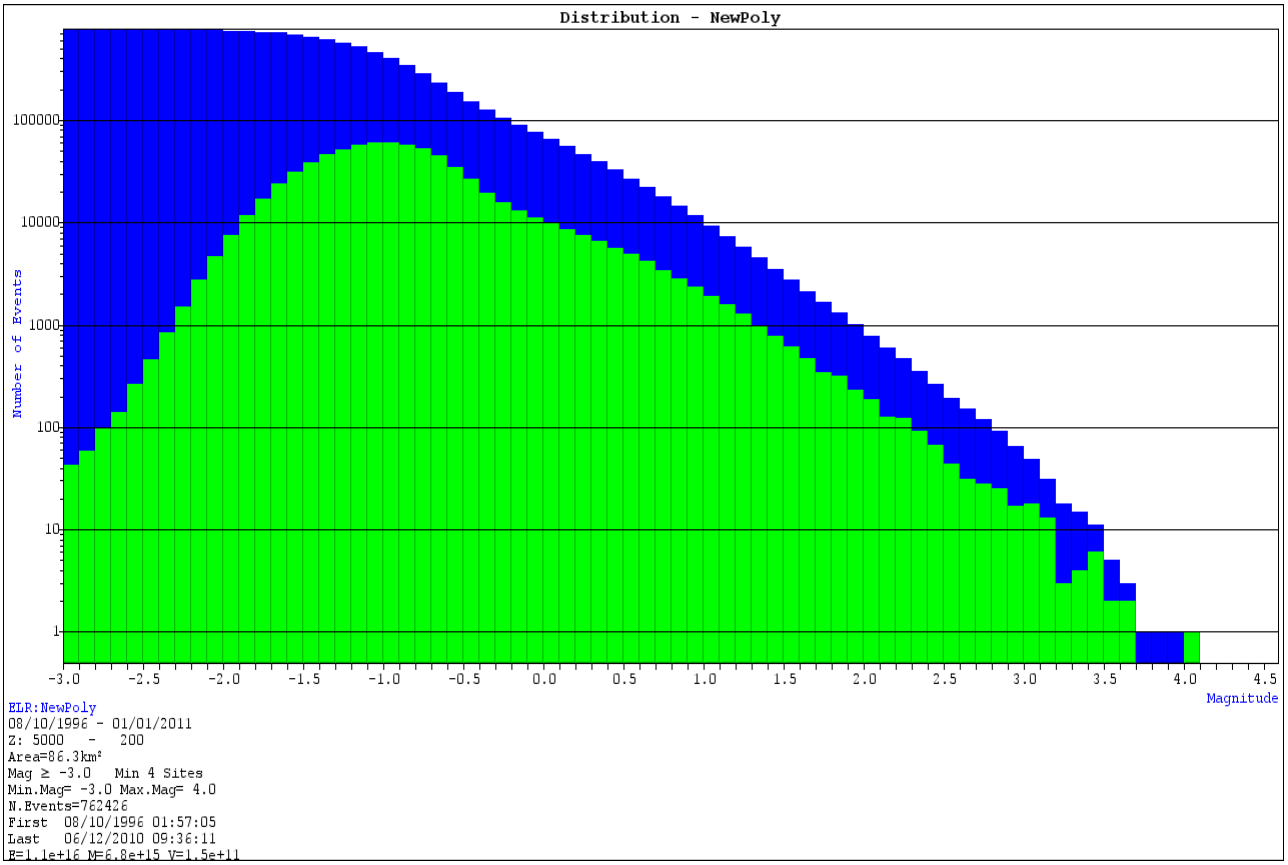

Figure 29: Magnitude distribution of all seismic events (1996 - 2011)

3.4. SOURCES OF MINING INDUCED SEISMICITY AT KUSASALETHU MINE

Not all of the seismic events recorded by the seismic network at Kusasalethu Mine result in damage to underground excavations. In general the protocol at Kusasalethu Mine is to consider all events with $M_L > 1.5$ as having the potential for damage. However, depending on the stress levels and ground conditions, smaller seismic events can also result in damage.

Analyses of the micro as well as the larger seismic events have identified different sources of seismicity within the Kusasalethu gold mining area and these are summarised below.

- Fracturing seismic events

  These are seismic events generated by the fracturing of the rock mass directly after blasting and are recorded in areas where the sensitivity of the seismic network is

capable of detecting seismic events with seismic moments equivalent to approximately $M_L < 0.0$ i.e. $\log_{10} Mo < 9.0$. These micro events provide qualitative information on the state of stress of the solid rock ahead of the face. These smaller events usually identify stope faces that are close to holing as well as imminent failure or crushing of pillars.

- Local structural seismic events

These are seismic events triggered along dykes and faults in the vicinity of active mining. Magnitudes generally range from $M_L = 0.0$ to about 3.0, depending on the complexity and size of the geological structures.

The micro- to medium seismic events that occur on these geological structures (i.e. those that slip incrementally or fracture under stress) provide qualitative information on the changes to the state of stress or strain on and around these discontinuities in the rock mass. All geological structures (faults and dykes) are potential sources of hazardous seismicity, but the level of seismic hazard varies according to the nature and/or complexity of the geological structures.

Faults and dykes are very common at Kusasalethu Mine and are the sources of larger seismic events. The Sequential Grid mining allows for effective clamping of geological structures which reduces the severity of major failures under normal circumstances.

Violent failures on geological structures are infrequent, but can occur even with the introduction of bracket pillars. Essrich (1998) showed that seismicity occurred on a number of geological structures when mining was taking place in the immediate vicinity of certain bracketed structures.

- Regional seismic events

Southern Africa is located in the interior of the large African Plate bounded in the south by the mid-Atlantic and mid-Indian Ocean Ridges. This is generally a tension environment and seismicity by world standards is moderate and has a shallow character. Occasionally earthquakes do occur, for example the 1908 event in Klerksdorp, the 1912 event in the Orange Free State and the Ceres-Tulbagh event of 1969. More recently, the area has seen the occurrence of earthquakes in Mozambique associated with the African rift system (2010).

From a mining induced seismic perspective, events with magnitudes up to 5.0 have occurred at depths of more than 2000 m. This can be compared to the seismicity experienced in the compressive stress environment of the Polish Coalfields where events with magnitude up to 4.5 have occurred (Gibowicz, 1979). This highlights the influence of the continental tectonic forces on the induced seismicity in particular areas. The triggering mechanism for these regional larger seismic events is most likely related to fluctuations in stress gradients, stress transfer across the regional area and small increases in stress to sites that are already in a state of unstable equilibrium. These types of seismic events are also usually associated with larger regional type faults and dykes characterized by large throws and which traverse the mine. A typical example of such a regional event is the dynamic failure that occurred on Kusasalethu Mine during April 2003 with M_L = 4.0 and which was located on the Grass dyke.

In addition to these three sources of seismicity, the following components of typical mining layouts also have an influence on the occurrence of seismic events:

- Static/Regional abutments

The starting up of new raise lines from the next production level (for example between 102 and 98 levels) creates regional abutments that can pose a significant seismic hazard. The creation of these regional abutments currently poses strata control problems, especially with regards to ground conditions in panels started up adjacent to these abutments.

- Pillar abutments

  A significant number of pillar abutments coincide with faults and/or dykes. Frequent, smaller and medium size events were recorded on the dip pillars in the back areas, but no large failures have been recorded as those observed on strike stabilizing pillars in other deep gold mines.

- Stope faces

Face bursting is a common occurrence and poses a seismic hazard on this mine. Violent failure of the face due to the build up of strain energy can result in serious accidents and even death. To minimize the risk of face bursting, face perpendicular preconditioning is conducted on an everyday to address this hazard. Figure 31 shows typical damage associated with a face burst.

Figure 30: Damage caused by a face burst

- Leads and lags

Excessive lead/lags of more than 10 m between adjacent panels are a common source of seismicity on Kusasalethu Mine. The strata control problems associated with incorrect lead/lags together with the occurrence of larger seismicity can result in extensive damage to the face and gully closest to this configuration.

3.5. SEISMIC DATA ANALYSES

The new Multi-raise mining method was implemented from raise line 35 between 98 and 102 levels at the end of 2006. Figure 32 shows the western section of the mine where the Multi-raise mining method was implemented together with all seismic events with M_L> = 2.0 since 2000 until March 2009 with the Mmax = 3.1. Only 2 seismic events with $M_L \geq 3.0$ have been recorded in the area, the last of these occurred on 31 July 2002.

Figure 33 shows the larger magnitude events with $M_L \geq 2.0$ that have occurred in the area from 2000 until 2009. The migration of the seismic activity in a southern direction coincides with the general trend in mining. The colours representing the seismic activity in this plot are based on annual intervals as portrayed in the legend.

The data at Kusasalethu Mine has been subject to the following external influences over the period of interest. These have had the undesired effect of introducing artificial trends to the data making interpretation of the recorded seismicity somewhat difficult. It is therefore important to keep these in mind during any analysis of the data set:

- The Institute for Mine Seismology (IMS) only have the relevant seismograms for events since 2005. This has resulted in difficulties when trying to re-calculate source parameters on the older seismic data with recent software upgrades.

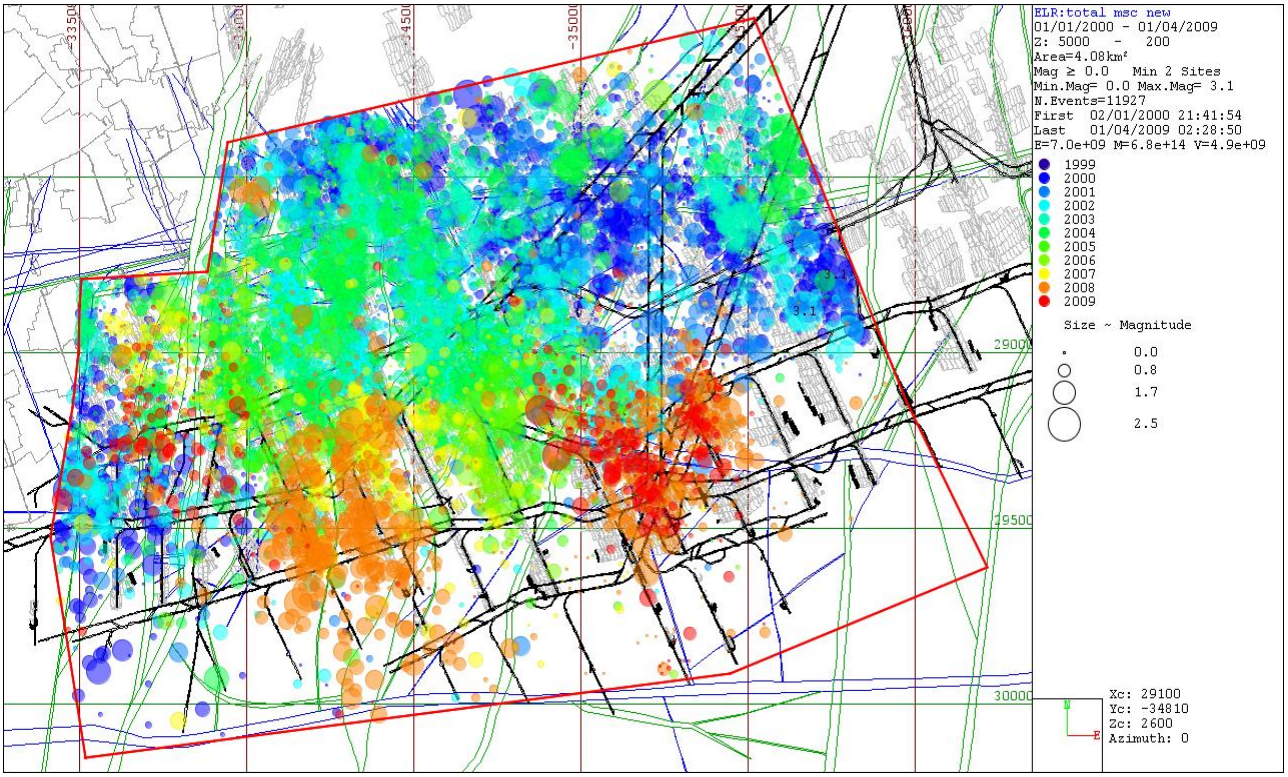

Figure 31: Location of all seismic events recorded by seismic system since 2000 with $M_L \geq 0.0$

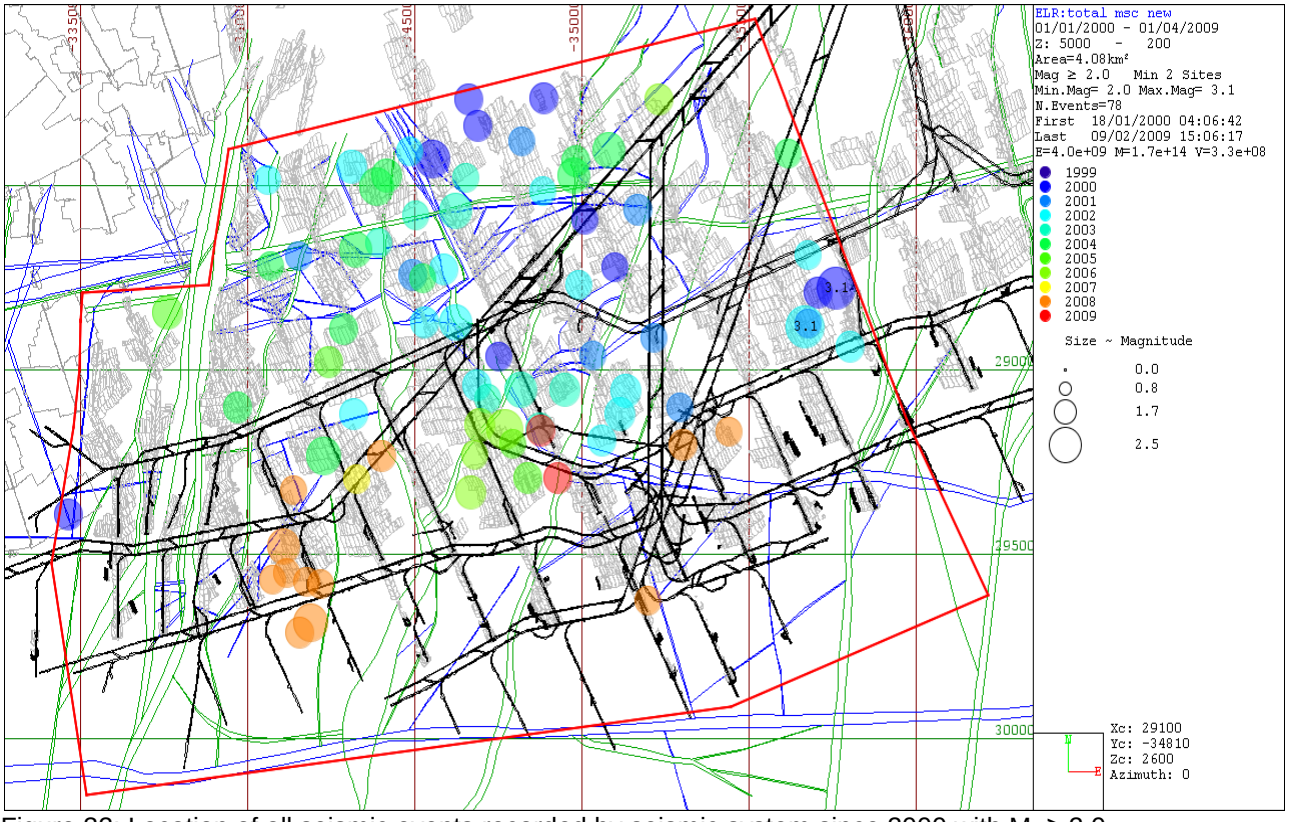

Figure 32: Location of all seismic events recorded by seismic system since 2000 with $M_L \geq 2.0$

- There also has been a change in the consultants responsible for the processing of seismic events over the time period involving this analysis. The history of the maintenance and administration of the seismic network involves three different seismological consulting companies. These changes may have influenced the quantity of accepted/rejected events as well as the precision and accuracy of the resulting source parameters.
- There have been several generations of upgrades to the seismological processing software since 2000, both with their own imprints on the natural data trends.
- The seismic system also underwent significant hardware and software upgrades to the latest geophysical seismometer (GS) models in 2009, a factor that seems to have had an effect on the overall sensitivity of the system response.

The time series depicting the occurrence of seismic activity with $M_L \geq 0.0$ for the period 2000 to March 2009 is shown in Figure 34. The reason for selecting the cut-off date as March 2009 is explained in Section 3.6. The distribution is based on yearly intervals and the following important features emerge from this representation of the seismic activity:

- There has been a general decrease in seismicity since 2005 with a peak in 2008 which is closely connected to the production as can be seen in Figure 35 which follows a similar trend.
- The decrease in activity for 2009 is due to the fact that the data set represents only the first three months of 2009.

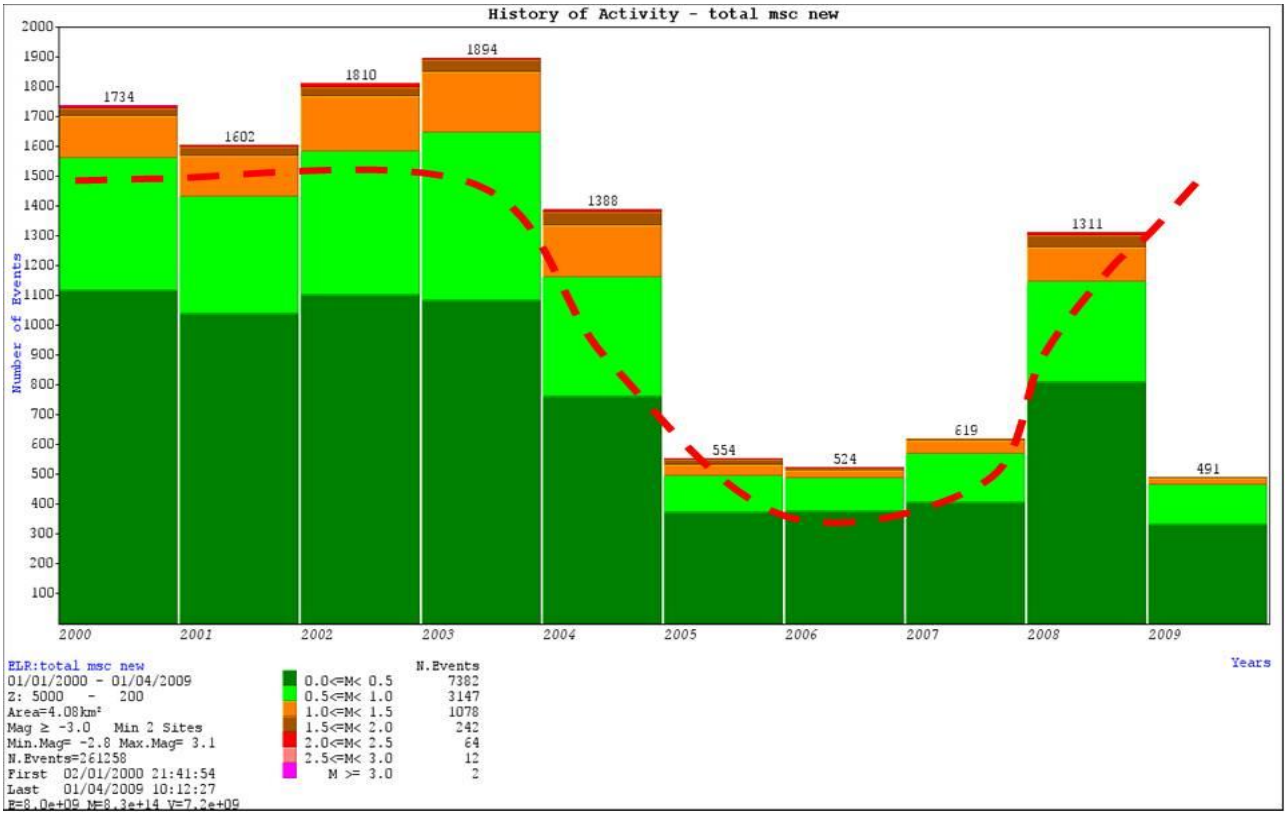

Figure 33: Activity per year since 2000 for all seismic events with $M_L \geq 0.0$ (up to March 2009)

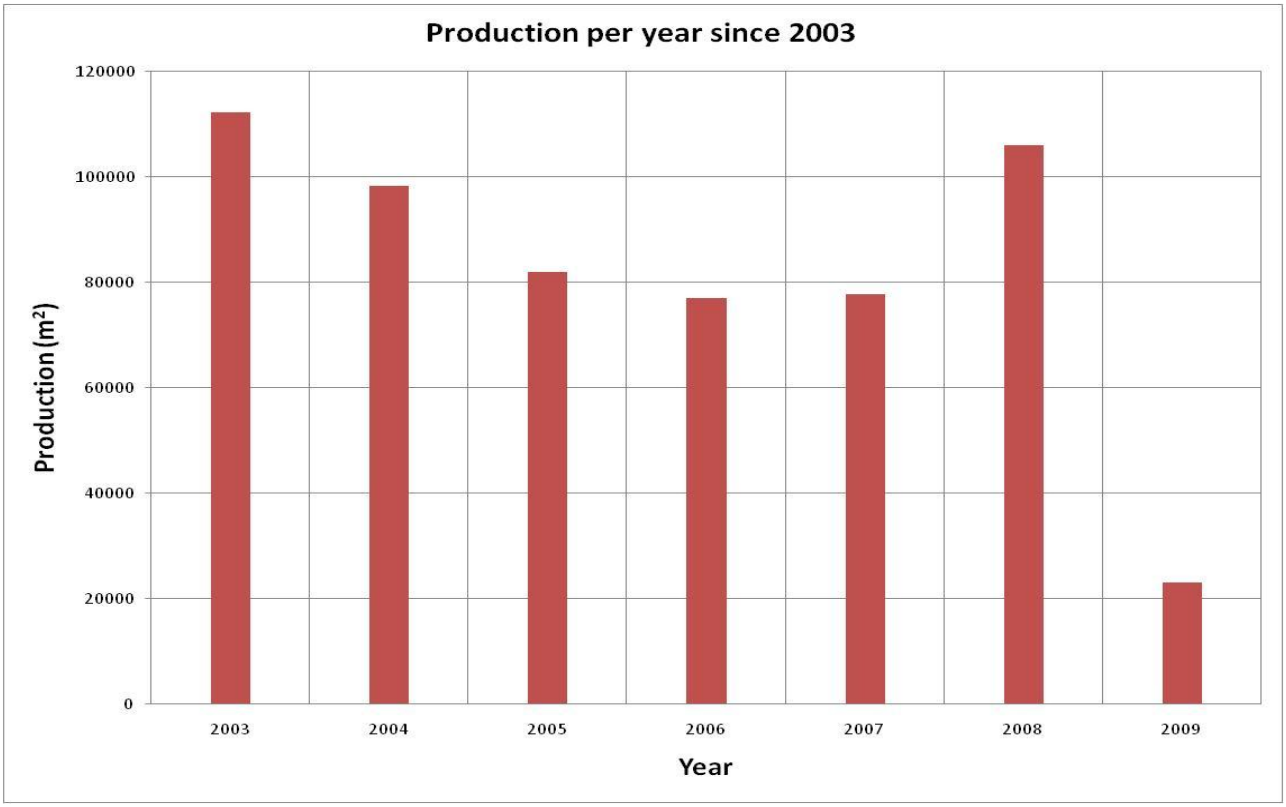

Figure 34: Production per year from 2003 to 2009

3.6. PRODUCTION DATA

3.6.1. Introduction

The relationship between mining seismicity and production (volume extraction) is an important one and has been reported by authors such as Van Der Heever (1984). Although the link has probably not been investigated as much as the seismicity itself, recent work by Mendecki (2005), has linked the volume of ground extracted to hazard estimates of seismicity. This study will attempt to investigate the strength of this link using the statistical principles of cross correlation. The changes to the Sequential Grid layout were introduced during 2007. The major change to the mine design was that multiple raise lines could be mined simultaneously. The layout of the dip stability pillars and the principle of mining towards the solid first remained in place for the new mine design.

3.6.2. Previous comparison

In the past two comparisons were conducted between the Sequential Grid mine design and the Longwall mining using alternative methods. One of the studies was conducted as part of a SIMRAC project in 1997 (SIMRAC GAP 303, 1997) and the other one was conducted by F Essrich (Essrich, 1996) in 1996. Table 3 shows the results obtained from the two different comparisons and from both assessments it is evident that the seismic hazard associated with the Sequential Grid method is less than the hazard associated with the longwall mining method.

Table 3: Comparison of seismicity generated by the Sequential Grid (SG) and Longwall mining (after Essrich, 1996 and SIMRAC, 1997).

	SIMRAC, GAP 303		F Essrich	
Parameter	SG	Longwall	SG	Longwall
Total mined (centares)	318357	197402	12500	11800
Average m^2 / event with $M_L \geq 2.0$ (total number of events)	22740 (14)	8973 (22)	12500 (1)	2360 (5)
Magnitude of largest event recorded	3.0	2.9	-	-

Table 4 shows the results obtained for the recent comparison of the Sequential Grid and Multi-raise method conducted by the author. The number of seismic events is normalized to the area mined for each mine design. It can be seen that for seismic events with $M_L \geq 2.0$, approximately 11% more mining can be done using the Multi-raise mine design than is the case for the original design. This means that the seismic hazard due to potentially damaging seismic events appears to be slightly lower in the Multi-raise layout than in the original design.

Table 4: Comparison of seismicity generated by the Sequential Grid and Multi-raise mine design.

Parameter	SG	MR
Average mined (centares)	427079	206972
Average m^2 / event with $M_L \geq 2.0$ (total number of events)	12202	13798
Magnitude of largest event recorded	3.1	2.6

3.6.3. Data analyses

Production data (Figure 36) was obtained for a selected dating back to July 2002. Prior to this, the production information is unfortunately not available. The production and associated seismicity for the 7 year period were analysed to determine if any changes in the seismic attributes could be attributed to the subsequent changes in mine design (change from Sequential Grid to Multi-raise sequence).

The production figures (m^2) since July 2002 were firstly compared with the number of seismic events recorded with $M_L \geq 0.0$ i.e. activity rate. The two series are compared in Figure 36 and the following points emerge:

- A good downward correlation is visible since the end of 2003 until July 2006,
- Since July 2006 until March 2009 the production rate is much higher than the associated seismic response, but the two series appear to follow the same trend.

- Visible examination of the two series reveals a good positive correlation up to March 2009. Beyond that the series appears to shows a strong negative correlation. Reasons for this negative correlation are not clear and this is considered beyond the scope of this study, this dissertation will therefore only focus on examining the seismic data prior to March 2009.

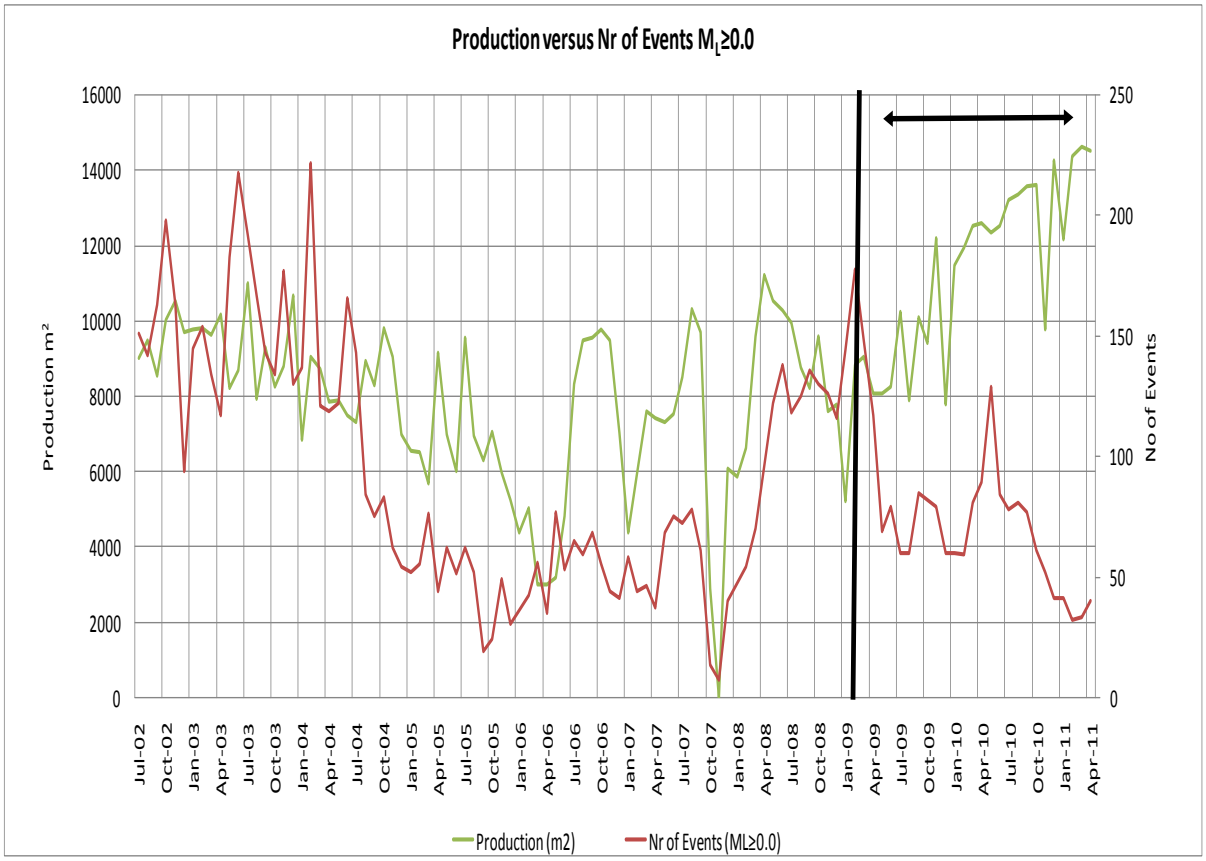

Figure 35: Production (m^2) compared with the number of seismic events ($M_L \geq 0.0$) per month since July 2002

A graphic representation of the dataset, indicating the section of data to be analyzed, is shown in Figure 37.

In this dissertation the attempt has been made to investigate the relationship between selected seismic and production variables in more detail. The most familiar measure of linear dependence between two quantities (variables) is the correlation coefficient (Pearson's correlation coefficient), Davis (2002). A correlation is a number between -1 and +1 that measures the degree of association between two variables. The

correlation coefficient is obtained by dividing the covariance of the two variables by the product of their standard deviations.

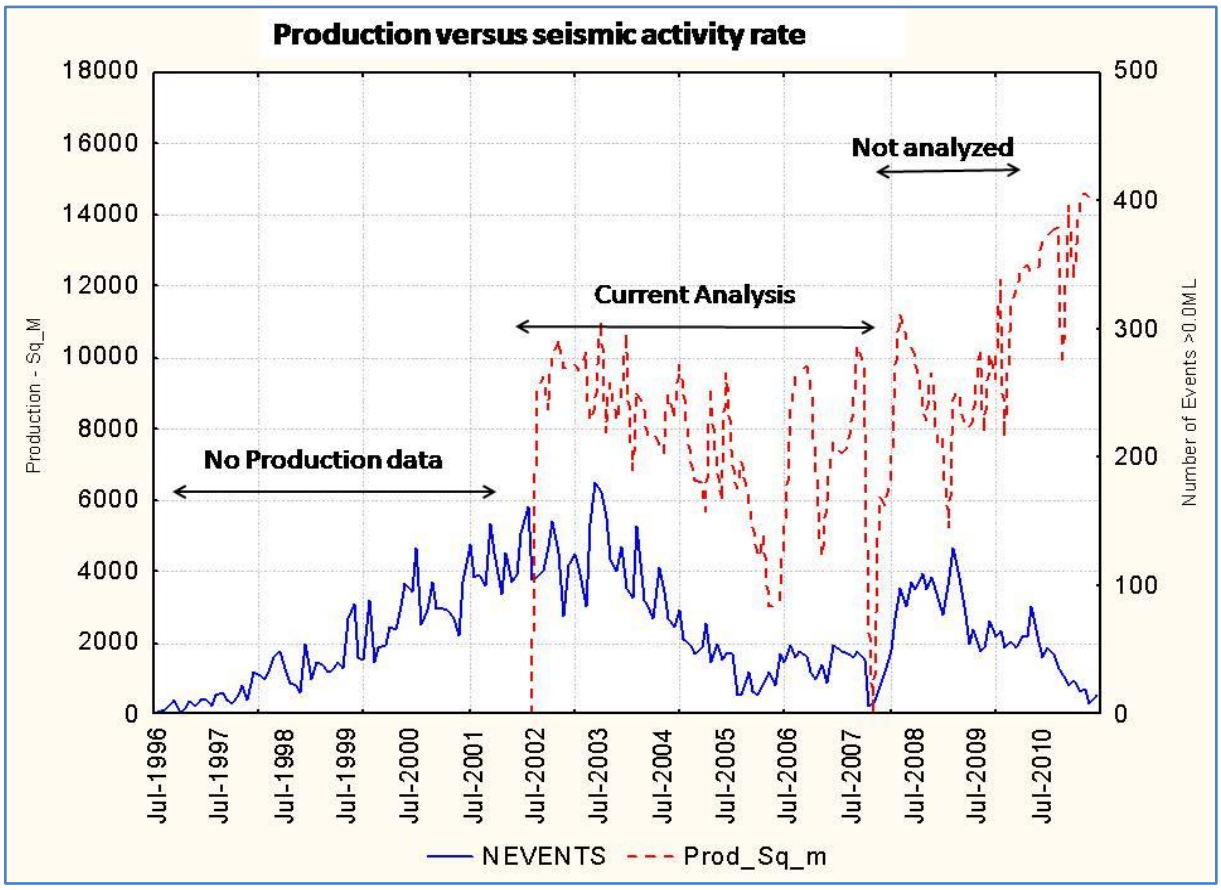

Figure 36: Graph shows the section of the data that will be analyzed.

The population correlation coefficient $\rho_{X,Y}$ between two random variables X and Y with expected values μ_X and μ_Y and standard deviations σ_X and σ_Y is defined as:

$$\rho_{x,y} = \mathbf{corr}(x, y) = \frac{\mathbf{cov}(x.y)}{\sigma_x \sigma_y} = \frac{\mathbf{E}[(x-\mu_x)(y-\mu_y)]}{\sigma_x \sigma_y} \qquad (2)$$

where E is the expected value operator, *cov* means covariance, and, *corr* a widely used alternative notation for Pearson's correlation. The Pearson correlation is defined only if both of the standard deviations are finite and both of them are nonzero.

All correlation coefficients range from -1.00 to +1.00. A correlation coefficient of -1.00 tells you that there is a perfect negative relationship between the two variables. This

means that as values on one variable increase there is a perfectly predictable decrease in values on the other variable. In other words, as one variable goes up, the other goes in the opposite direction (it goes down).

A correlation coefficient of +1.00 tells you that there is a perfect positive relationship between the two variables. This means that as values on one variable increase there is a perfectly predictable increase in values on the other variable. In other words, as one variable goes up so does the other. A correlation coefficient of 0.00 tells you that there is a zero correlation, or no relationship, between the two variables.

In the case of mining related data, the variation in mining processes over time suggest the use of a time series to evaluate the presence of a linear dependence between variables using a cross correlation function. If we have a series of *n* measurements of *X* and *Y* through time written as x_i and y_i where i = 1, 2, ..., n, then the sample correlation coefficient can be used to calculate the correlation coefficient at any position in the series using paired samples from the two respective series.

Correlation coefficients can also be calculated at various lags between the series by effectively sliding one series past the other and using n^* as the number of overlapping positions between the respective series estimate the population Pearson correlation r between X and Y. The sample correlation coefficient is written

$$r_{xy} = \frac{\sum_{i=1}^{n^*}(x_i-\bar{x})(y_i-\bar{y})}{(n^*-1)s_x s_y} = \frac{\sum_{i=1}^{n^*}(x_i-\bar{x})(y_i-\bar{y})}{\sqrt{\sum_{i=1}^{n^*}(x_i-\bar{x})^2 \sum_{i=1}^{n^*}(y_i-\bar{y})^2}} \qquad (3)$$

where x and y are the sample means of *X* and *Y*, and s_x and s_y are the sample standard deviations of *X* and *Y*.
This can also be written as:

$$r_{xy} = \frac{\sum x_i y_i - n^* \bar{x}\bar{y}}{(n^*-1)s_x s_y} = \frac{n^* \sum x_i y_i - \sum x_i y_i}{\sqrt{n^* \sum x_i^2 - (\sum x_i)^2}\sqrt{n^* \sum y_i^2 - (\sum y_i)^2}} \qquad (4)$$

The standard error of the cross correlation coefficient can be estimated by the relationship SE =1/(n*-k) where k represents the number of lags and n* represents the number of overlapping points between the two series. Correlations are calculated at various lags (positive and negative) and the resulting values are plotted by means of a correllolgram.

Figure 38 shows the Pearson's correlation between the number of events, $M_L \geq 0.0$ per month and the monthly production (in square meters) for the period July 2002 up to March 2009. Both series were smoothed using a 5 point moving average in order to make comparisons in terms of the trend components.

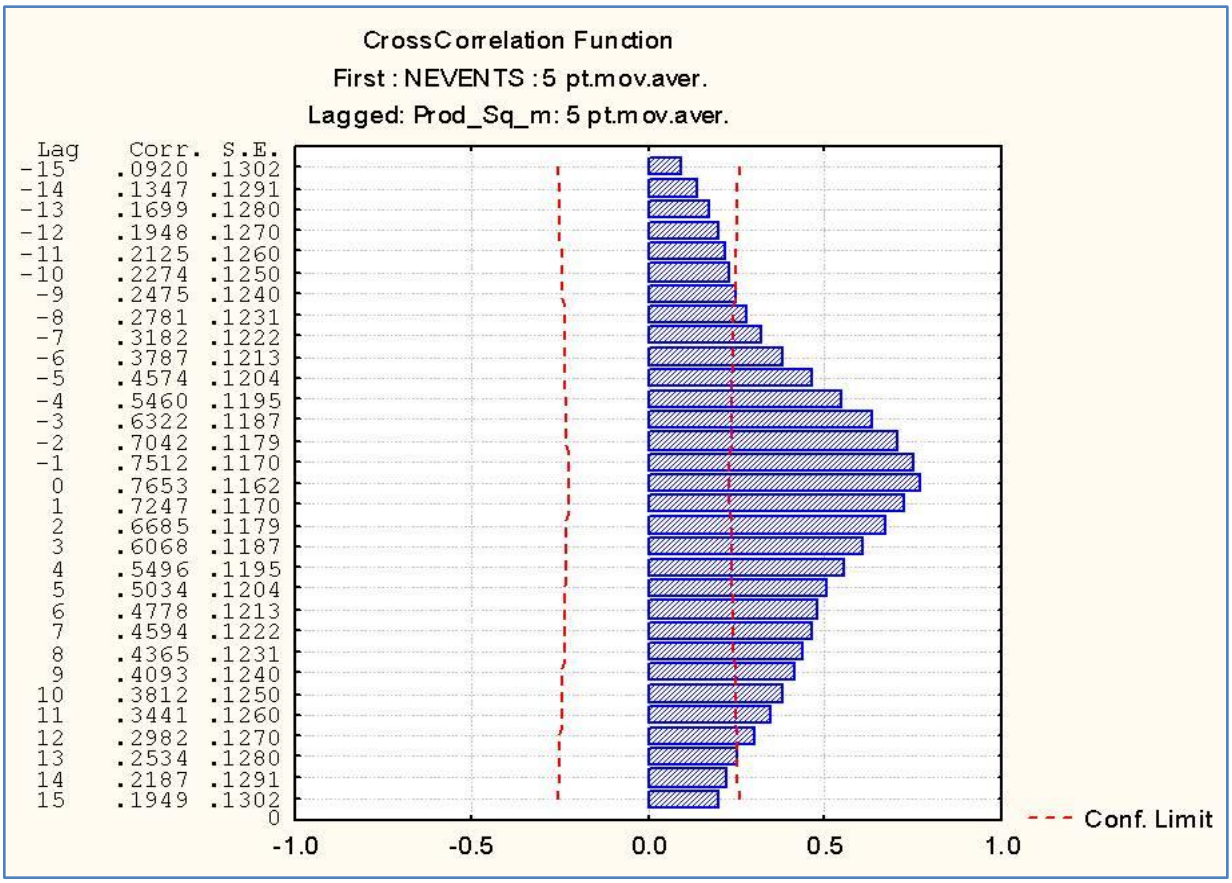

Figure 37: Correllolgram showing the cross correlation between production and number of seismic events with $M_L \geq 0.0$

It can be noted from this graph that at lag 0 i.e. alignment of original axes, the correlation coefficient, r, is 0.7653, suggesting a strong positive correlation without any lag between the two data sets.

The next two figures (39 and 40) show the relationship – in terms of trend - between production rate (m^2) and seismic moment (10^{12} NM) as well as the correlation coefficient for the two parameters as described above. The seismic moment used in this section of the dissertation is calculated as follows according to Aki and Richards, 1980:

The low frequency level Ω_0 of the far-field displacement spectrum either of P or S waves is directly related to the seismic moment,

$$Mo = \frac{4\pi p_o c_0^3 R\Omega_0}{F_c R_c S_c} \qquad (5)$$

Where,

P_0 is the density of the source material,

C_0 is either P-wave velocity or the S-wave velocity at the source,

R is the distance between the source and the receiver,

F_c accounts for the radiation of either P or S waves,

R_c accounts for the free-surface amplification of either P- and S-wave amplitudes, and

S_c is the site correction for either P or S waves.

The following can be noted from Figure 39 comparing production with the amount of seismic moment released:

- For the period 2002 until beginning of 2006 the monthly production and seismic moment depicts a decreasing trend.

- For a 6 month period early in 2006 the two parameters show little correlation with each other but the two parameters again start to reveal a good positive correlation from July 2006 onwards.

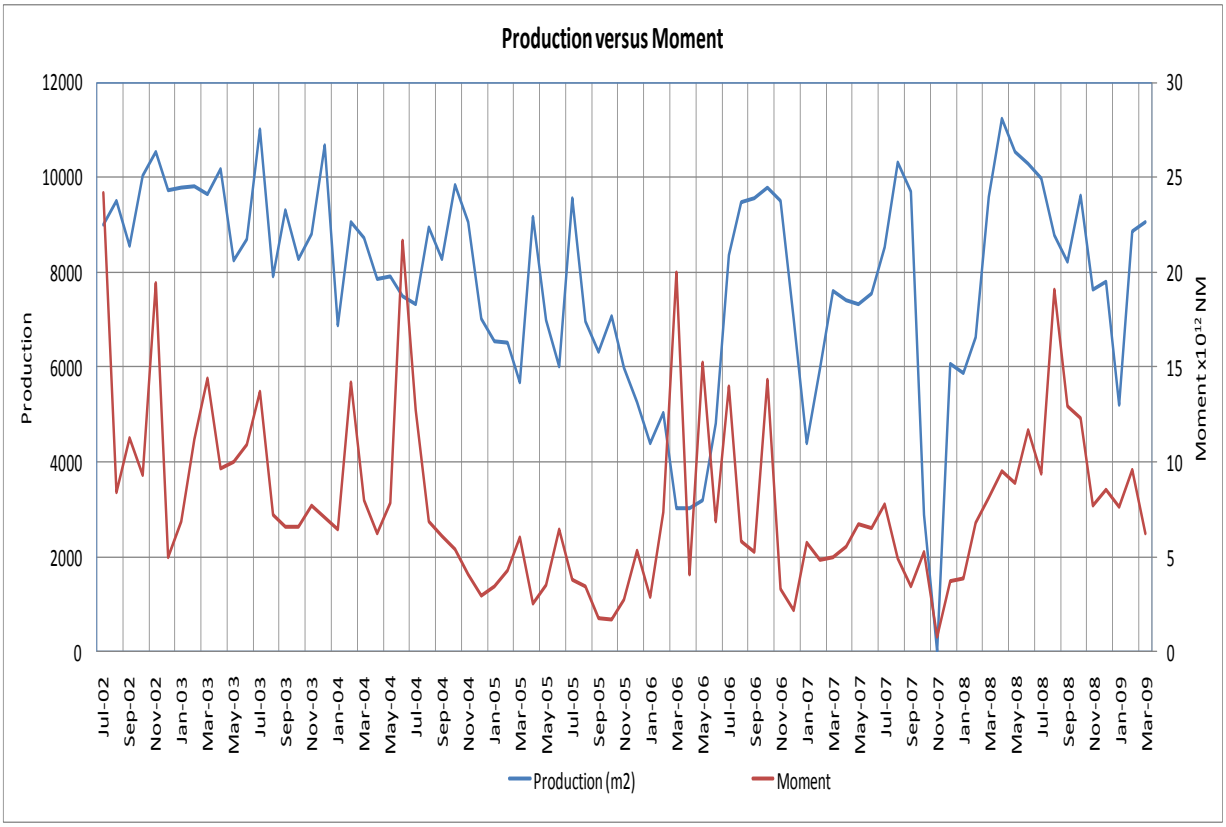

Figure 38: Production (m^2) compared with moment being released ($x10^{12}$ NM) for all seismic events ($M_L \geq 0.0$) per month since July 2002

Figure 40 shows the cross correlation between the seismic moment and production using a 3 point moving average for both series. It can be noted from the graph that at lag +2 the cross correlation is 0.4555, suggesting a correlation between the two datasets with a lag of two month in the moment. The cross correlation is relatively low suggesting that there is not a strong link between the amount of deformation and production. One of the explanations for this poor correlation can be due to the limited number of larger magnitude seismic events. The magnitude distribution for both data sets shows a sparse distribution from $M_L = 1.8$ and above.

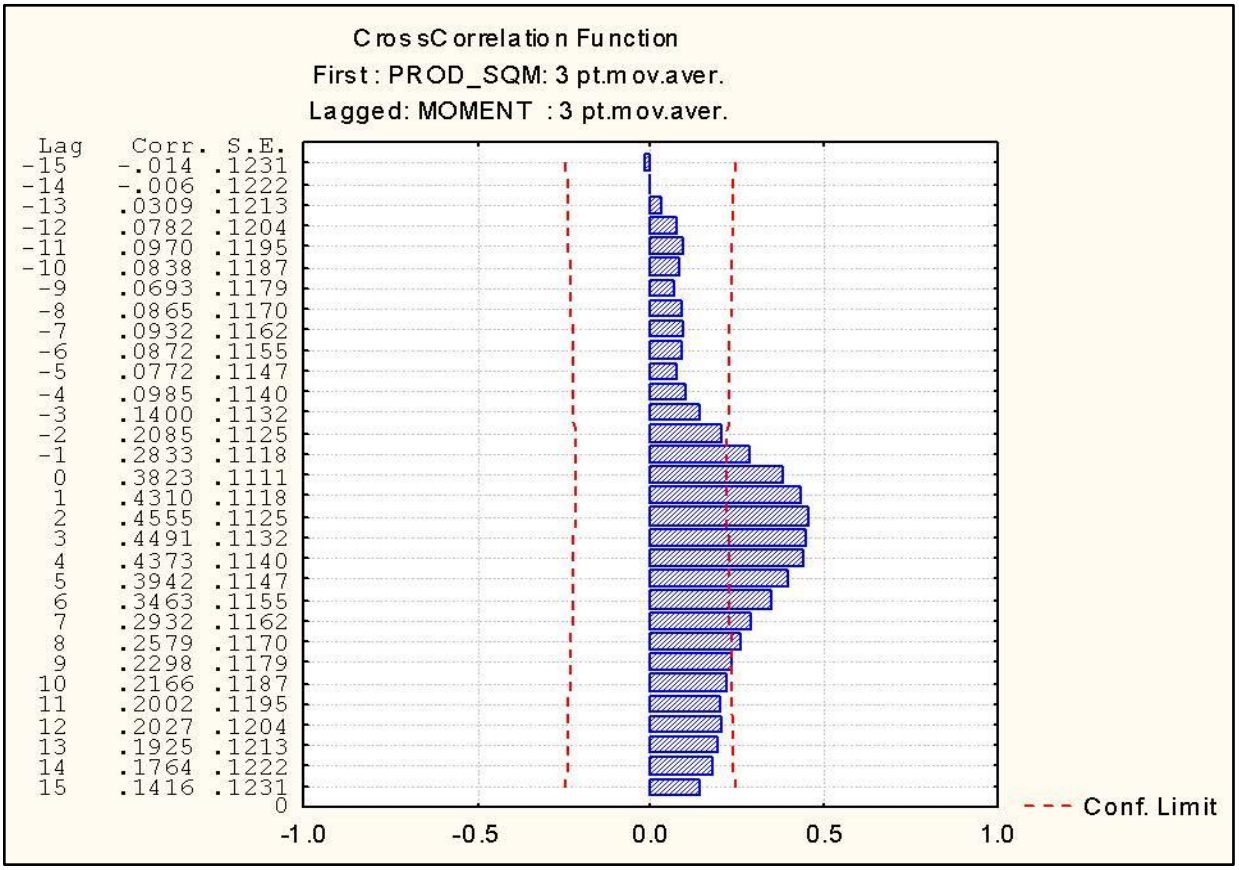

Figure 39: Pearson's correlation between production and seismic moment

Figure 41 shows the comparison between the production and the maximum magnitude that occurred per month for the same time period as selected above. The two sets of data show a good relationship for almost the whole time period.

An analysis was attempted using correlations between the two time periods for the respective mining methods on Kusasalethu Mine. This was difficult to do on account of the variable time periods for the Sequential Grid and Multi-raise mining methods. Correlations based on the periods/frequency and long term trends require equal time periods for the generation of reliable results. In addition long term trends require time periods greater than the frequency of the movements in the data more especially since moving averages are used to smooth the data for any possible trends. It was difficult to satisfy these conditions for the current analyses.

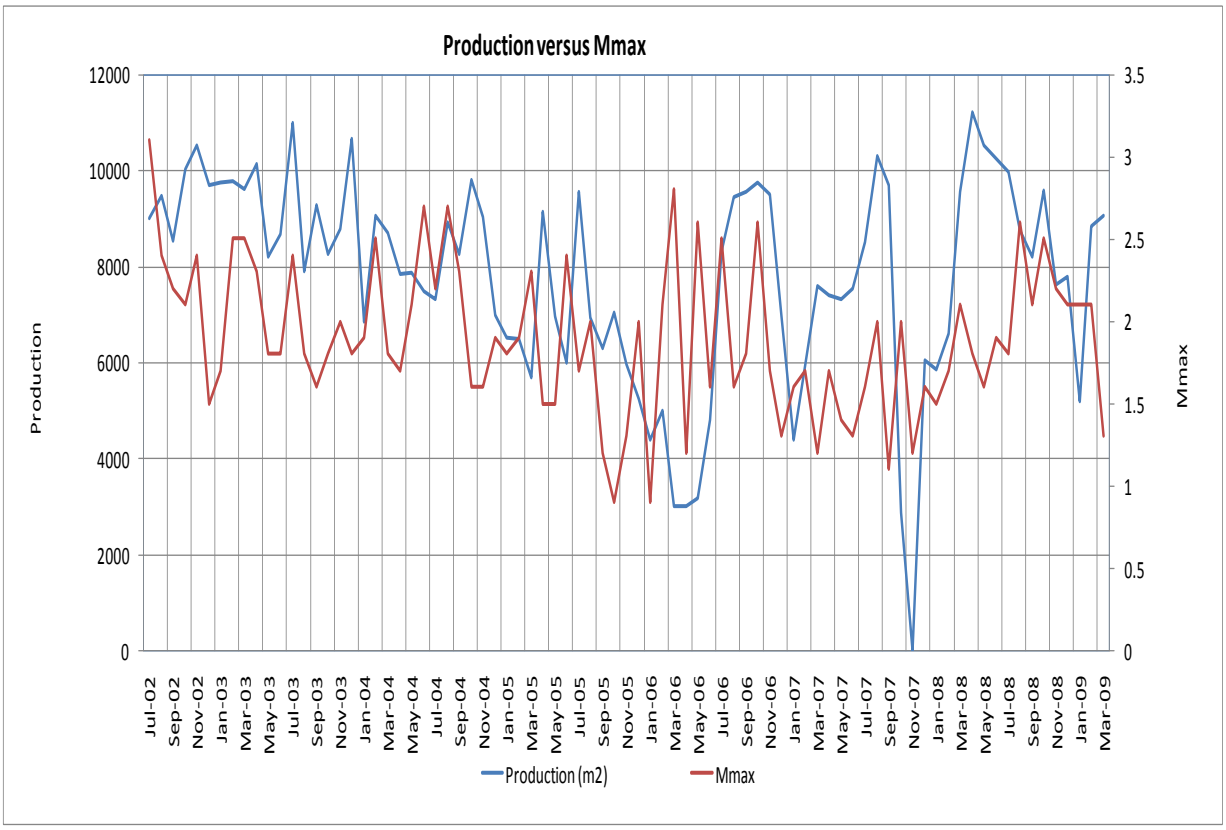

Figure 40: Production (m^2) compared with Mmax (maximum magnitude recorded) per month since July 2002

3.7. SEISMIC HAZARD ESTIMATIONS

The probabilistic assessment of the seismic hazard involves specifying the likelihood, maximum magnitude, location, and nature of seismic events that might have damaging effects at underground working areas and trying to estimate the peak acceleration of the ground shaking close to underground infrastructure. Seismic hazard is defined as the probability of occurrence of a seismic event or ground motion exceeding a specified level, within a given period of time according to Jager (1999).The occurrence of mine tremors is not strictly a random process but a statistical approach to the analysis of seismic events and provides a reasonable basis for seismic hazard assessments to assist in estimating expected losses or assessing different mine designs.

Observations indicate that seismic events induced by mining activities show some of the same characteristics as those noticeable in crustal seismology. One of the relationships

that is readily applied between both fields of seismology is the frequency-magnitude relationship that was introduced by Gutenberg and Richter in 1944,

$$\log n = a - bm \qquad (6)$$

where *n* is the number of seismic events with magnitude *m,* and *a* and b are intercept and slope parameters for the logarithmic relationship.

Equation 6 can be interpreted in two ways. Firstly as a cumulative relationship where “n” represents the number of events with magnitude equal or larger than “m” in a given time interval. Secondly as a density law where “n” represents the number of events in a certain small magnitude range around the value of m. The parameter ‘a’ is the intercept parameter and a measure of the level of seismicity, whereas the parameter b, which is the slope indicator and typically close to 1 for natural earthquakes, describes the relative number and distribution of event magnitudes within a given time interval (Kijko, 1996).

Numerous papers have been documented on the above frequency-magnitude relationship and they all show that the relationship holds for virtually all magnitude ranges. Criticism of equation 6 is centred on its unsatisfactory behaviour for the larger magnitude seismic events where it overestimates the likelihood of occurrence of these events. Lomnitz showed in 1979 that this tendency was build into the formula while Taylor, 1990, attributed the non-linear effect of the frequency-magnitude relationship to either observational or source effects.

Various research projects dedicated to equation 6 investigated the physical significance of the relation and its parameters. Rock deformation experiments done by Scholz (1968) showed that the b-value variations are directly related to the stress conditions where b decreased as stress increased. He believed that the state of stress plays a more important role than the heterogeneity of the rock. Similar results were obtained by Gibowicz in 1973. Therefore the parameter b can be considered as a parameter controlling the capability of the medium in releasing the accumulated energy.

Determining the maximum magnitude capable of occurring in any active mining area can be achieved by either of two methods namely a deterministic or a probabilistic approach. The visualization program, *Korhaan*, used in this dissertation to determine the seismic hazard and Mmax, uses the probabilistic method, explained in detail below.

The oldest approach to find Mmax through the use of statistical procedures which was probably applied for the first time by Nordquist (1945) is the Gumbel Type-I distribution. Epstein and Lomnitz (1966) later proved that the Gumbel Type-I distribution can be derived directly from the assumption that seismic events follow the Poisson distribution and the Gutenberg-Richter frequency-magnitude relationship.

A more comprehensive probabilistic approach for estimating the maximum magnitude, Mmax, was suggested by Kijko and Sellevoll (1989) and was further refined by Kijko and Graham (1998) to consider the uncertainties in the input magnitude data. To describe the seismic event magnitude, they used a truncated exponential probability distribution function with lower cut-off magnitude Mmin, and an upper bound magnitude Mmax along with a statistical parameter β = b ln 10, where b defines the Gutenberg - Richter's relationship. Thus for seismic hazard the truncated Gutenberg-Richter relation is usually applied and the cumulative distribution function is:

$$F(m) = \frac{1-\exp[-\beta(m-M_{min})]}{1-\exp[-\beta(M_{max}-M_{\min})]} \qquad (7)$$

where M_{min} is the threshold of completeness, i.e. minimum magnitude for which all seismic events are recorded, M_{max} is the maximum possible magnitude that can occur and **β** is the parameter of distribution, β= b ln(10).

This was then used to define the probability distribution of the Maximum magnitude for an observation period of T years. By constraining the observed largest magnitude to be the expected value of the largest observed magnitude, Kijko and Graham (1998) has obtained an estimator for M_{max}, which requires knowledge of the mean seismic activity rate λ and the parameter b.

$$N(m,T) = \lambda T[1 - F(m)] \qquad (8)$$

To estimate M_{max}, Kijko and Graham (1998) developed a joint maximum likelihood function using mixed data files, consisting of an incomplete part of the seismic catalogue containing only large historical events for a very long period and the complete part of the catalogue for a short recent period. The incomplete part is described by extreme-value distribution based on the double truncated magnitude distribution defined in terms of parameter, β, and the complete part by the Poisson probability density function with a mean occurrence rate, λ. By including β and λ, an iterative procedure is used to get the maximum likelihood estimate of M_{max} along with parameters λ and β.

To get a reliable estimation of the seismic hazard it is essential to consider all seismic activity with their spatial distribution around the site of interest. The probabilistic seismic hazard estimation method provides a way to consider the effect of the total expected seismicity over a specific period. This method provides information on the mean return periods of events of certain magnitude seismic events, the probability of them occurring within a given time period and the expected maximum magnitude that can occur during the life of mining (Gibowicz & Kijko, 1994 and Kijko, 1996).

Seismic hazard analysis requires an assessment of the future seismic potential. It is, therefore, necessary to estimate the maximum event magnitude and recurrence time period that might be generated by a particular active fault or particular mining configuration/ mining method.

One of the basic elements in assessing seismic hazards is to recognize seismic sources that could affect the particular location at which the hazard is being evaluated. These sources are often called seismogenic sources. Defining and understanding seismogenic sources is often the major part of a seismic hazard analysis and requires knowledge of the regional and local geology as well as past seismicity. Earthquake hazard parameters such as, maximum expected magnitude, M_{max}, activity rate, and b value of the Gutenberg-Richter relation have been evaluated for each seismogenic zone.

In the application of statistical estimations of seismic hazard within Harmony Gold mines, several assessments have been carried out over a period of time. The following limitations of the methodology have been identified (Stankiewicz, 1998a and b, Stankiewicz, 2000, Ebrahim-Trollope, 2001):

- Mining has a dynamic nature and changes constantly in space and time therefore this method cannot be extrapolated over very long periods of time without analyzing the mining direction and volume which are only two of the variables that can cause differences in the hazard calculated for a particular mining area.
- The method must be used comparatively between similar geotechnical areas where at least one of the areas has previously been mined out. In other words you can “predict” what might happen for a particular mining area when a similar area has been mined out in the past. Method of mining, mining rate and geology plays an important factor when comparing and selecting mining areas for analyses.
- The method is applicable to a single source mechanism and therefore all source mechanism as discussed beforehand needs to be identified for a particular geotechnical area. There is a distinctive bi-modal distribution for seismic events with different source mechanisms. It is therefore important to understand the different sources of seismicity in a region before interpreting the result obtained for the hazard estimation. The choice and size of the selected area must be geologically similar to the mining area of interest.
- The method requires a consistent and reliable database. For example no changes to software programs can be made that might result in source parameters being calculated differently. A loss of periods of seismic data will also detrimental as this will influence the results obtained by the seismic analyses.
- The selection of the mining area and the time period for the seismic hazard estimation can be problematic and therefore care needs to be taken when the selection of the area is done to ensure that an acceptable log-linear distribution is obtained that will not result in the over- or underestimation of the seismic hazard. The lack of an acceptable log-linear distribution often highlights the possible errors in the choice of mining area or time period.

- The hazard estimation results obtained from the analysis are averaged over the time period of the analysis and more hazardous time periods within the period selected cannot be identified.

Despite the lack of a complete database for the smaller areas and consequently a less than acceptable truncated Gutenberg-Richter distribution, the hazard results to date suggest a reasonably accurate estimate of seismic hazard. It is important to remember the incomplete seismic dataset when conclusions are made from the hazard estimation results.

3.7.1. Seismic hazard analyses for mining layouts

To identify and determine the seismic hazard associated with a specific mine design, the seismicity of the area in question needs to be determined prior to the change in mining method as well as a significant time period after the method was changed. The two analyses then need to be compared to determine if the changed mine design resulted in any significant changes to the response in seismicity. The area as shown in Figure 43 was used to select the two areas where the two mine designs were implemented and the two areas selected are depicted.

3.7.1.1. Seismic hazard estimation for Sequential Grid mine design

The probabilistic seismic hazard according to the program, *Korhaan*, was determined for the top of the west section of Kusasalethu Mine as depicted in Figure 42. Figure 43 shows all seismic events with $M_L \geq 2.0$ for time period October 2004 until December 2006 with the largest event being a $M_L = 3.1$. A relative good Gutenberg - Richter relationship is obtained from the seismic data set available. The data set is a bit sparse from magnitude larger than 1.8 and a peak is visible for magnitudes between 2.0 and 2.2.

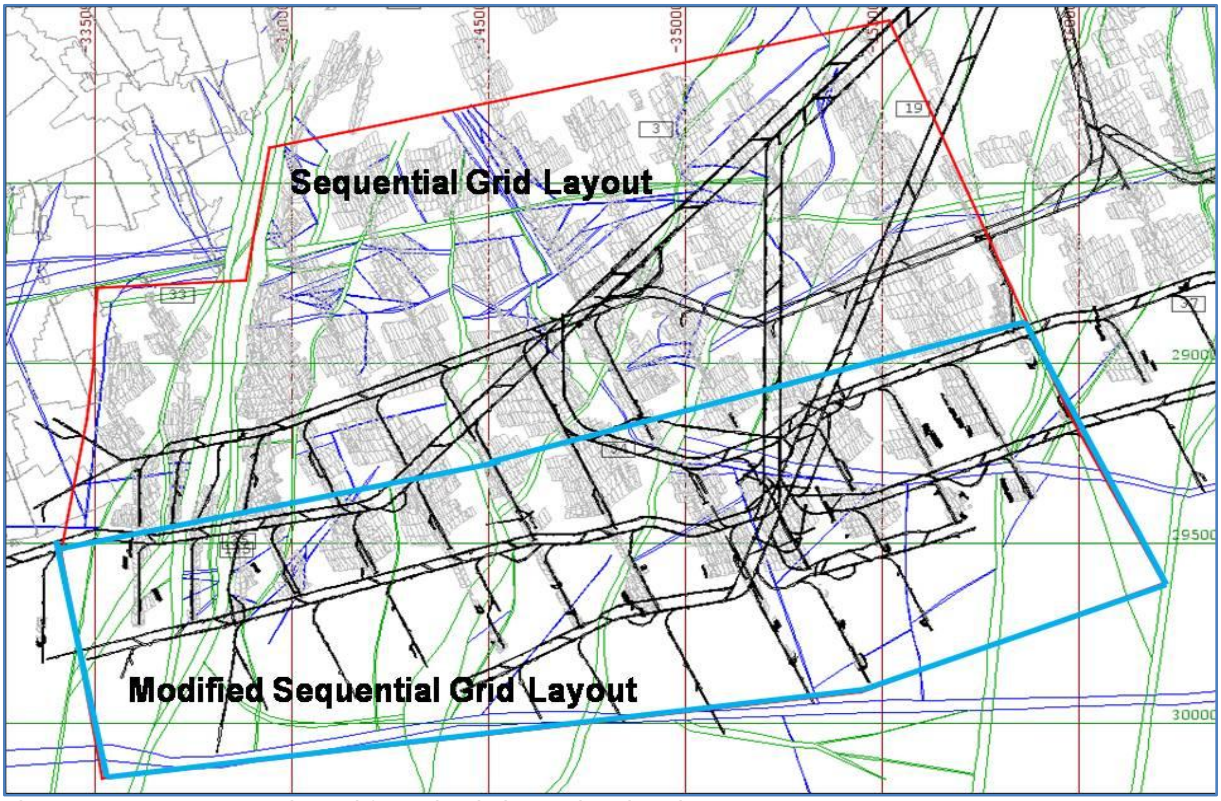

Figure 41: Two areas selected for seismic hazard estimation

The results obtained from the seismic assessment for the original Sequential Grid design are as follows and more detail can be obtained from Figures 44 and 45:

- Largest magnitude seismic event expected according to the seismic hazard estimation is $M_L = 2.9$
- The hazard magnitude for the distribution is 3.27
- The Mmax to occur within one year is 2.5
- The Mmax to occur within two years is 2.7
- The Mmax to occur within five years is 2.8
- Four events with $M_L \geq 1.0$ can be expected every month.
- The return period of a $M_L = 2.5$ is approximately eleven months.

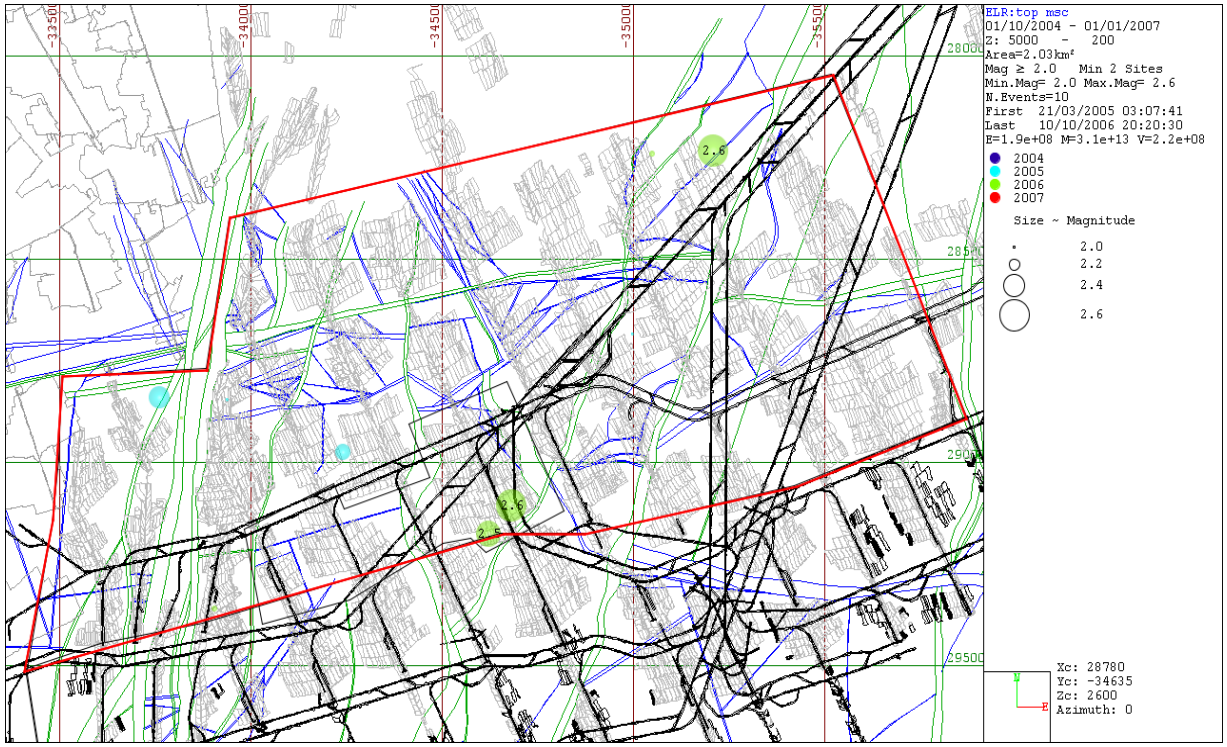

Figure 42: Location of all seismic events recorded by seismic system between October 2004 until December 2006 with $M_L \geq 2.0$ for the top of the west mine

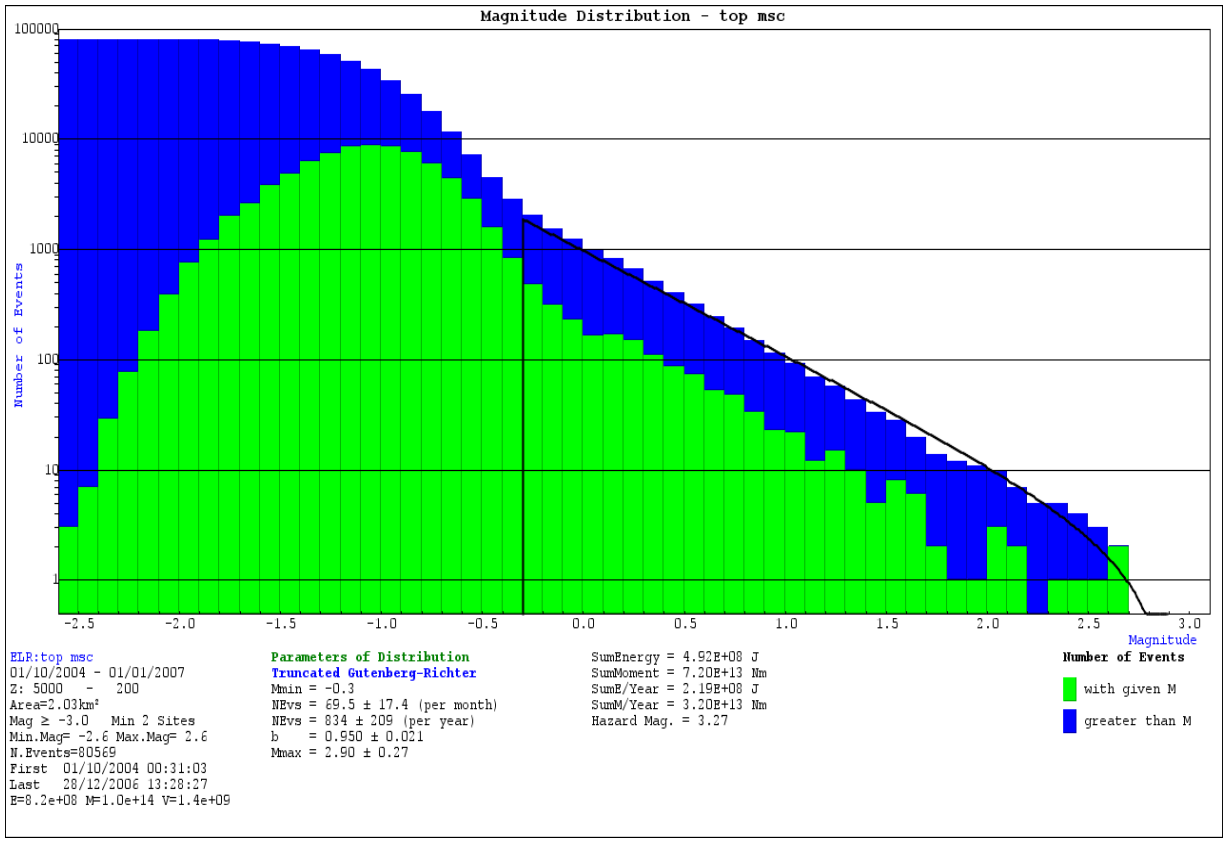

Figure 43: Gutenberg - Richter relationship – Sequential Grid mine design

Seismic Hazard - top msc

Summary of Data

ELR:top msc
01/10/2004 - 01/01/2007
Z: 5000 - 200
Area=2.03km²
Mag ≥ -3.0 Min 2 Sites
Min.Mag= -2.6 Max.Mag= 2.6
N.Events=80569
First 01/10/2004 00:31:03
Last 28/12/2006 13:28:27
E=8.2e+08 M=1.0e+14 V=1.4e+09

Parameters of Distribution

Truncated Gutenberg-Richter
Mmin = -0.3
NEvs = 69.5 ± 17.4 (per month)
NEvs = 834 ± 209 (per year)
b = 0.950 ± 0.021
Mmax = 2.90 ± 0.27

Mean Return Periods

Mag.	Number of Events /Month	/Year	Return Period months	years
0.0	36.00	432.0	0.028	0.00
0.5	12.01	144.1	0.083	0.01
1.0	3.98	47.7	0.251	0.02
1.5	1.29	15.5	0.775	0.06
2.0	0.39	4.7	2.565	0.21
2.5	0.09	1.1	11.304	0.94

Probabilities of Seismic Event

Mag.	1 month	3 months	6 months	1 year	2 years	5 years
0.0	100.0%	100.0%	100.0%	100.0%	100.0%	100.0%
0.5	100.0%	100.0%	100.0%	100.0%	100.0%	100.0%
1.0	98.1%	100.0%	100.0%	100.0%	100.0%	100.0%
1.5	72.5%	97.9%	100.0%	100.0%	100.0%	100.0%
2.0	32.3%	68.9%	90.4%	99.1%	100.0%	100.0%
2.5	8.5%	23.3%	41.2%	65.4%	88.0%	99.5%

Maximum Expected Magnitude

In 1 year M = 2.52
In 2 years M = 2.67
In 5 years M = 2.79

Seismic Events Distribution

Magn >	0.0	0.5	1.0	1.5	2.0	2.5
Theor.	972	324	107	35	11	2
Observed	1000	323	92	28	10	3

Hazard Magnitude

Hazard Mag. = 3.27
SumEnergy = 4.92E+08 J SumEnergy/Year = 2.19E+08 J
SumMoment = 7.20E+13 Nm SumMoment/Year = 3.20E+13 Nm

Figure 44: Seismic hazard estimation- Sequential Grid mine design

3.7.1.2. Seismic hazard estimation for Multi-raise mine design

The probabilistic seismic hazard according to the program, *Korhaan*, was determined for the bottom of the west section of Kusasalethu Mine as depicted in Figure 42. Figure 46 shows all seismic events with $M_L \geq 2.0$ for time period January 2007 until March 2009 with the largest event being a $M_L = 2.7$.

A relative good Gutenberg - Richter relationship is obtained from the seismic data set available. The data set has the same trend as for the original design for the larger magnitude events and it is a bit sparse from magnitude larger than 2.5 and a peak is visible for magnitudes between 2.0 and 2.5.

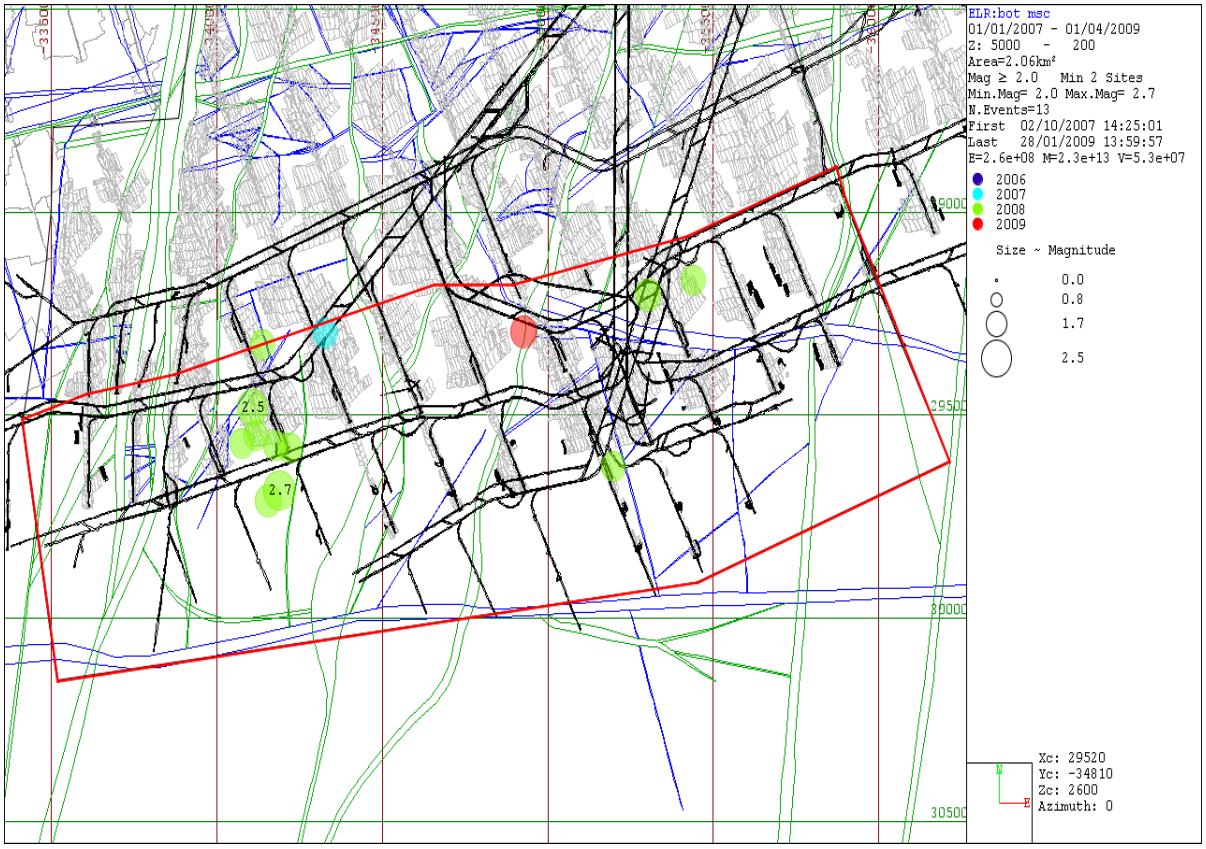

Figure 45: Location of all seismic events recorded by seismic system since 1996 with $M_L \geq 2.0$ for the bottom of the west mine

The results obtained from the seismic assessment for the change in design (Multi-raise) are as follows and more detail can be obtained from Figure 47 and 48:

- Largest magnitude seismic event expected according to the seismic hazard estimation, $M_L = 2.9$
- The hazard magnitude for the distribution is 3.38
- The Mmax within one year is 2.5.
- The Mmax within two years is 2.7
- The Mmax within five years is 2.8
- Six seismic events with $M_L \geq 1.0$ can be expected every month.
- The return period of a $M_L = 2.5$ is approximately eleven months.

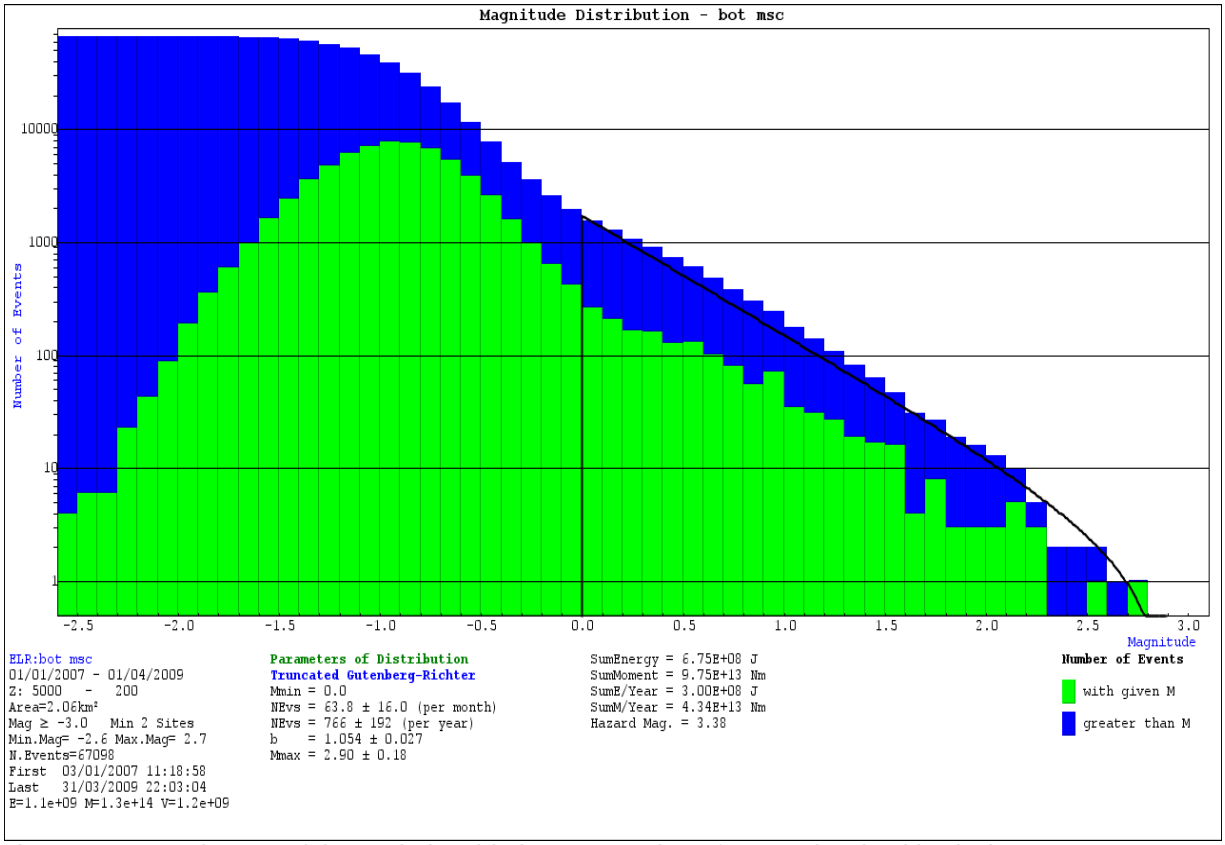

Figure 46: Gutenberg – Richter relationship bottom section of west mine (Multi-raise)

Seismic Hazard - bot msc

Summary of Data

ELR:bot msc
01/01/2007 - 01/04/2009
Z: 5000 - 200
Area=2.06km²
Mag ≥ -3.0 Min 2 Sites
Min.Mag= -2.6 Max.Mag= 2.7
N.Events=67098
First 03/01/2007 11:18:58
Last 31/03/2009 22:03:04
E=1.1e+09 M=1.3e+14 V=1.2e+09

Parameters of Distribution

Truncated Gutenberg-Richter
Mmin = 0.0
NEvs = 63.8 ± 16.0 (per month)
NEvs = 766 ± 192 (per year)
b = 1.054 ± 0.027
Mmax = 2.90 ± 0.18

Mean Return Periods

Mag.	Number of Events /Month	/Year	Return Period months	years
0.0	63.81	765.7	0.016	0.00
0.5	18.91	227.0	0.053	0.00
1.0	5.58	66.9	0.179	0.01
1.5	1.62	19.4	0.618	0.05
2.0	0.44	5.3	2.267	0.19
2.5	0.09	1.1	10.903	0.91

Probabilities of Seismic Event

Mag.	1 month	3 months	6 months	1 year	2 years	5 years
0.0	100.0%	100.0%	100.0%	100.0%	100.0%	100.0%
0.5	100.0%	100.0%	100.0%	100.0%	100.0%	100.0%
1.0	99.6%	100.0%	100.0%	100.0%	100.0%	100.0%
1.5	80.2%	99.2%	100.0%	100.0%	100.0%	100.0%
2.0	35.7%	73.4%	92.9%	99.5%	100.0%	100.0%
2.5	8.8%	24.1%	42.3%	66.7%	88.9%	99.6%

Maximum Expected Magnitude

In 1 year M = 2.52
In 2 years M = 2.67
In 5 years M = 2.79

Seismic Events Distribution

Magn >	0.0	0.5	1.0	1.5	2.0	2.5
Theor.	1721	510	150	44	12	2
Observed	1544	615	176	47	13	2

Hazard Magnitude

Hazard Mag. = 3.38
SumEnergy = 6.75E+08 J SumEnergy/Year = 3.00E+08 J
SumMoment = 9.75E+13 Nm SumMoment/Year = 4.34E+13 Nm

Figure 47: Seismic hazard estimation - bottom section of west mine (Multi-raise)

Table 5 compares the seismic hazard of the original Sequential mine design with the Multi-raise mine design to determine if any significant changes could be identified in the seismic character. The results obtained from the current study reveal no significant differences between the two mining methods in terms of the relevant maximum magnitude and return period for seismic events with $M_L \geq 2.5$ seismic hazard parameters. The number of seismic events with $M_L = 1.0$ shows a 33% increase for the Multi-raise mine design when compared to the Sequential Grid mine design.

Table 5: Comparison of Seismic Hazard between Sequential Grid and Multi-raise mine design.

	Sequential Grid	Multi-raise
Time span	01/10/04 – 01/07/07	01/07/07 – 01/04/09
Largest seismic event that occurred	2.6	2.7
Mmax expected	2.9	2.9
Return period of $M_L = 1.0$	4 per month	6 per month
Return period of $M_L = 2.5$	1 per year	1 per year

3.8. SUMMARY

- The new Multi-raise mining method was implemented from raise line 34 between 98 and 102 levels at the end of 2006.
- The database used for the analyses starts in 2000 with only 2 seismic events with $M_L \geq 3.0$ have been recorded, the last of these occurred on 31 July 2002.
- The seismic data set at Kusasalethu Mine has been subject to the following external influences over the period of interest e.g. changes to hardware and software. These have had the undesired effect of introducing artificial trends to the data making interpretation of the recorded seismicity somewhat difficult and needs to be taken into consideration when the results are interpreted.
- A previous study into the effectiveness of the Sequential Grid mine design was undertaken by Essrich in 1996 which concluded that the Sequential Grid mine design was less hazardous than Longwall design. A repeat of this study indicated that the seismic hazard due to potentially damaging seismic events ($M_L \geq 2.0$) is lower in the Multi-raise layout than in the original design. It is important to note that

the extraction ratio between the two methods differs and the conditions for the Multi-raise design can therefore still deteriorate in future as the extraction ratio increases.

- The Pearson's correlation between the number of events, $M_L \geq 0.0$ per month and the monthly production were analyses. The results suggested a strong correlation without any lag between the two data sets. This, however, could not be repeated for the series, production and moment released, where a poor correlation was found.
- The seismic hazard results for the original Sequential mine design with the Multi-raise mine design reveal no significant differences between the two mining methods in terms of the relevant maximum magnitude and return period for seismic events with $M_L \geq 2.5$ seismic hazard parameters.
- The number of seismic events with $M_L = 1.0$ shows a 33% increase for the Multi-raise mine design when compared to the Sequential Grid mine design.
- This can be probably be explained by the fact that more seismicity can be expected with the Multi-raise mine design due to the section where the design was implemented was deeper than the area where the Sequential Grid design was implemented in the past.

Chapter 4

MODELLED MOMENT ESTIMATES

4.1. INTRODUCTION

For a given change in mining configuration (i.e. for a mining step) one can estimate potential seismic hazard by numerical modelling. Numerous methods have been applied in the past, a few examples important in the SA gold mining are include Ryder, 1988 and Wiles et al., 2001 and more recently Hofmann, 2012 and Scheepers et al., 2012.

Here the author applied a method (developed by IMS) to estimate the moment tensor of the deformation event associated with each mining step. The mining volume is enclosed in a box or sphere which plays the role of the source volume. Assuming all deformation associated with a particular mining step is associated with one seismic 'event', one can estimate the resulting moment from the changes in the elastic displacements and tractions on the elements of the box or sphere. The method was recently described by Malovichko et al., 2012.

4.2. METHOD

The method to model seismic moment associated with a mining step as described by Malovichko et al. (2012), was recently further developed by the IMS numerical modelling unit. In summary the method involves the following steps:

- Define a sphere around the mining volume of interest that contains all the material subjected to a deformation or dislocation associated with a mining step. This volume must be small enough to capture the elastic stress- and strain change caused by the mining, but large enough to ensure that the material outside it is linear elastic.

- Discritize the sphere surface by small flat elements. The elements must be small enough to justify a constant-traction and constant-displacement approximation for each element, but large enough to allow timeous numerical calculations.
- Run the static stress analyses tool for the state before the and after the mining step and compute the changes in tractions and displacements at the centroids of the elements on the sphere.
- Calculate the moment tensor as per the Appendix in Malovichko et al. 2012.

The seismic moment that is calculated is called the Modelled Moment for each mining step. The results of the Modelled Moment analyses for the Kusasalethu mining layouts were calibrated using the seismic history of Kusasalethu Mine and the IMS in-house numerical modelling program, ISSM.

4.3. MODELLED MOMENT ESTIMATES FOR KUSASALETHU MINE LAYOUTS

The numerical modelling in-house program of IMS called ISSM (Integrated Static Stress Model) was used to conduct the numerical modelling. ISSM is an indirect boundary element method. It models the rock mass as a linear elastic continuum, but can also model the following non-linear behaviour:

- Preventing complete /over closure of tabular excavations
- Effect of backfill
- Ride on structures

Figures 49 and 50 show the location and all the mining blocks (green squares) contributing to the spheres (1 to 8 depicted in Figure 51) that was selected for the analyses as described in Section 4.2. The brown areas represent the mining steps. The spheres enclosing these mining blocks are shown in Figure 51. Spheres needs to be the same size to compare the modelled moment magnitudes derived from the analyses. Different sphere sizes will influence the obtained modelled moment magnitudes from the analyses.

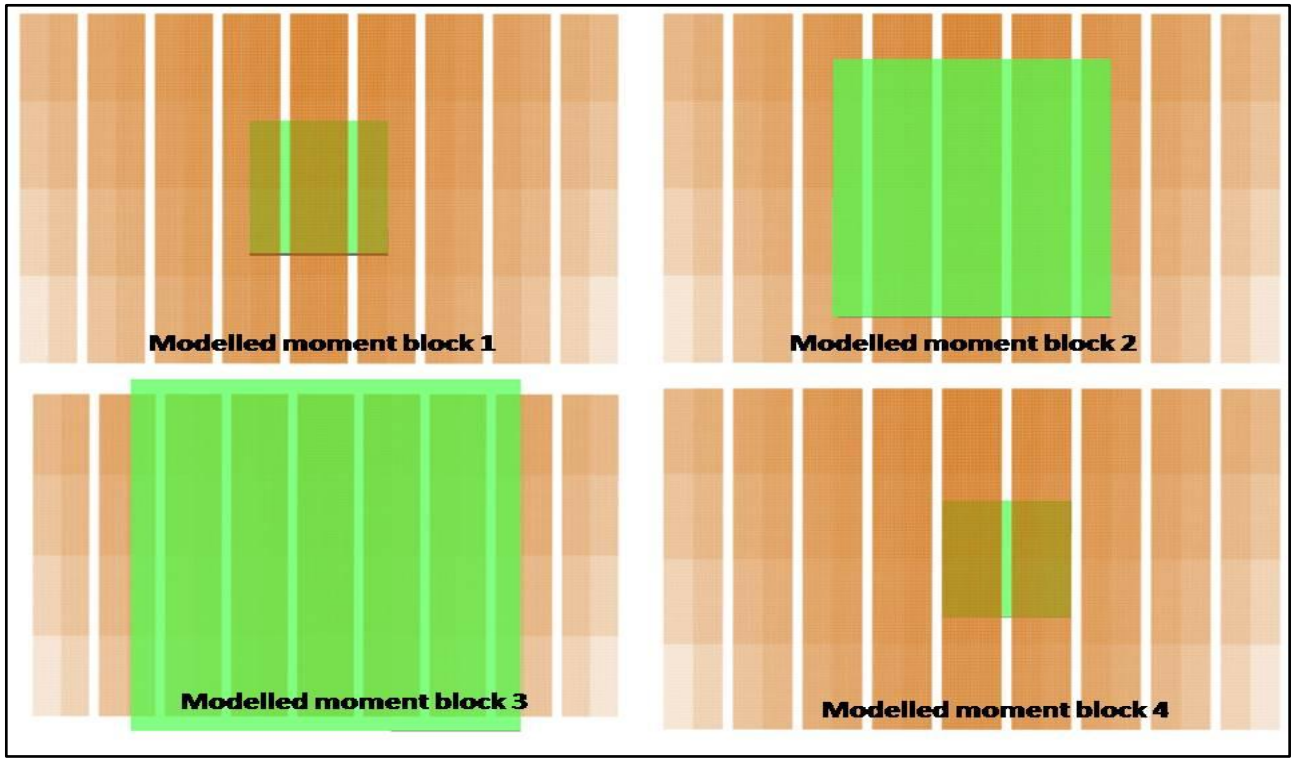

Figure 48: Modelled Moment mining block locations (Spheres 1 to 4)

Figures 52, 53 and 54 plots the Modelled Moment results for each selected sphere for both of the two mining methods. Note the following from these figures:

- The 3 spheres (spheres 2, 3 and 8) with the largest Modelled Moment magnitudes at the end of the mining cycles are the same for both of the mining methods, ranging between 2.0 and 2.5.
- The 3 spheres with the largest Modelled Moment magnitudes are also the 3 largest spheres, including the most mining.
- The other 5 spheres (spheres 1,4,5,6 and 7) have very similar Modelled Magnitudes at the end of the mining cycle.
- The results of all the spheres follow a similar road to the final step (see Figures 52 and 53), with the Multi-raise method reaching higher magnitudes earlier on. This is due to the shorter extraction time when compared with the Sequential Grid layout.

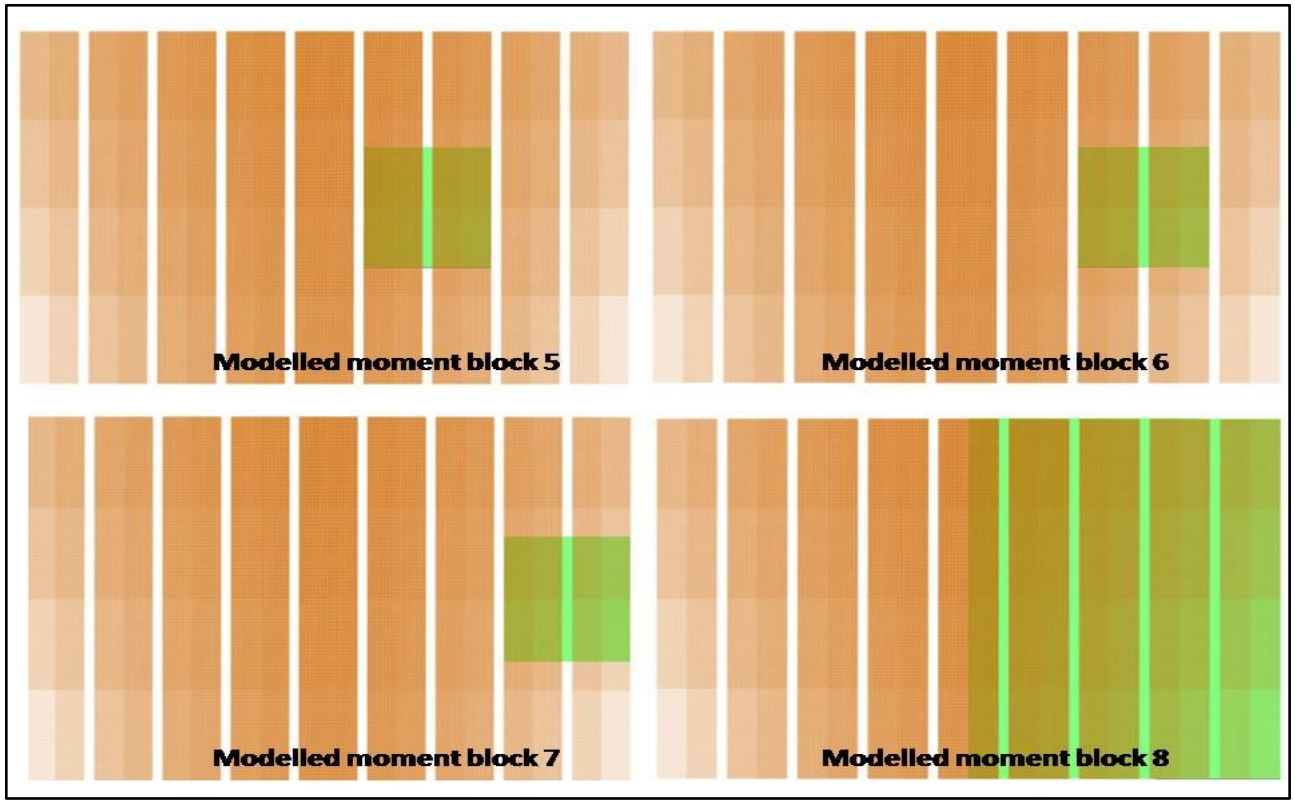

Figure 49: Mining block locations (Spheres 5 to 8)

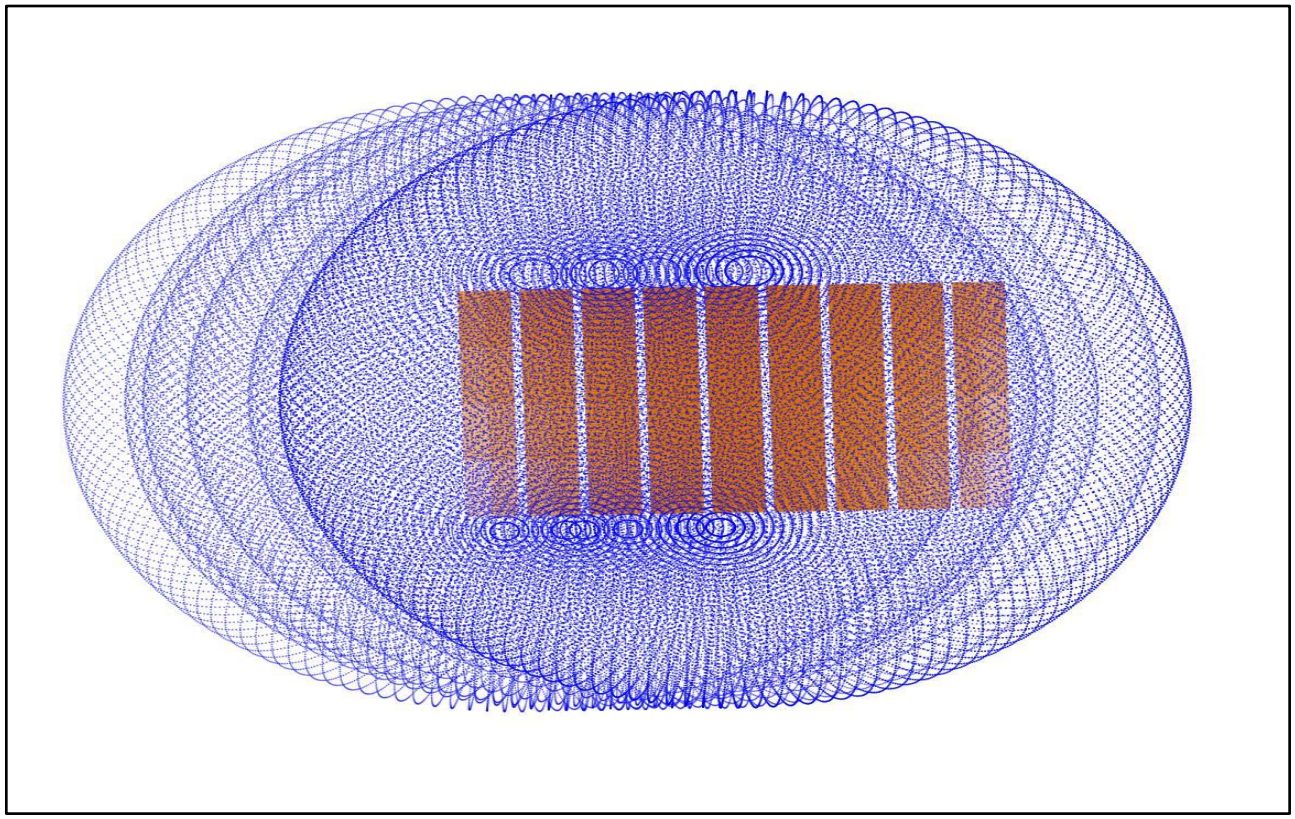

Figure 50: Location of spheres of the selected modeling the modeled moment for the mining blocks.

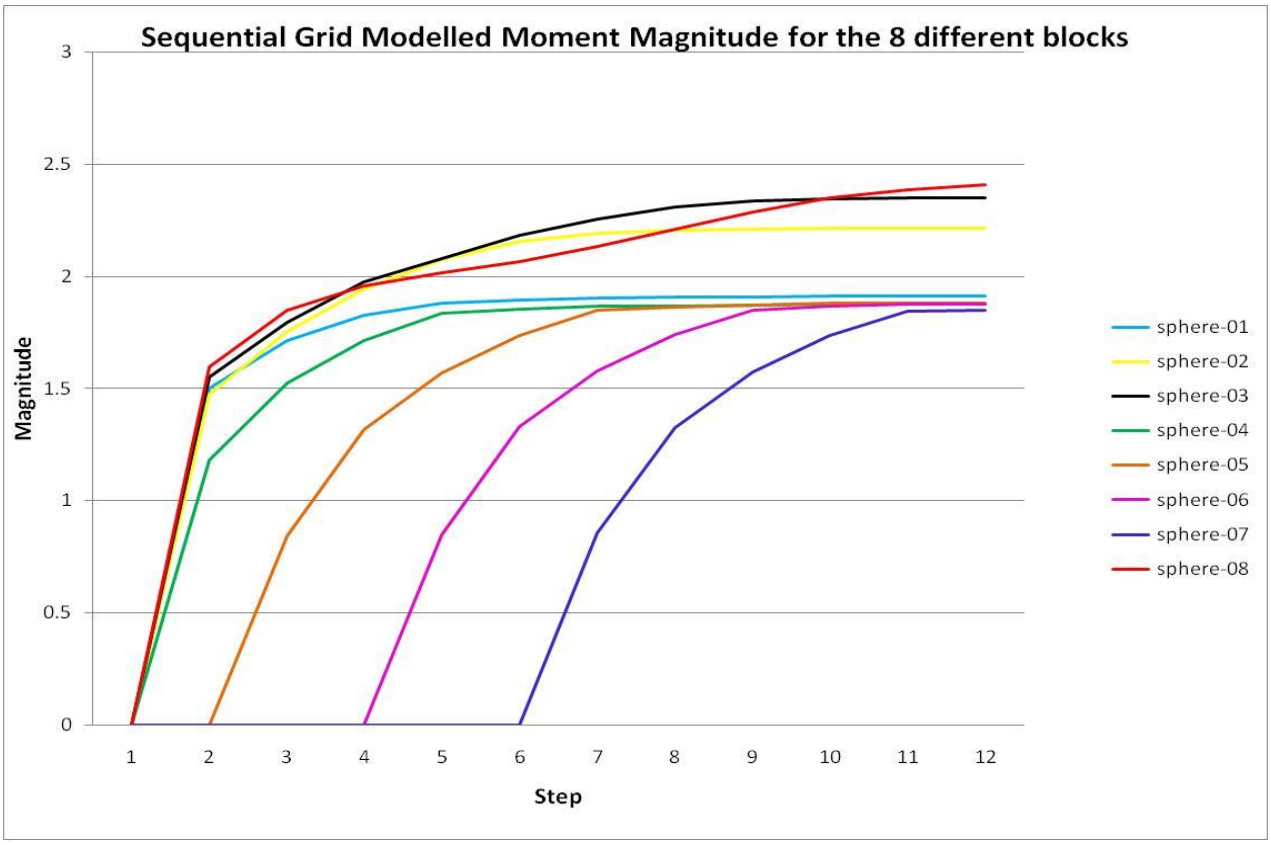

Figure 51: Sequential Grid Modelled Moment Magnitudes for the 8 different spheres

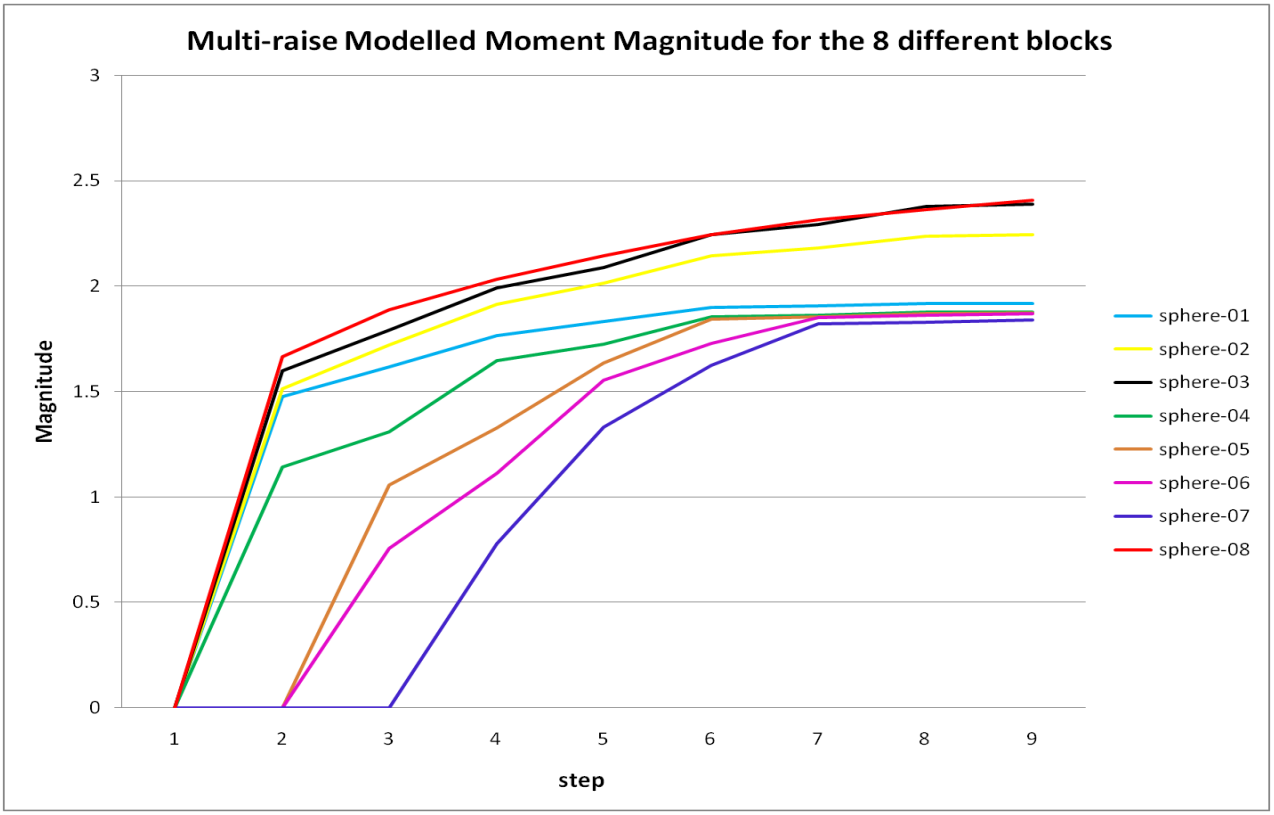

Figure 52: Multi raise Modelled Moment Magnitude for the 8 different spheres

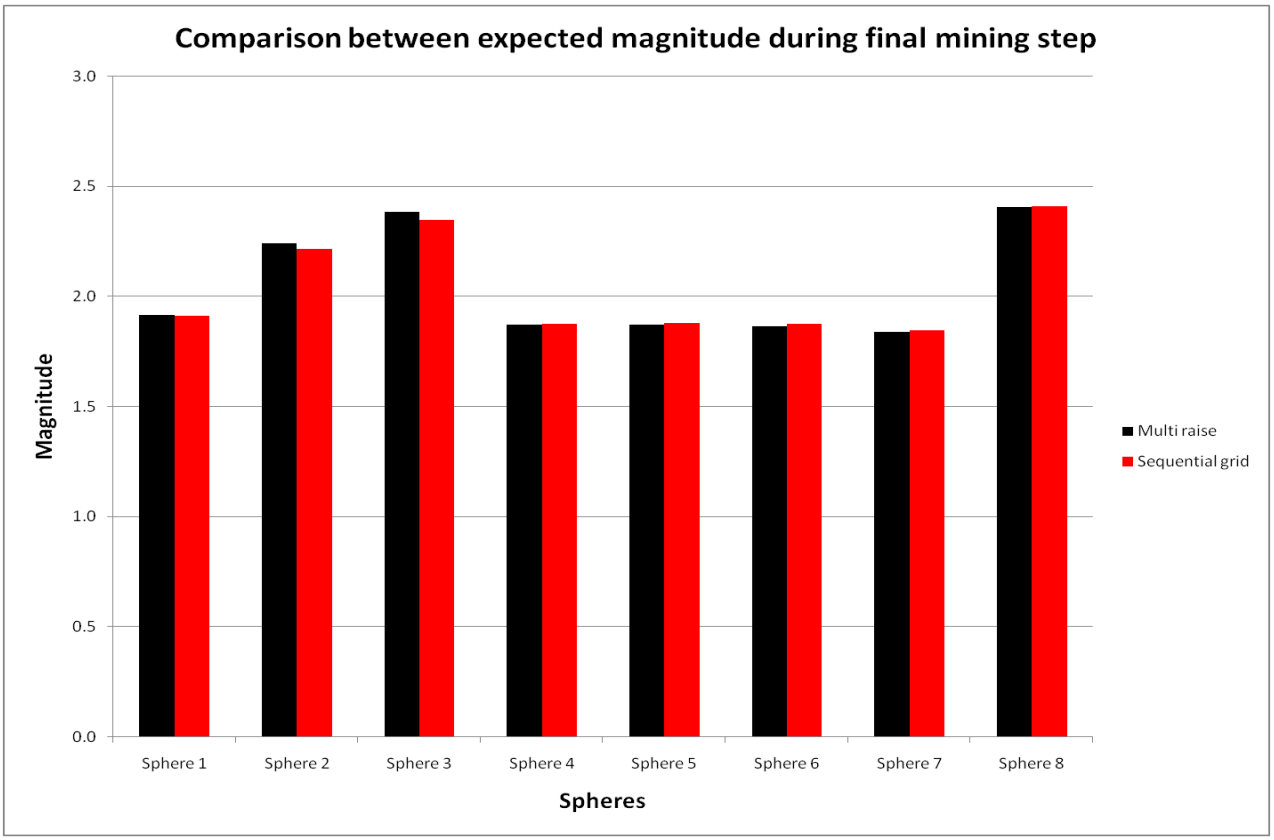

Figure 53: Comparison between expected magnitudes during final mining step for both mining methods

In conclusion, when comparing the results obtained from the Modelled Moment method, little difference can be noticed between the two different mining methods. The only difference in the Multi-raise sequence is that the seismicity is generated much earlier in the mining steps compared with the Sequential Grid design i.e. see Figures 52 and 53.

Further numerical modelling was done by the program, MINSIM, to determine if the modelling parameters show any significant difference when comparing the two mine designs.

Chapter 5

NUMERICAL TECHNIQUES USED IN THIS DISSERTATION

5.1. NUMERICAL MODELLING PROGRAM – MINSIM

The MINSIM-D computer package was initially designed and developed in the early 1980's by John Ryder and John Napier. This work arose as a result of the need in the industry at that time for an updated numerical-based application to improve the analysis of elastic stresses and strains around tabular excavations. The program was originally maintained by the CSIR, but in 2006 ownership was transferred to GMSI. The latest version of MINSIM 2000 is currently widely used in the mining industry in South Africa.

MINSIM makes use of the boundary element method (and specifically the displacement discontinuity approach) to calculate the distribution of stresses and strains around mining excavations. Boundary element methods are beneficial as only the boundaries of the excavations being investigated needs to be discretised. In addition to the excavation surfaces, boundary elements can also be used to model the free surface for shallow mining problems, joint surfaces where joints are considered explicitly and material interfaces for anisotropic applications in rock engineering.

MINSIM in particular uses the technique known as the *Displacement Discontinuity Method (DDM)*, so named because the analysis is based on the solution of an elongated slit in an elastic continuum with shearing and normal displacements associated with the slit. This method is usually restricted to isotropic elastic materials. All of the numerical modelling conducted in this dissertation has been conducted using the *Displacement Discontinuity method*, as embodied in MINSIM 2000.

5.2. THE EFFECT OF GRID SIZE ON THE CALCULATION OF APS

The concept of an average value for the stress distribution in a pillar is referred to as the average pillar stress (APS). Although averages are generally simple to calculate given the availability of appropriate data, average values for the stress distributed within pillars is more complex, especially when working in the realm of displacement discontinuity numerical methods. Numerical models in the mining industry are used to estimate APS on a routine basis, but the fundamental properties of the methods involved are not well understood. This frequently led to erroneous estimates of average values and can lead to poor designs involving pillars.

The nominal tributary area theory used in the estimation of the average stress overestimates the stresses on pillars as it ignores the effect of barrier and boundary pillars.

The calculation of APS has been investigated by Napier and Malan (2011) using the displacement discontinuity boundary element method, TEXAN. Their findings, summarized below, reveal some of the difficulties that arise in the determination of this parameter.

- The *Displacement Discontinuity method* is frequent used by practitioners to determine average pillar stresses. There are limitations involved with this methodology that need to be taken into consideration:

    - The determination of APS using DDM's is affected by both the size and shape of the boundary elements selected for the analysis.
    - The displacement discontinuity approximation of a tabular excavation takes no account of the excavation dimensions normal to the plane of the reef. Consequently, the simulation models the pillar with an effective "zero height" and therefore cannot simulate the stress distribution at various heights in the pillars.

Napier and Malan (2011) showed that a simple extrapolation technique can be employed to obtain robust estimates of average pillar stress values to overcome the problems associated with the grid size.

In order to illustrate the effectiveness of the extrapolation procedure, a single strip pillar of width 20 m centrally located between two parallel-sided panels each having a span of 120 m was modelled in TEXAN. The layout was assumed to be horizontal and was solved in plane strain. If the primitive stress at the panel horizon is 100 MPa, then the average pillar stress can be determined analytically and in their case was equal to 516.24 MPa.

Figure 55 shows a plot of estimates of the average pillar stress as a function of the element grid size for the strip pillar as modelled by the numerical program, TEXAN (Napier, 2012).

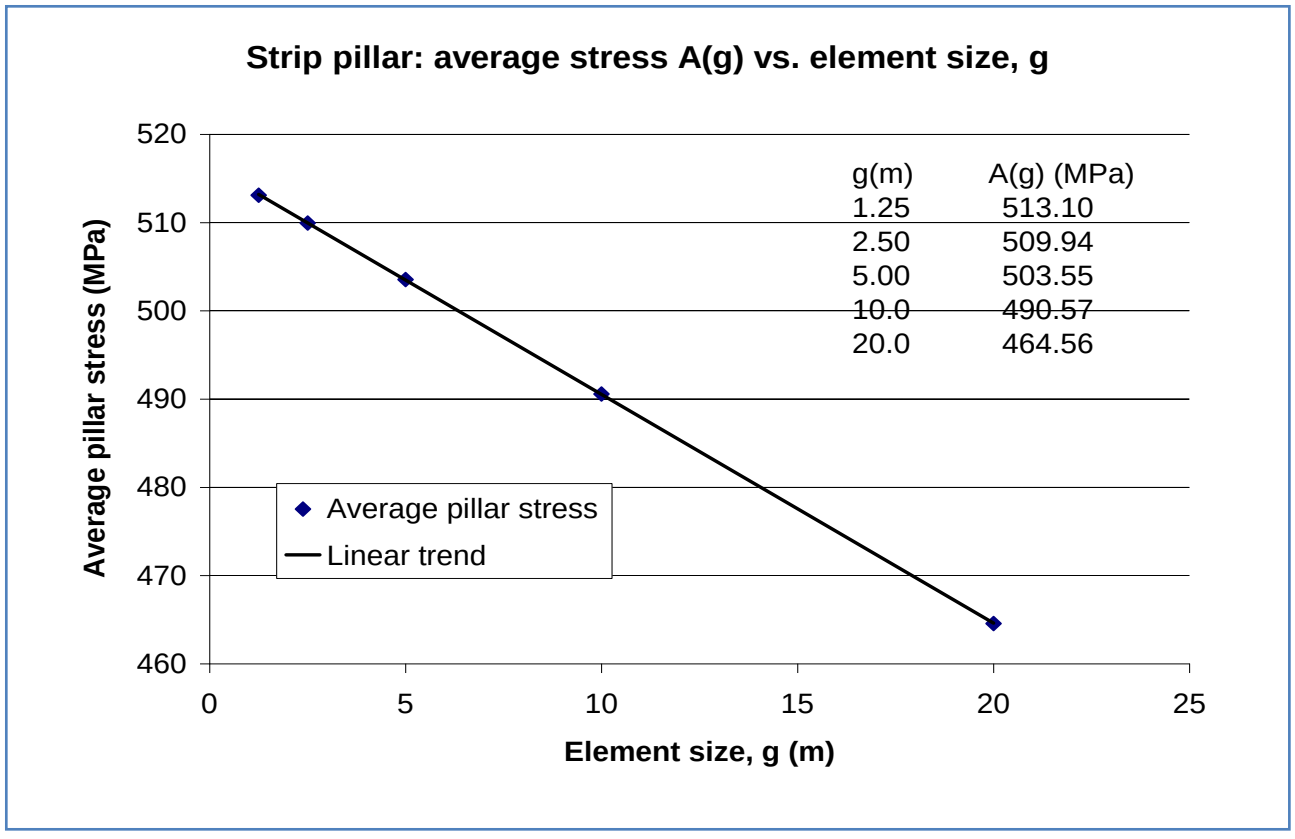

Figure 54: Single strip pillar average pillar stress magnitude estimated as a function of the element grid size. The pillar has a width of 20 m and is located between two parallel-sided panels each having a span of 120 m (after Napier and Malan, 2011)

It is clear from Figure 55 that the values of the estimated average pillar stress in this example follow a nearly perfect linear trend. The trend in this graph suggests a more accurate value of APS for smaller grid sizes as well as indicating the important role of grid size in the determination of APS values as element sizes tend to zero. Larger grid sizes can result in a significant under estimation of the APS.

Detailed calculations of APS, with MINSIM 2000, were conducted as part of the current dissertation in order to make comparisons between i.e. the ordinary Sequential Grid design and the modified or multi–raise design. A basic mining layout was used: 300 m x 30 m pillar in the middle of a 1000 m x 1000m mined area. The grid from the on-reef sheet was on the pillar boundary. Grid sizes of 10 m, 6 m and 3 m was selected for the initial analysis and the results are shown in Figure 56.

Once again it is clear from Figure 56 that the values of the estimated average pillar stress follow a nearly perfect linear trend. The trend in this graph suggests a more accurate value of APS for smaller grid sizes.

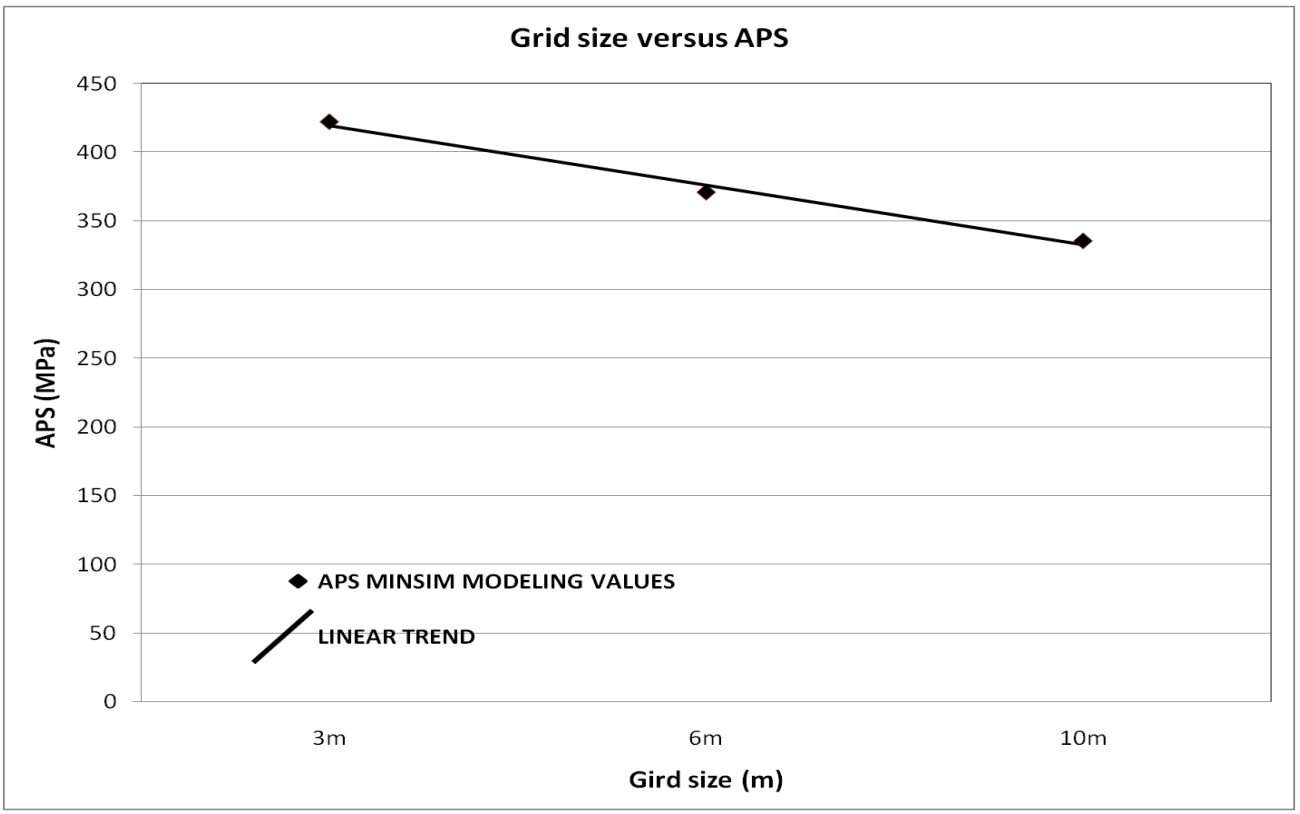

Figure 55: Effect of grid size on the average pillar stress as calculated by MINSIM 2000

In view of the fact that multiple different mining layouts were modelled as part of the dissertation, the relatively larger block size of 10 m was selected in order to save on computational time. Since the analysis effectively involved comparisons between different layouts, the precise or absolute values of APS could largely be ignored.

5.3. PROPOSED METHOD TO CALCULATE APS VALUES USING MINSIM 2000

The following paragraphs contain a sequence developed by the author to ensure that errors are minimised. This section is included to give guidance to new MINSIM 2000 users not familiar with the potential pitfalls of the numerical program.

Two methods can be used to determine the APS values of a specific pillar in a MINSIM 2000 model. The first being the software functions to SUM and AVERAGE values from the MINPOST platform. The second will be to export the data to a spreadsheet, manually delineating the pillar from the table of values and average the pillar values to determine the APS. This process may be almost impossible with complex pillars found typically on the mines and therefore it is recommended that the functions keys be used to save valuable time.

When the MINSIM functions keys are used the follow procedure needs to be followed:

Setup of sheet

When a new MINSIM 2000 job is being prepared for calculation, an expandable window is adjusted over the digitized mine plans in order to select the area of interest. Numerical modelling results are only obtainable for the area under the selected window sheet (see Figure 57).

The user needs to move and place the selected window sheet over the area of interest and then set the modelling parameters for the sheet. Figure 57 illustrates the property box for selection of the modelling parameters. The size of the sheet is depicted by means of the red square in Figure 57.

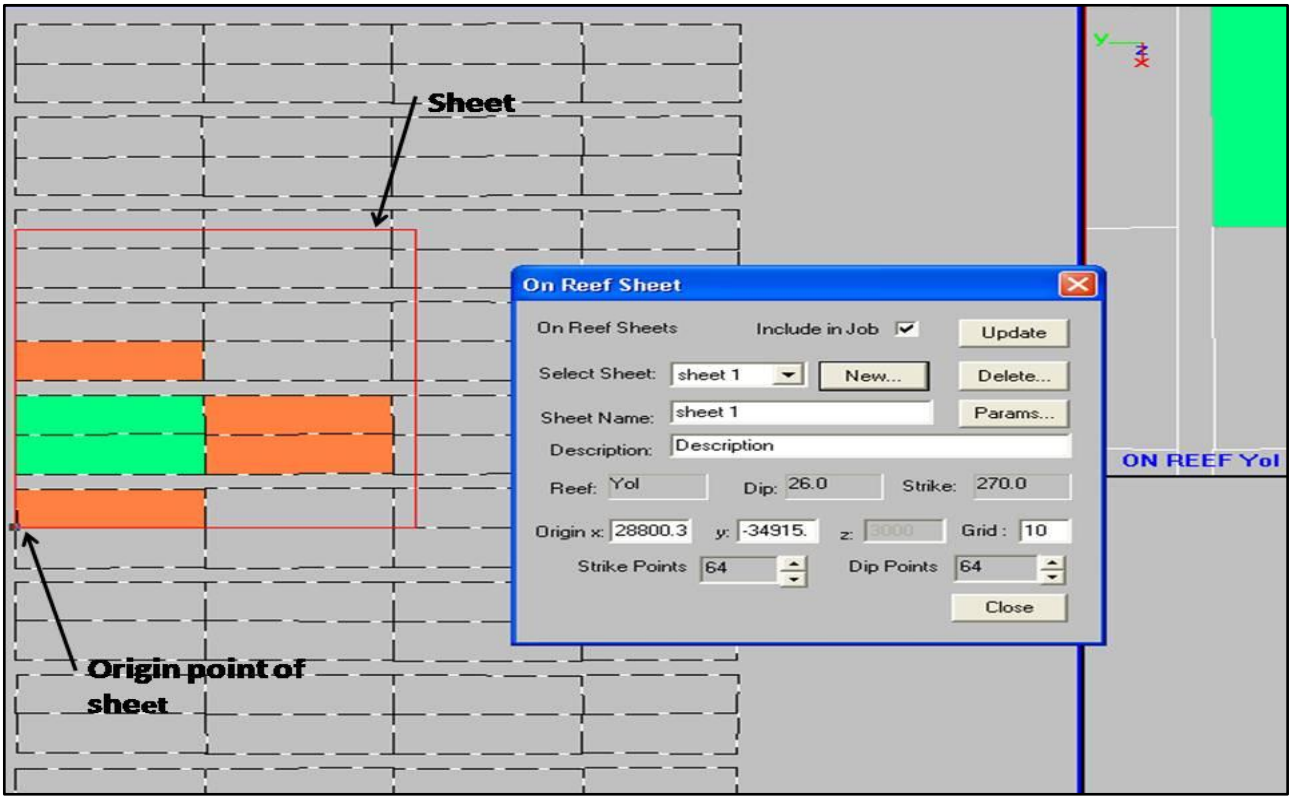

Figure 56: MINSIM 2000, setup of off reef sheet

The following parameters for the selected window sheet are set in the on reef sheet window as portrayed in Figure 57:

- Origin – specify here the location of the sheet relative to the mining (x,y) of the origin point.
- Grid – set the grid size
- Strike and Dip points – define the size of the sheet on dip and strike of the reef

Additional parameters for the sheet can also be setup by selecting the “Params” option in the sheet parameter box as depicted in Figure 58.

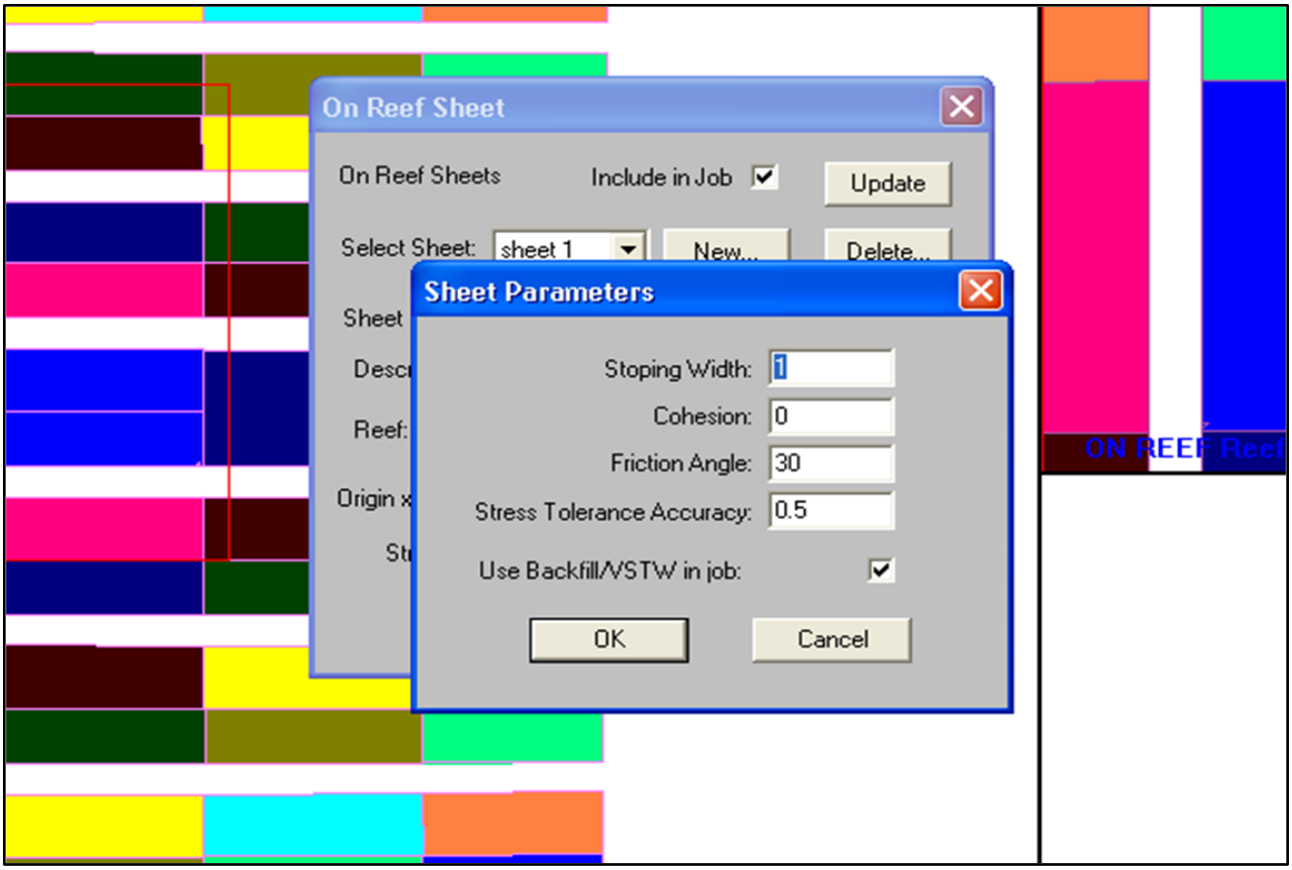

Figure 57: Set sheet parameters

Output format

The model results are calculated for the area that was selected by the window sheet in the setup process. The output of any specific model parameter from the program can be viewed using contour or colour plots as shown in Figures 59 and 60.

Obtaining APS value

In the post processor program (MINPOST), contours are drawn of the major principle stress (SIG1) parameter as shown on Figure 61. On this plot, the area of interest is selected around the pillar. The automated contour statistics return a pop-up screen with the Non-zero Average for the major principle stress (see Figure 61). Figure 61 shows the results obtained for the selected area where the pop-up screen shows the result of the APS calculated as the non-zero average as 93.8 MPa.

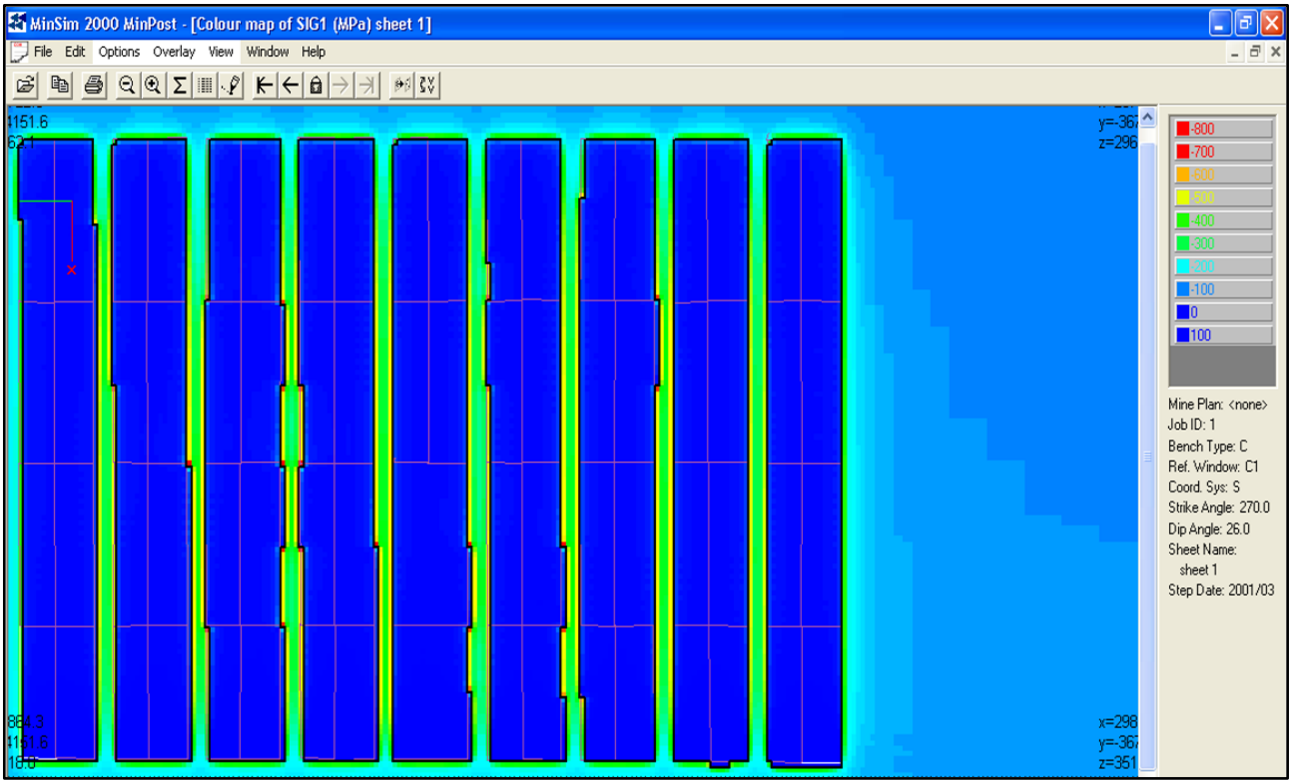

Figure 58: Colour output sheet

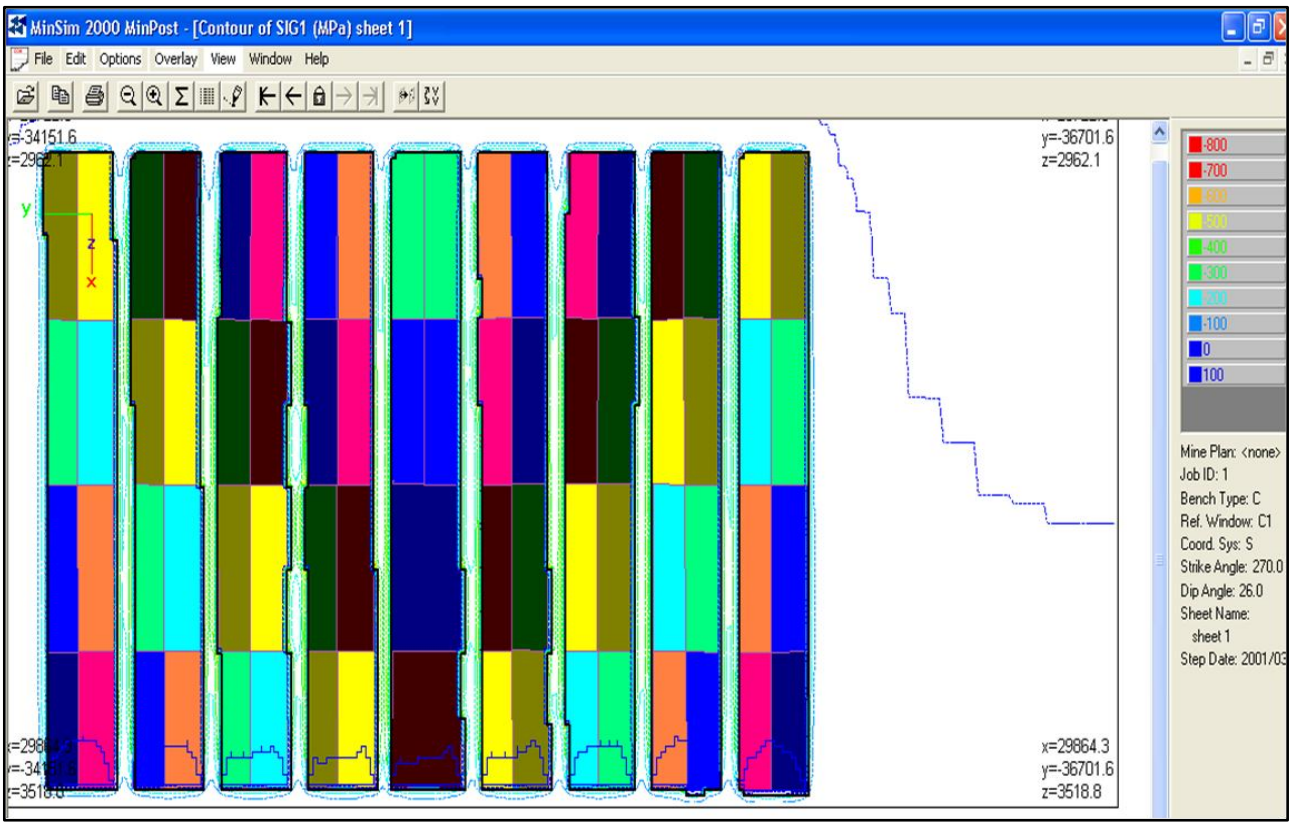

Figure 59: Contour output sheet

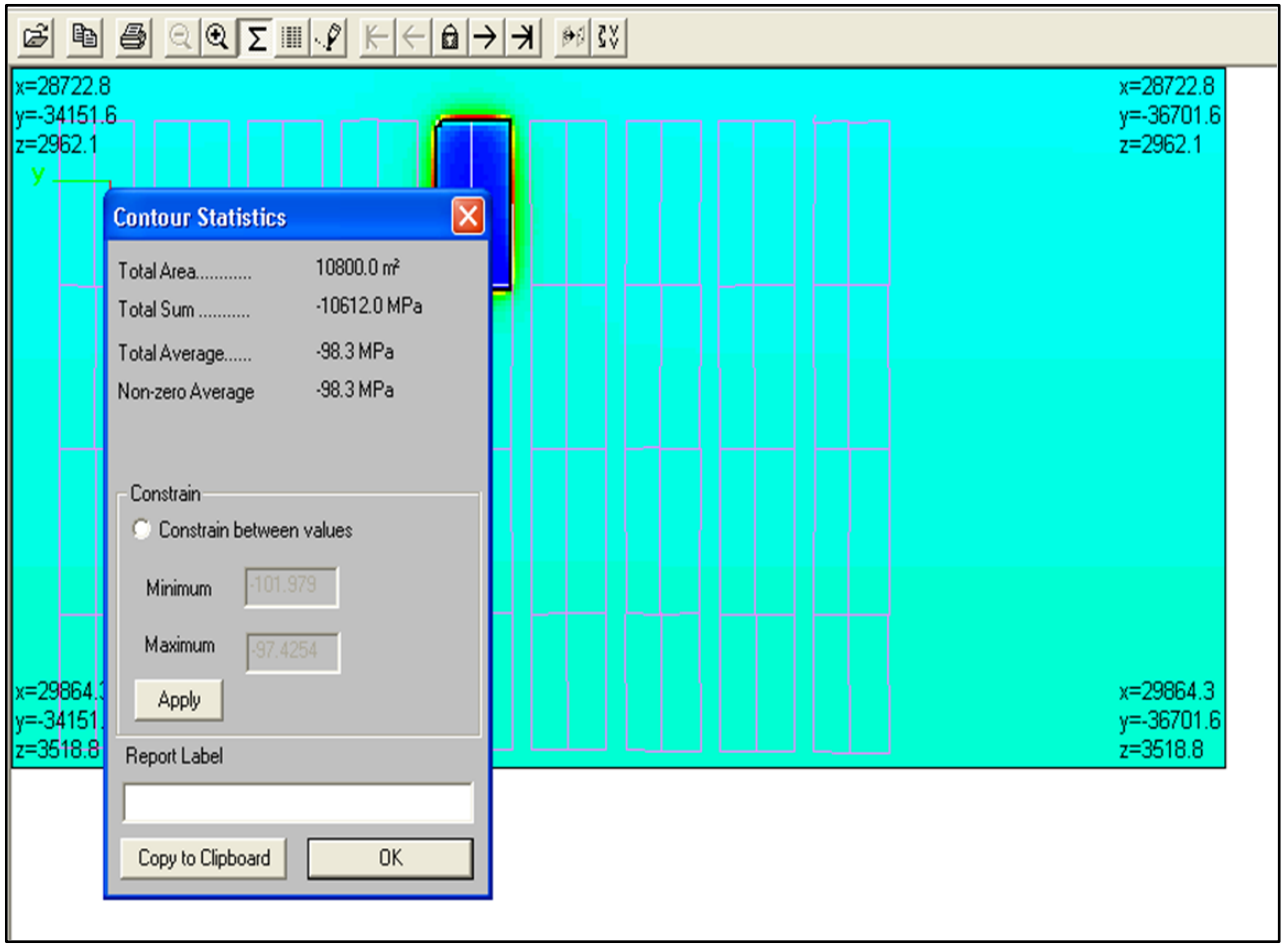

Figure 60: The results of the APS for the selected area.

5.4. PROCEDURE TO CALCULATE APS USING MINSIM FUNCTION KEY METHODOLOGY

The following procedure is suggested when average pillar stress is to be calculated using MINPOST and is essentially similar to that proposed by Maritz (2010):

i. Two models should be prepared for the calculation of the APS. Each model should have the same mining layout and step selection; however the difference should be in the grid size applied to the models. For ease of calculation, a 10 m and 5 m square grid size is recommended.

ii. In the post processor (MINPOST), plot a contour graph on SIG1 from the start-up window on the relevant on-reef sheet containing the pillar to be evaluated.

iii. Select the **Σ** icon from the command line.

iv. Draw a box around the pillar to be evaluated.

v. Tick the "*Constrain between values*" option and set the limits to highest value and the approximate virgin stress of the pillar (The virgin stress of the pillar should be calculated using the standard equation $\sigma_v=\rho gh$ where h is equal to the average depth of the pillar). Then click *Apply*.

vi. The *Non-zero average* in the statistics window will be the calculated APS.

vii. Tabulate the value for extrapolation purposes.

viii. Repeat steps i to vii for the second prepared grid size model.

ix. Extrapolate the two APS values from the different models to 0 m as shown in Figure 62. Where X and Y represent the grid sizes and APS values respectively.

x. If two mining scenarios are compared ensure that the origins of the grid sheets are set relative to the mining plans. See Section 3.5 for more detail.

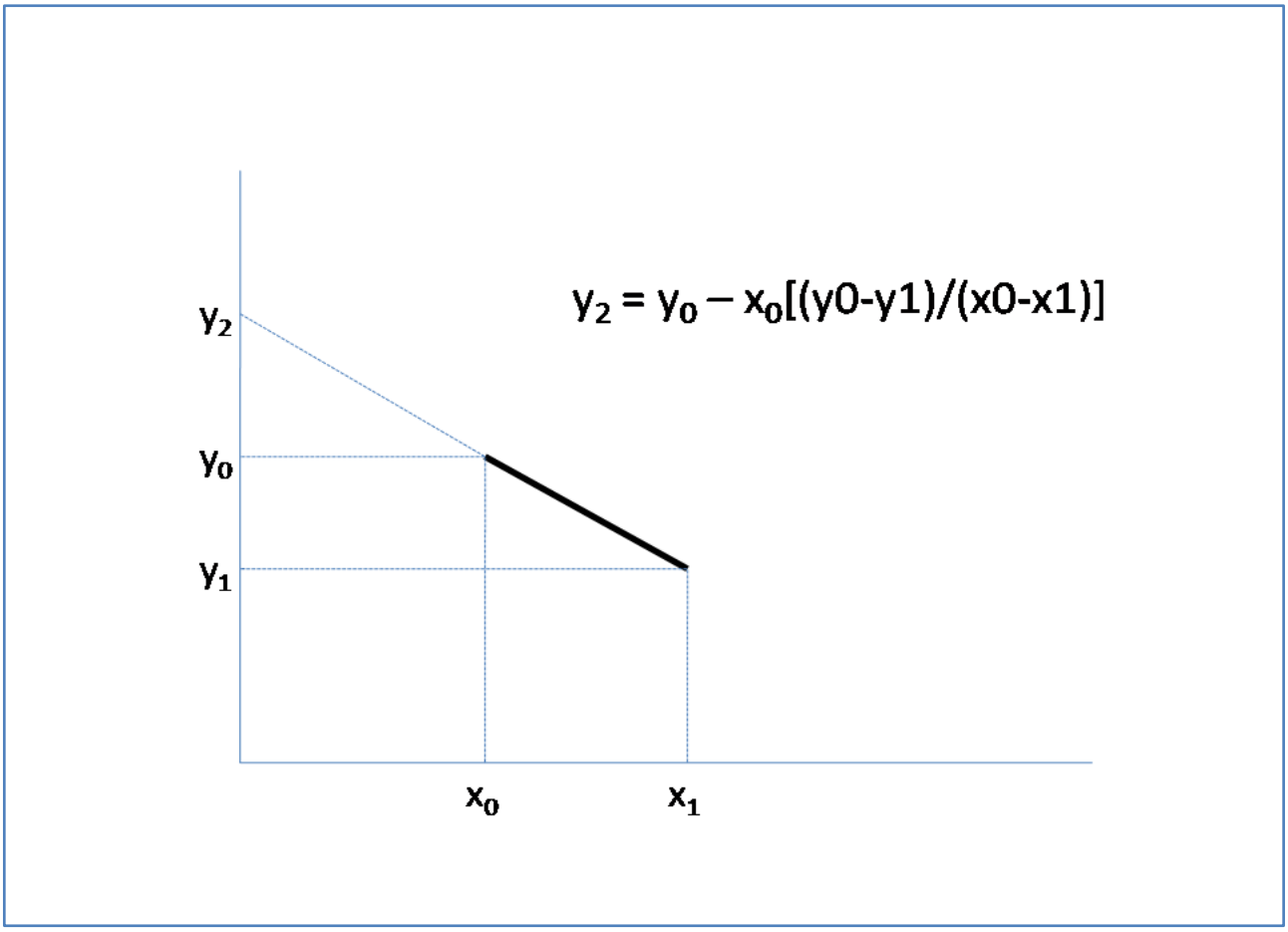

Figure 61: Extrapolation equation for determining the APS

5.5. APS VALUE COMPARISON FOR DIFFERENT MINING SCENARIONS

The calculation of APS in MINSIM 2000 is dependent on the positioning of the collocation points in the mesh. For analyses where the results involve different mining scenarios, it is critical to ensure that overlying grids and plans used in the numerical preparation are identified. Failure to ensure this will cause a difference in input parameters that may translate into different outputs of stress values. Effective comparisons can therefore not be done. This can be achieved by ensuring that the origins of the sheets (x,y,z) are the same for all cases where comparisons are involved.

Figure 63 shows the offset in the grid sheets that can result if the origin for respective MINSIM 2000 jobs is not set up to the same position. Figure 63 shows the misplacement of the grids on the digitized plans (colour contours) that will result if the origin points of the grids are not setup in the initial job preparation process.

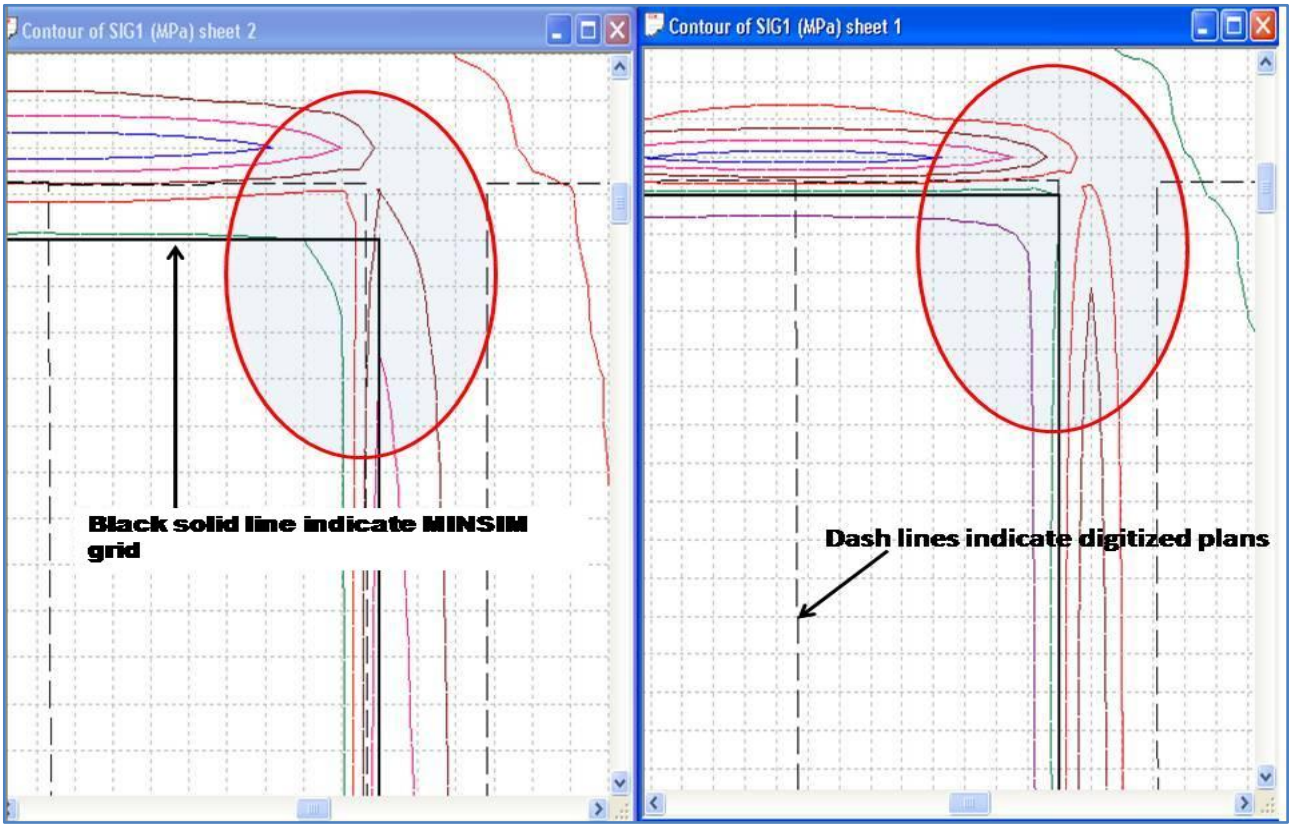

Figure 62: Difference of calculating major principal stress when the grid position was not set (line contour plots)

The method and procedure discussed above can assist with minimizing problems experienced in the past with the calculation of average pillar stress (APS) used on mines to determine the stability of rock engineering pillars.

In the next chapter the technique described above are used as one of the methods to determine the difference between the two mining methods, Sequential Grid and Multi-raise.

Chapter 6

NUMERICAL ANALYSES OF THE MODIFIED SEQUENTIAL GRID LAYOUT

6.1. INTRODUCTION

To determine the feasibility of the Multi-raise mine design, earlier numerical modelling was conducted by Brentley (2006) to determine if any major stress changes could be expected. His results were based on the proposed layout of the mining method and the results are discussed in Section 6.2. As a number of questions remained unanswered, additional numerical modelling was conducted by the author of this dissertation using MINSIM 2000. This was conducted to determine the changes in face stresses as well as average pillar stresses in an ideal mining layout. The results from this study are discussed in Section 6.3.

6.2. HISTORICAL INVESTIGATION INTO MULTI-RAISE MINING

The analysis (Brentley, 2006) modelled three mining sequences, but only the following two sequences were evaluated:

- Method A – Mining multiple raise lines with the bottom panel leading. Mining occurred in an easterly direction first followed by mining west.
- Method B – Standard Sequential Grid with bottom panel leading.

The numerical modelling was conducted using MINSIM 2000 and the following input parameters were used. These are similar to those used by Appelgate (1991) for the initial design of the Sequential grid mining layout:

- Grid size – 10 m

- Poisson's ratio – 0.2
- Young's Modulus – 70 GPA

The following variables were analysed:

- Energy release rates (ERR)
- Excess shear stress on the geological structures (ESS)
- Haulage stability

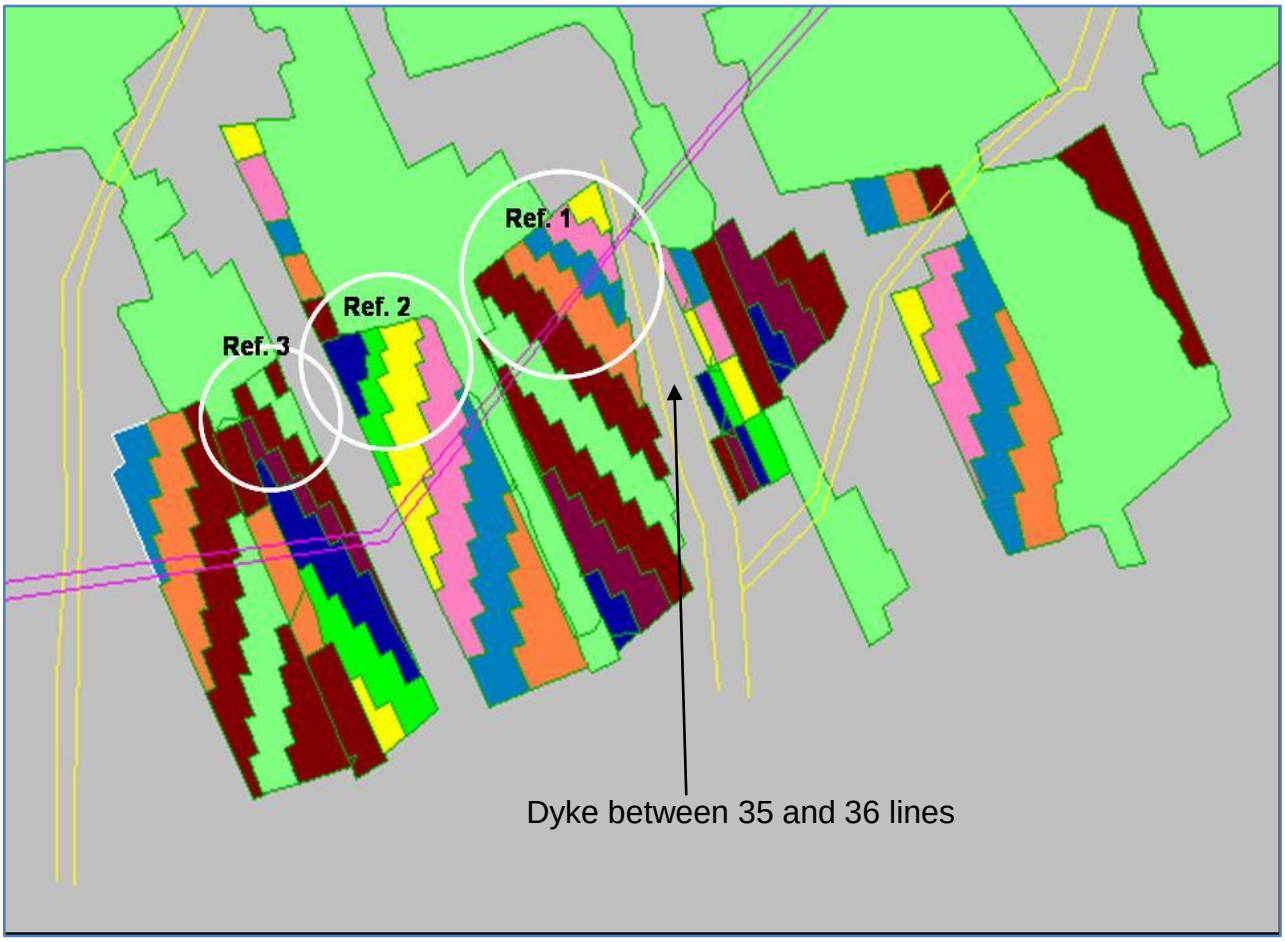

Figure 63: Numerical model with reference points (after Brentley, 2006)

Table 6 is a summary of the results obtained from the numerical modelling by Brentley (2006). Three reference points were chosen to evaluate the results, see Figure 64.

6.3. ENERGY RELEASE RATES AND FACE STRESS RESULTS FROM BRENTLEY (2006)

The data from Brentley (2006) is shown in Table 6. As there are some difficulty in interpreting and comparing this data with additional numerical modelling results, some of this work was repeated for the dissertation study.

Table 6: Summary of ERR and Face stress (after Brentley, 2006)

Mining Step	Results obtained from reference points as depicted in Figure 64			
	Method A		Method B	
	ERR (MJ/m²)	Face stresses (MPa)	ERR (MJ/m²)	Face stresses (MPa)
Reference Point 1				
5th last step	18 (15)	230	18 (15)	210
4th last step	19 (16)	235	19 (16)	220
3rd last step	18 (15)	230	17 (14)	220
2nd last step	17 (14)	250	17 (14)	220
Last step	8 (Ahead) (7)	190	9 (8)	190
Reference Point 2				
4th last step	30 (26)	330	30 (26)	320
3rd last step	32 (27)	340	28 (24)	315
2nd last step	33 (28)	330	30 (26)	300
Last step	23 (Ahead) (20)	290	19 (Ahead) (16)	270
Reference Point 3				
4th last step	6 (5)	190	7 (6)	215
3rd last step	9 (8)	210	11 (9)	230
2nd last step	10 (9)	190	13 (11)	240
Last step	10 (In line) (9)	190	6 (5)	260

() Estimated ERR values based on 15% benefit using backfill.

The following preliminary conclusions could be derived from the table:

- For reference point 1, the values for ERR and the face stresses range between 8 and 19 MJ/m² and 190 and 250 MPa for both sequences. From this it can therefore be deduced that good to acceptable hangingwall conditions are expected, irrespective of the sequence chosen.
- At reference point 2, the ERR and on-reef stresses range between 16 and 33 MJ/m² and 270 and 340 MPa respectively for the three sequences. The high values of stress and ERR can be attributed to the large stoping span which is governed by fault orientation and is planned to be 220 m. This is clarified in Table 7 where the results obtained after reducing the stope span to 170 m is summarized.

Table 7: ERR and face stresses (Method B, reference point 2) with 170m span (after Brentley, 2006)

Mining Step	ERR MJ/m²	On-reef (MPa)
4th last step	18 (15)	250
3rd last step	21 (18)	270
2nd last step	24 (20)	290
Last step	17 (14)	260

- Values for ERR and face stresses at reference point 3 vary from 5 to13 MJ/m² and 190 to 260 MPa respectively for both the sequences.

Although the ERR criterion is not an absolute measure for expected conditions, it does provide the user with an acceptable criterion for comparing designs in similar mining areas.

The reason for evaluating the practice of a mining configuration of bottom panel leading (underhand configuration) was to limit the strata control issues associated with the wide gully headings of each panel as would be in the case of top panel leading (overhand configuration). Stoping with top panel leading will mean that the panel adjacent to the old mined-out area is mined as a leading panel.

Historically, on Kusasalethu, the maximum acceptable ERR for any given panel has been 30 MJ/m² (Applegate, 1991). Studies done on Kusasalethu Mine by visual observation

from underground and then comparing the results done by the numerical modelling indicated that:

- ERR < 10 MJ/m² = Good conditions
- ERR 11 – 20 MJ/m² = Acceptable conditions
- ERR > 20 MJ/m² = Difficult to support

Similarly where:

- σ on-reef < 200 MPa = Good conditions
- σ on-reef 201 – 300 MPa = Acceptable conditions
- σ on-reef > 300 MPa = Difficult to support

In addition, Applegate (1991) indicates that the placing of classified tailings close to the face reduces the ERR value by some 20 % and improves face conditions due to its strata control benefits.

6.4. HAULAGE STABILITY

Off-reef benchmark sheets were placed 90 m below reef position by Brentley (2006) in order to determine the effect the changes in stress will have on the stability of the footwall haulages which are influenced by the stoping and final dip pillar positions. Table 8 is a summary of the results obtained from the numerical modelling.

Table 8: Maximum values of principle stress expected for a haulage 90 m below reef (after Brentley, 2006).

Sequence	Maximum Principal Stress
Method A	90 MPa
Method B	85 MPa

From the results, it is evident that the haulages will be subjected to similar field stresses for the two sequences modelled.

6.5. EXCESS SHEAR STRESS

A dip orientated dyke, situated between the 98-35 and 36 raise lines (see Figure 64), was subject to an ESS analysis in order to, firstly evaluate the change in ESS on the structure for the two mining sequences and, secondly to estimate the likely maximum event magnitude (M_{max}) should slip along the structure occur.

The estimate of the likely maximum event magnitudes were calculated using the formulae:

$$Mo = \mu AD \qquad (8)$$

Where,

μ = Modulus of rigidity
A = Area of ESS lobes
D = Expected slip

ESS is used to assess the potential for slip along a pre-existing major geological structure, in this case a dyke. The comparison indicates that the expected M_{max} is in the region of M_L = 3.0 to M_L = 3.2.

A summary of the results are represented in Figure 65 and the following is evident:

- Mining towards the dip orientated dyke increases the potential for slip as can be expected as the field stresses will increase ahead of the advancing faces.
- The numerical modelled maximum event magnitude is M_{max} = 3.1 for both the original Sequential Grid and the Multi-raise method which could be expected in the final stages of extraction.

In summary, from the preliminary modelling conducted by Brentley (2006), it appears that there is little difference when comparing the original Sequential Grid and the Multi-raise layouts. This study was repeated for this dissertation by the author owing to the difficulty in interpreting and comparing the Brentley (2006) results. The problem areas are:

- It is not clear where and how the various parameters were determined, e.g. was the ERR the average values along the current faces or in front of a single panel.
- Face stress as a design criteria can be problematic as the value calculated will depend on the grid size.
- Maximum principle stress may not be the optimum parameter to investigate haulage stability as other parameters such as Rock Wall Condition Factor (RCF) may be more suitable.

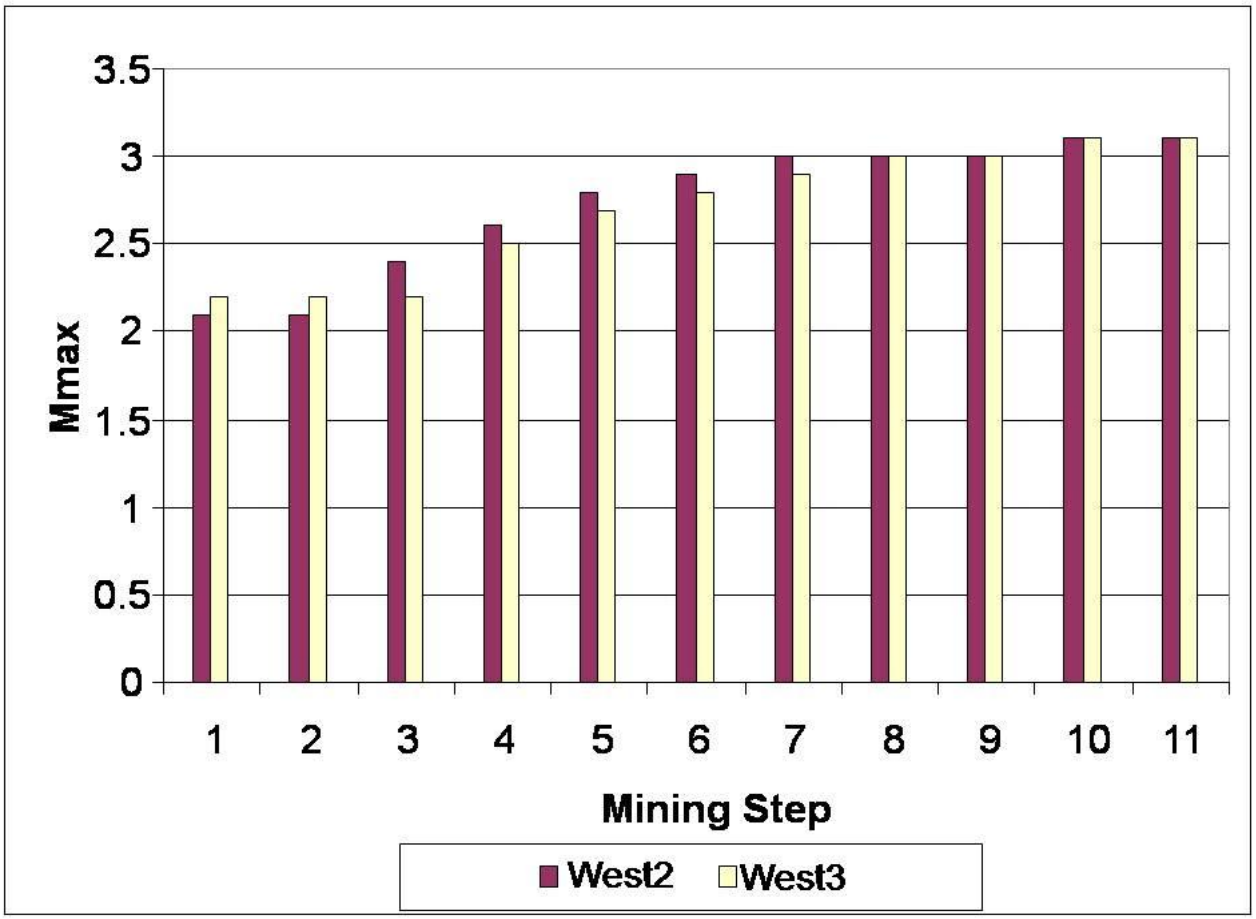

Figure 64: Summary of numerical modelled ESS results (after Brentley, 2006)

6.6. ADDITIONAL NUMERICAL MODELLING CONDUCTED FOR THIS STUDY

Numerical modelling was conducted to compare the stress changes between the Multi-raise sequence and the original Sequential Grid sequence. The design parameters used in this study is similar to the study conducted by Brentley (2006) as described in Section 6.2 above.

To compare the two mining sequences, two numerical modelling parameters, average pillar stress (APS) and energy released rates (ERR), were compared to determine the most favourable design. Figure 66 depicts the location where the APS and ERR values where obtained from the numerical modelling results, to compare the two design methods with each other. Two areas were identified where numerical results will be obtained from, the red rectangle (in the middle of the mining layout) depicts the total pillar area and the black arrow depicts the smaller top pillar area.

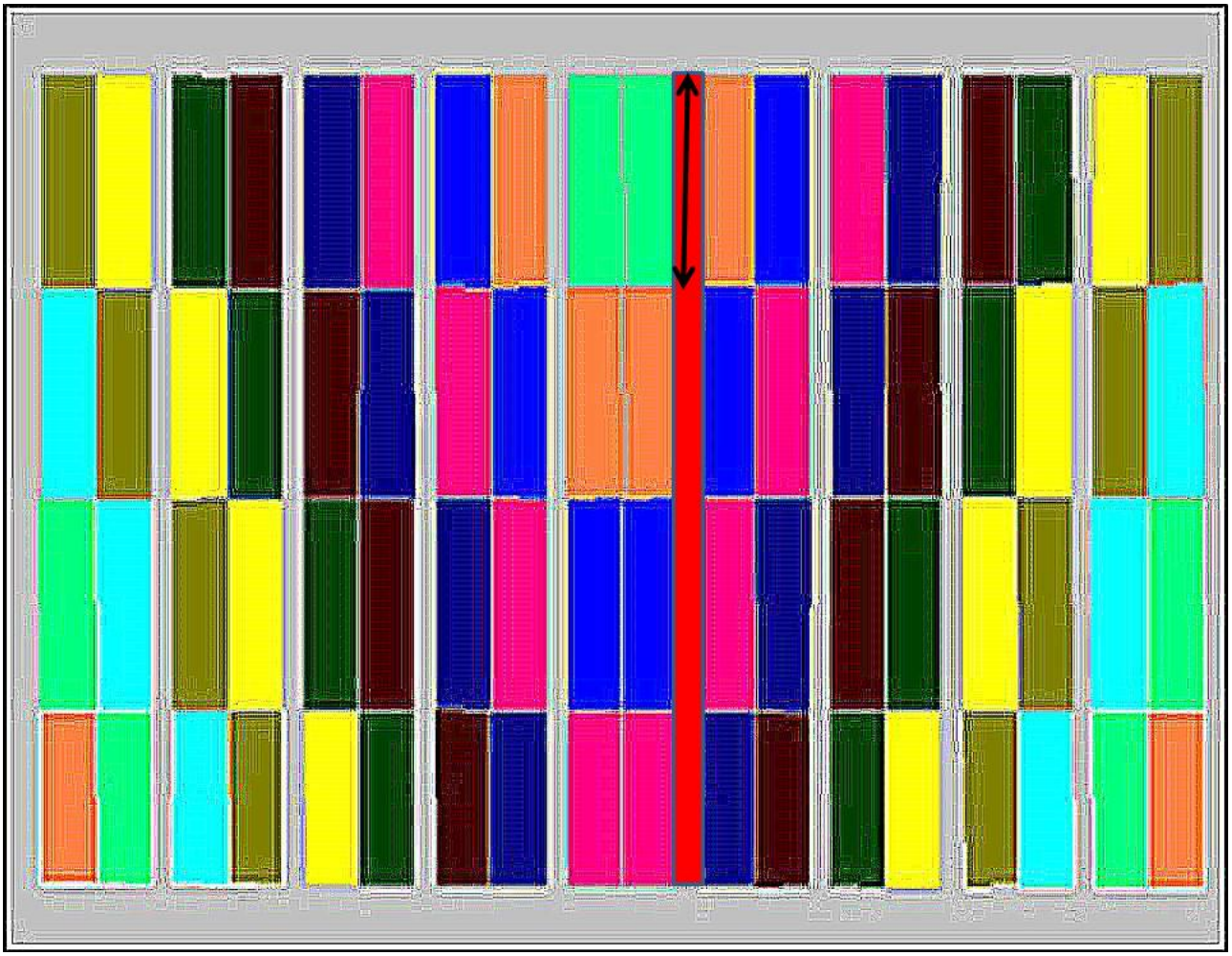

Figure 65: Depicted location where APS and ERR values where analyze

6.7. ENERGY RELEASE RATES (ERR)

The removal of rock during the mining processes results in the increase of stresses ahead of the mined areas due to sag of the overlying strata. The ERR concept was introduced in

the 1960's, as it is a simple and handy measure to determine the stress concentrations ahead of the mined areas. ERR takes into account the effect of depth and the geometry of the mined out areas and are related to the extent of the volumetric convergence that occurs in the back areas. ERR calculation and the explanation of the parameters used, is discussed in Section 1.3.

Figure 67 shows the average ERR values as a function of mining step for the total pillar area (calculated on one side of the red rectangle). Figure 68 shows the ERR values obtained for the pillar separating the first two raise lines (top pillar), depicted with a black arrow in Figure 66.

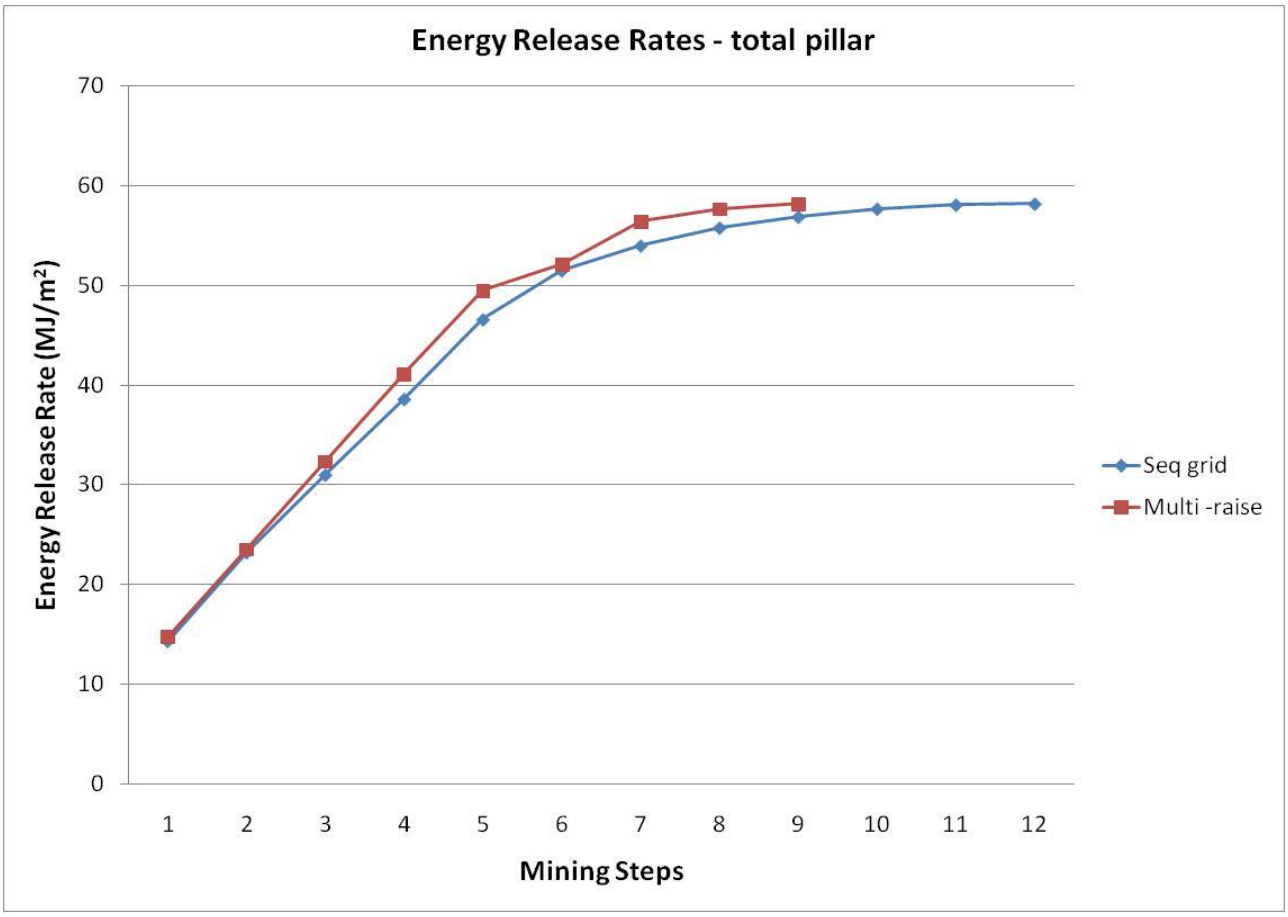

Figure 66: ERR according to mining steps for the Sequential Grid and Multi-raise design (total pillar)

The following can be noted from the results obtained for the average ERR values (total pillar area) as shown on Figure 67:

- The two mine designs follow a similar trend when comparing the average ERR values for the total length of the pillar.

- The maximum ERR value (58.2 MJ/m^2) are obtained during step 12 for the Sequential Grid sequence and during step 9 for the Multi-raise sequence.
- The average ERR value obtained in the initial steps is higher for the Multi-raise when compared to the Sequential Grid design. A maximum difference for the two sequences where obtained during step 5 of 5.9 %.

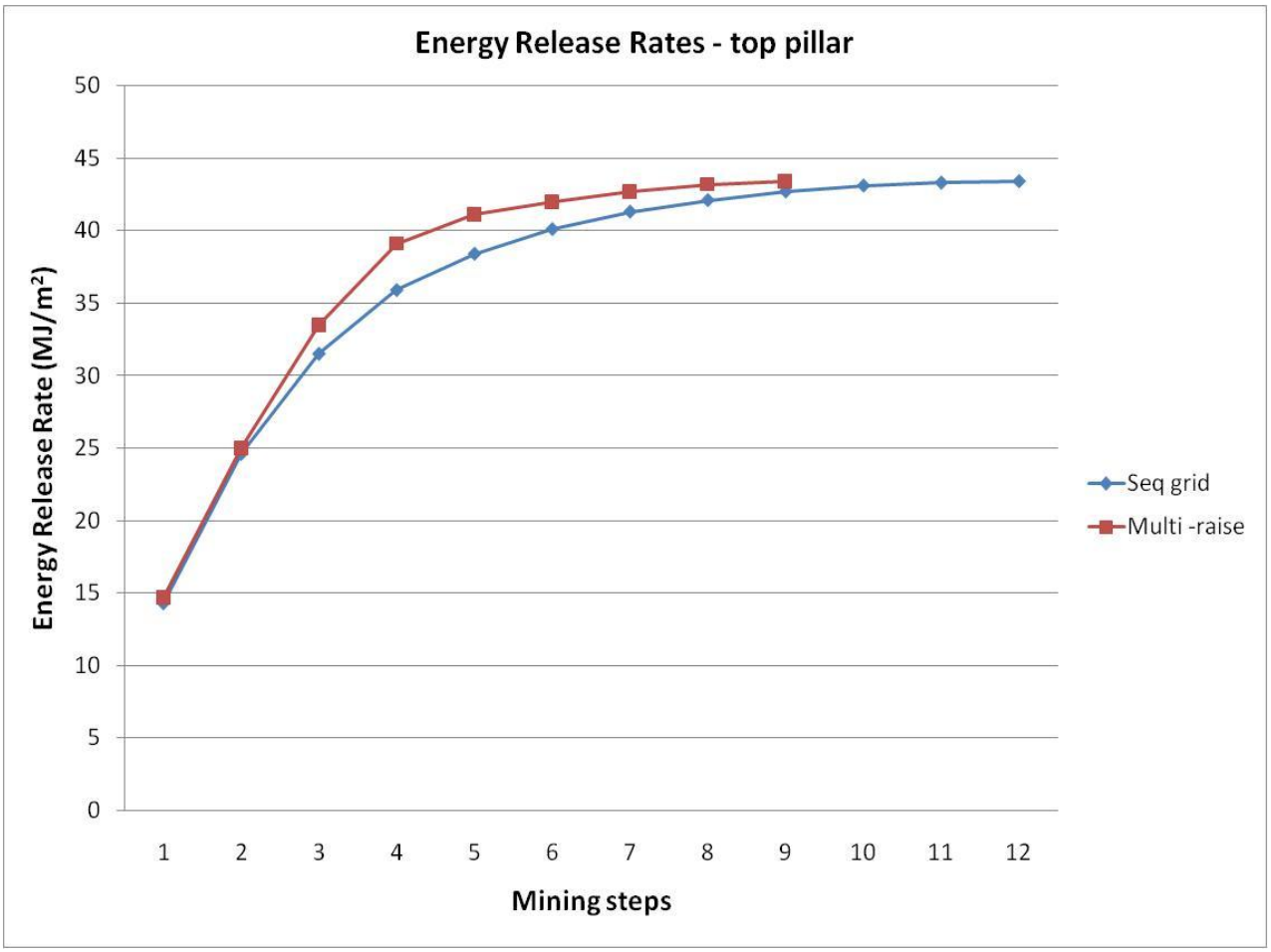

Figure 67: ERR according to mining steps for the Sequential Grid and Multi-raise design (top pillar)

The following can be noted from the results obtained for the average ERR values (top pillar area) as shown on Figure 68:

- The two mine designs follow a similar trend when comparing the average ERR values for the top pillar area.
- The maximum ERR value (43.4 MJ/m^2) are obtained during step 12 for the Sequential Grid sequence and during step 9 for the Multi-raise sequence.

- The average ERR value obtained in the initial steps is higher for the Multi-raise sequence when compared to the Sequential Grid sequence. A maximum difference for the two sequences where obtained during step 4 of 8.1 %.

6.8. AVERAGE PILLAR STRESS (APS)

APS is used to design and assess the stability and performance of pillars. If the mining and pillar layout is regular, tributary area theory can be used to determine the APS value for a specific pillar as follows:

$$APS = \frac{q_v}{1-e} \qquad (9)$$

Where, q_v is the virgin stress and e the extraction ratio.

The APS as determined by the numerical modelling program, MINSIM 2000, is shown in Figure 69 and 70 respectively for the total pillar and the top pillar area.

The following can be noted from the results obtained for the APS values (top pillar area) as shown on Figure 69:

- The difference between the two mining methods when comparing the APS is minimal when examining the values obtained for the total length of the pillar. Both sequences follow a similar APS trend.
- The APS value obtained per step is higher for the Multi-raise sequence when compared to the Sequential Grid sequence. A maximum difference for the two sequences where obtained during step 4 of 4.5 %.
- The maximum APS value (335.4 MPa) is obtained during step 12 for the Sequential Grid sequence and during step 9 for the Multi-raise sequence.

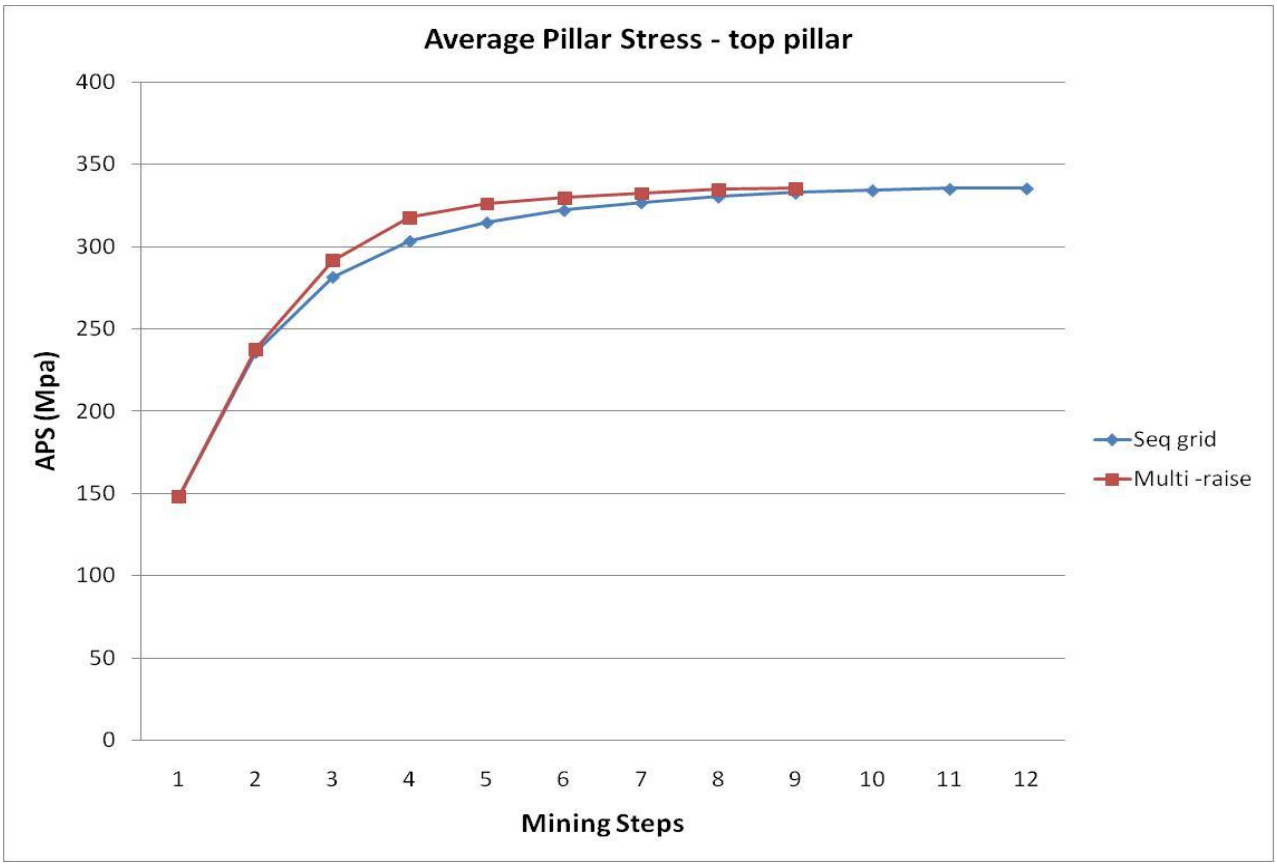

Figure 68: APS according to mining steps for the Sequential Grid and Multi-raise design (top pillar)

The following can be noted from the results obtained for the APS values (total pillar area) as shown on Figure 70:

- The difference between the two design methods when comparing the APS is minimal when comparing the values obtained for the total length of the pillar. Both sequences follow a similar trend.
- The APS value obtained per step is slightly higher for the Multi-raise sequence when compared to the Sequential Grid sequence. A maximum difference for the two sequences where obtained during step 5 of 3.0 %.
- The maximum APS value (386.4 MPa) is obtained during step 12 for the Sequential Grid sequence and during step 9 for the Multi-raise sequence.

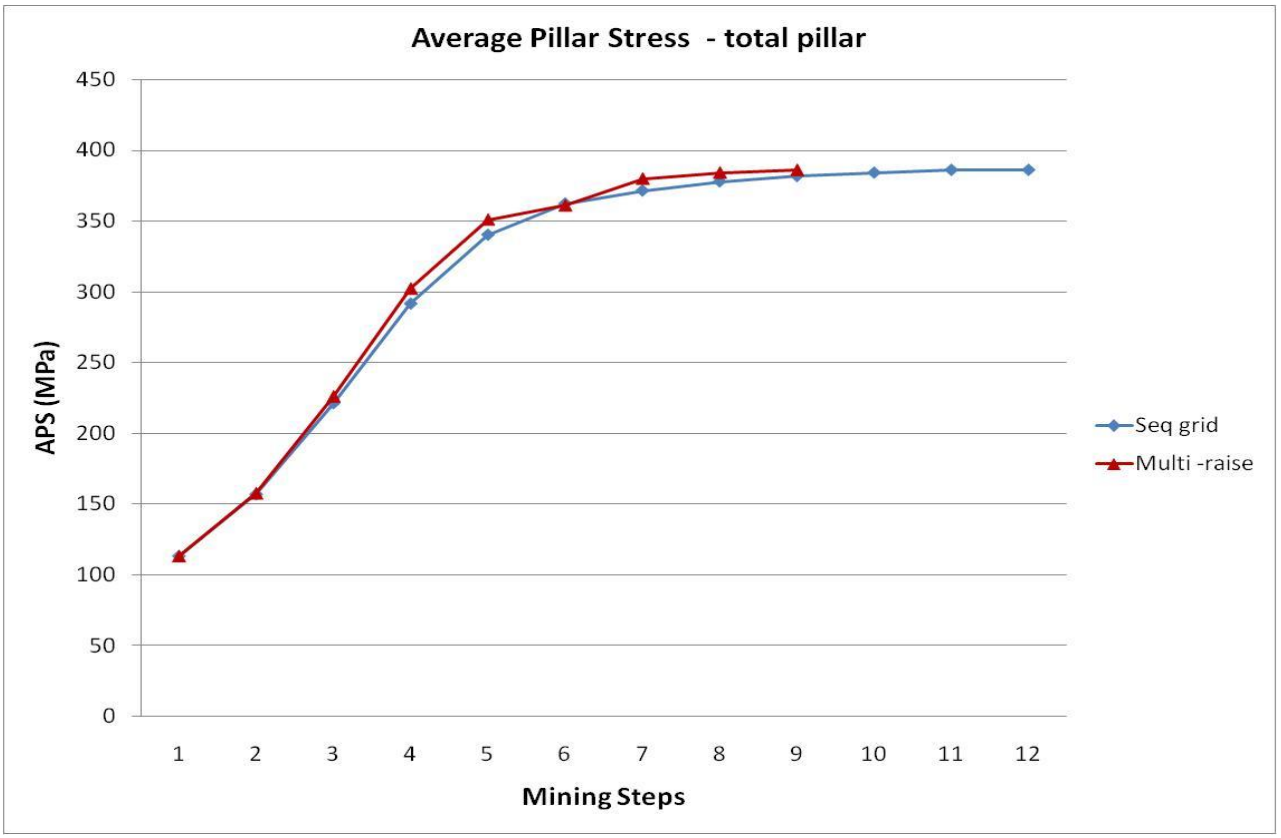

Figure 69: APS according to mining steps for the Sequential Grid and Multi-raise design (total pillar)

According to Brentley, 2006, the maximum average pillar stress (APS) to prevent foundation failure for Kusasalethu is 625 MPa. This is determined by using the conventional criteria:

$$DesignAPS \leq f_a x UCS \qquad (10)$$

Where f_a is an empirical factor typical taken as 2.5 (COMRO, 1988). The UCS of the weakest rock at Kusasalethu is the footwall quartzite with a uni-axial compressive strength of 250 MPa.

Figure 70 shows that not at any stage during the extraction process the APS values exceed 625 MPa for a 10 m grid size. It can be seen that the maximum APS for a grid size of 3 m as discuss in Section 3 the APS value increases to 446 MPa.

In the next chapter alternative designs were modelled to determine if other changes can be made to the design of the Sequential Grid method to address its shortcomings.

Chapter 7

ALTERNATIVE MINE DESIGNS

7.1. INTRODUCTION

Further MINSIM numerical modelling was conducted by the author to investigate alternative mining sequences that will address the biggest shortcoming of the original Sequential Grid design, namely the low rates of production.

The two alternative mining layouts were investigated and the results of the two designs are presented below:

- Double attack points
- Dip stability pillars of 40 m widths with 160 m mining spans.

The same numerical modelling and input parameters (for MINSIM 2000) were used as in described in Chapter 6.

7.2. ALTERNATIVES MINING LAYOUTS - DOUBLE ATTACK POINTS

The main concept of this layout is that two smaller Sequential Grids are formed by having two attack points. It is important to note that the basic principles of the Sequential Grid layout remains intact and needs to be adhere to:

- Only single sided mining is allowed
- The 70 m rule applies where panels are not allowed to mine towards each other within this distance
- Lead/lags to be kept within 10 m.

- Grid mining is performed so as to mine towards the shaft first and then away from the shaft

One major problem that can be identified with this layout is that development needs to be done far in advance to allow this concept to be fully effective. This might prove to be the downfall of this layout (although it will result in addressing the problem of low rates of production) as development progress is usually the main restraint of production. Figure 71 shows a schematic representation of the Double Attack point layout. Note the two separate “V” – shaped mining sequences.

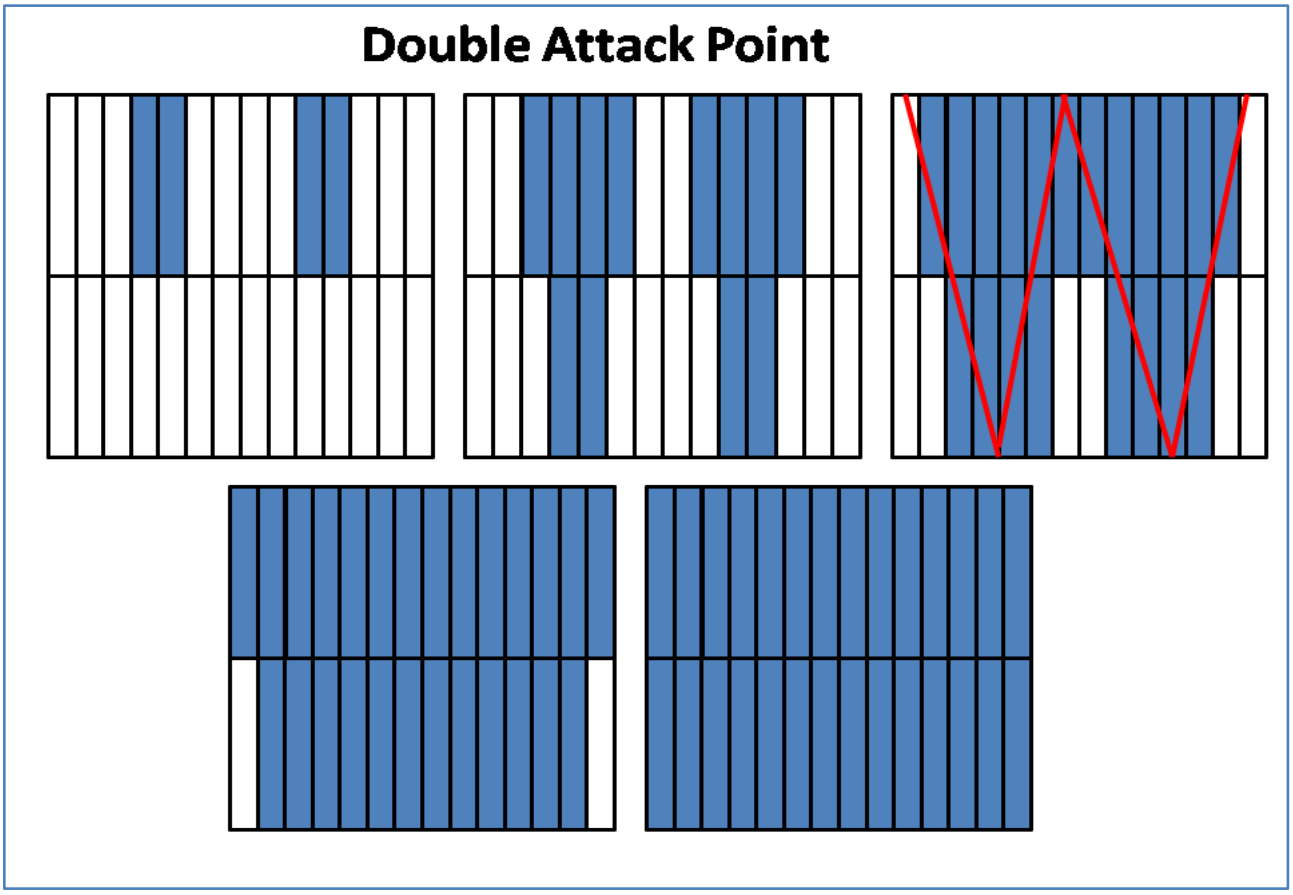

Figure 70: Schematic of the Double Attack point layout

The APS as determined by the numerical modelling program, MINSIM 2000, is shown in Figure 72 for the total pillar area. Note that the same points of interest (total pillar and top pillar areas) where selected to compare the two mine design method as described in Section 6.7, Figure 66.

The following can be noted from the results obtained for the APS values (total pillar area) as shown in Figure 72:

- The APS for the Double Attack layout remains significantly lower than the APS values obtained for the Sequential Grid and Multi-raise layouts. The main reason for this result is that the pillar where the APS values are obtained from (see Figure 66) will experience low APS values due to mining occurring in the vicinity only during the final stages of the total extraction process.
- The maximum APS value (335.4 MPa) is obtained during the last step of the Double Attack layout (Step 10).

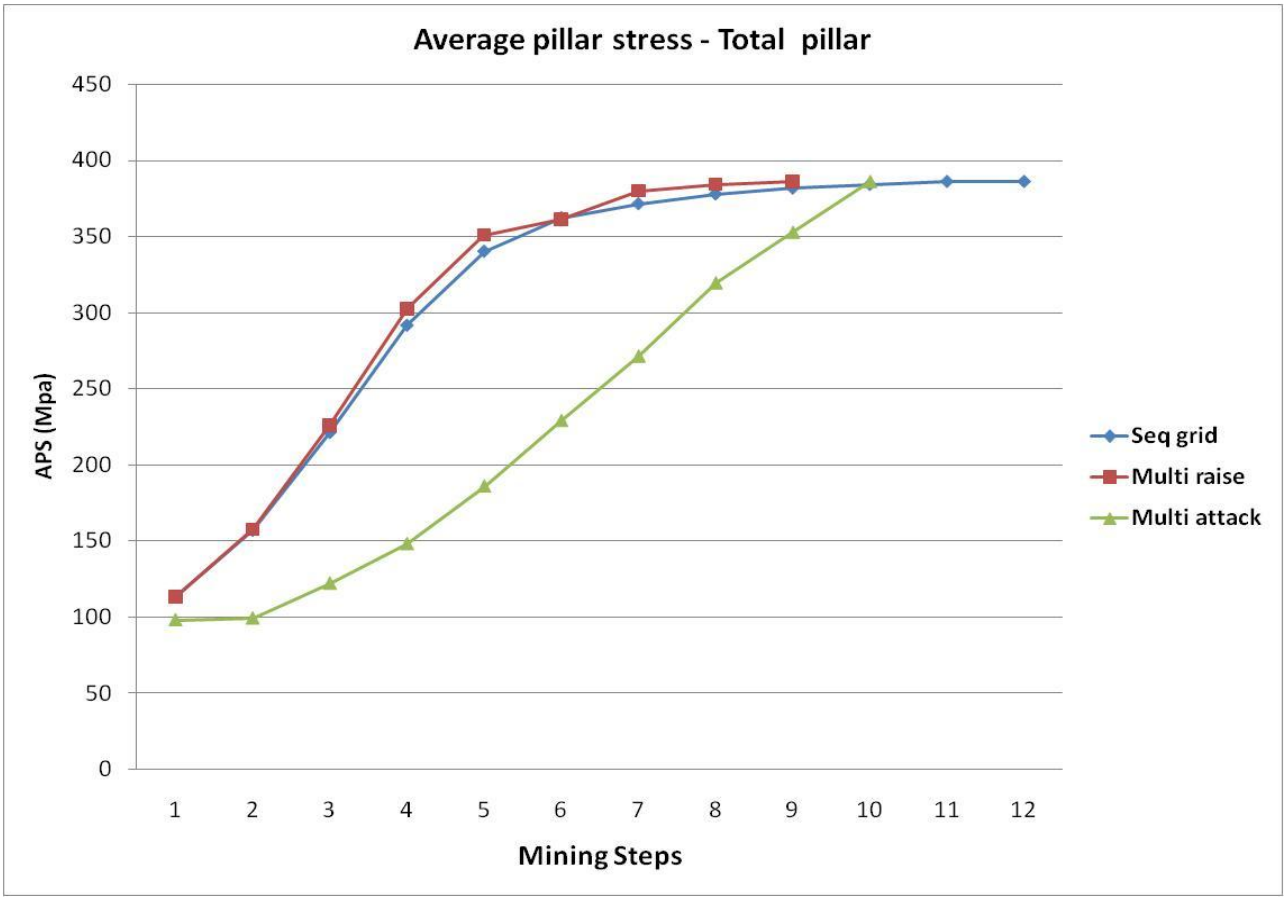

Figure 71: APS values according to mining steps for the Double Attack point layout (total pillar)

Figure 73 shows the ERR values (obtained from MINSIM 2000) for the total pillar area compared to the two other methods.

The following can be noted from the results obtained for the average ERR values (total pillar area) as shown in Figure 73:

- Once again the ERR vales for the Multi attack layout remains significantly lower than the ERR values obtained for the Sequential Grid and Multi-raise layouts. The main reason for this result is that the pillar where the ERR values are obtained from (see Figure 66) will experience low ERR values due to mining occurring close to it only during the final stages of extraction.
- The maximum ERR value (58.2 MJ/m^2) are obtained during the final step 10 of the layout.

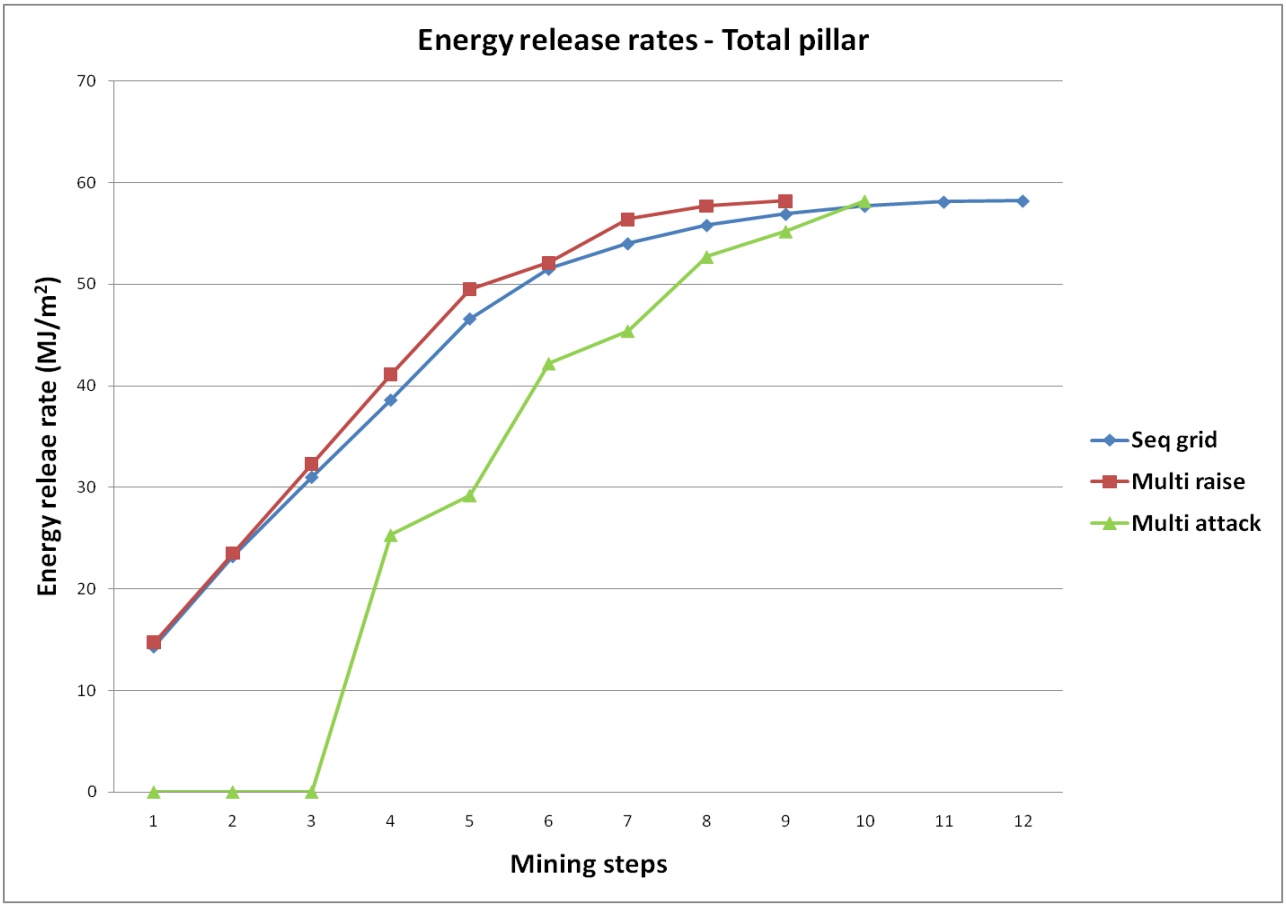

Figure 72: ERR values according to mining steps for the Double Attack point layout (total pillar)

7.3. ALTERNATIVE MINING LAYOUTS - DIP STABILITY PILLARS 40M WITH 160M MINING SPANS

Decreasing the extraction ratio is the main concept behind this layout. Increasing the dip stability pillars to 40 m and decreasing the mining spans between the stability pillars will result in a decrease in the extraction ratio. This will have a beneficial effect on the stress at the face and on the stability pillars. The extraction rate will decrease from 85 % with 30 m wide pillars to 80 % with 40 m wide pillars.

Increasing the pillar widths by 10 m and decreasing the mining spans between the stability pillars by 10 m were conducted for both the Sequential Grid and the Multi-raise layouts. The results were compared with the original layout of the two methods as discussed earlier in the dissertation.

The following can be noted from Figure 74 where the APS values were obtained for the whole pillar area as shown in Figure 66:

- The APS value obtained per step is higher for the 30 m stability pillar layouts when compared with the two 40 m stability pillar layouts. This can be expected as APS values are closely connected to the extraction ratio as discuss in detail below.
- 30 m Multi-raise sequence when compared to the 40 m Multi-raise differ a maximum of 26.6 % during step 5.
- 30 m Sequential Grid sequence when compared to the 40 m Sequential Grid sequence differ by a maximum of 10.4 % during step11.
- The maximum APS value (386.4 MPa) for the 30 m pillar designs is obtained during step 12 for the Sequential Grid and during step 9 for the Multi-raise sequences.
- The maximum APS value (346.1 MPa) for the 40 m pillar designs is obtained during step 12 for the Sequential Grid and during step 9 for the Multi-raise sequences.

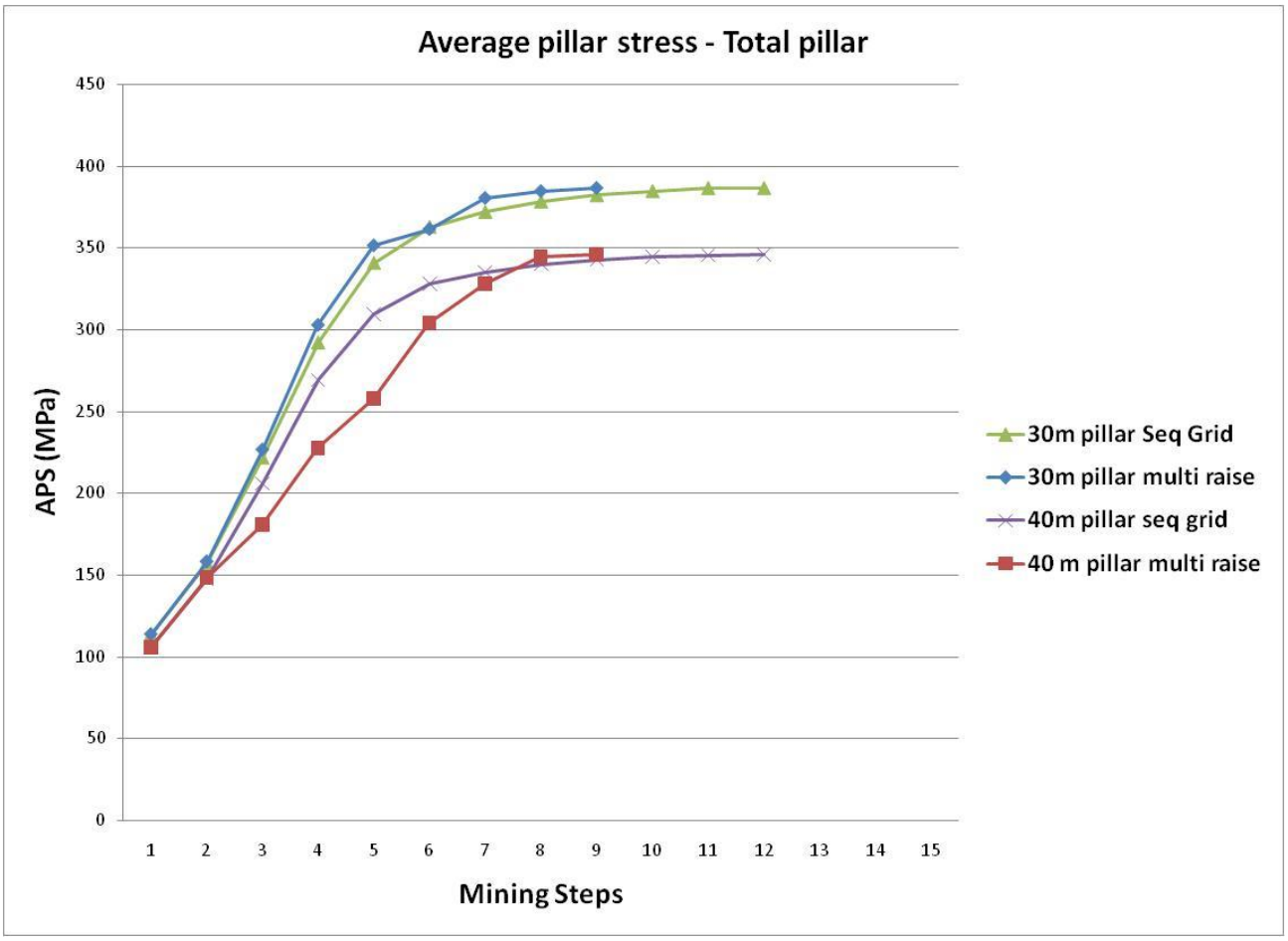

Figure 73: APS values according to mining steps for the 30 m and 40m pillar layout (total pillar)

Figure 75 shows the ERR values (obtained from MINSIM 2000) as calculated for the one side of the pillar as shown in Figure 66.

The following can be noted from the results obtained for the average ERR values (total pillar area) as shown on Figure 75:

- The ERR values obtained for the different sequences differ significantly for the 30 m and 40 m sequences respectively. A reduction of 21 % in the ERR values are obtained when the dip stability pillars are increased by 10 m and the mining spans decreased by 10 m.
- The maximum ERR value of 58.2 MJ/m^2 is obtained for the 30 m mining layouts layout while the maximum ERR value for the 40 m mining layouts is 45.7 %.

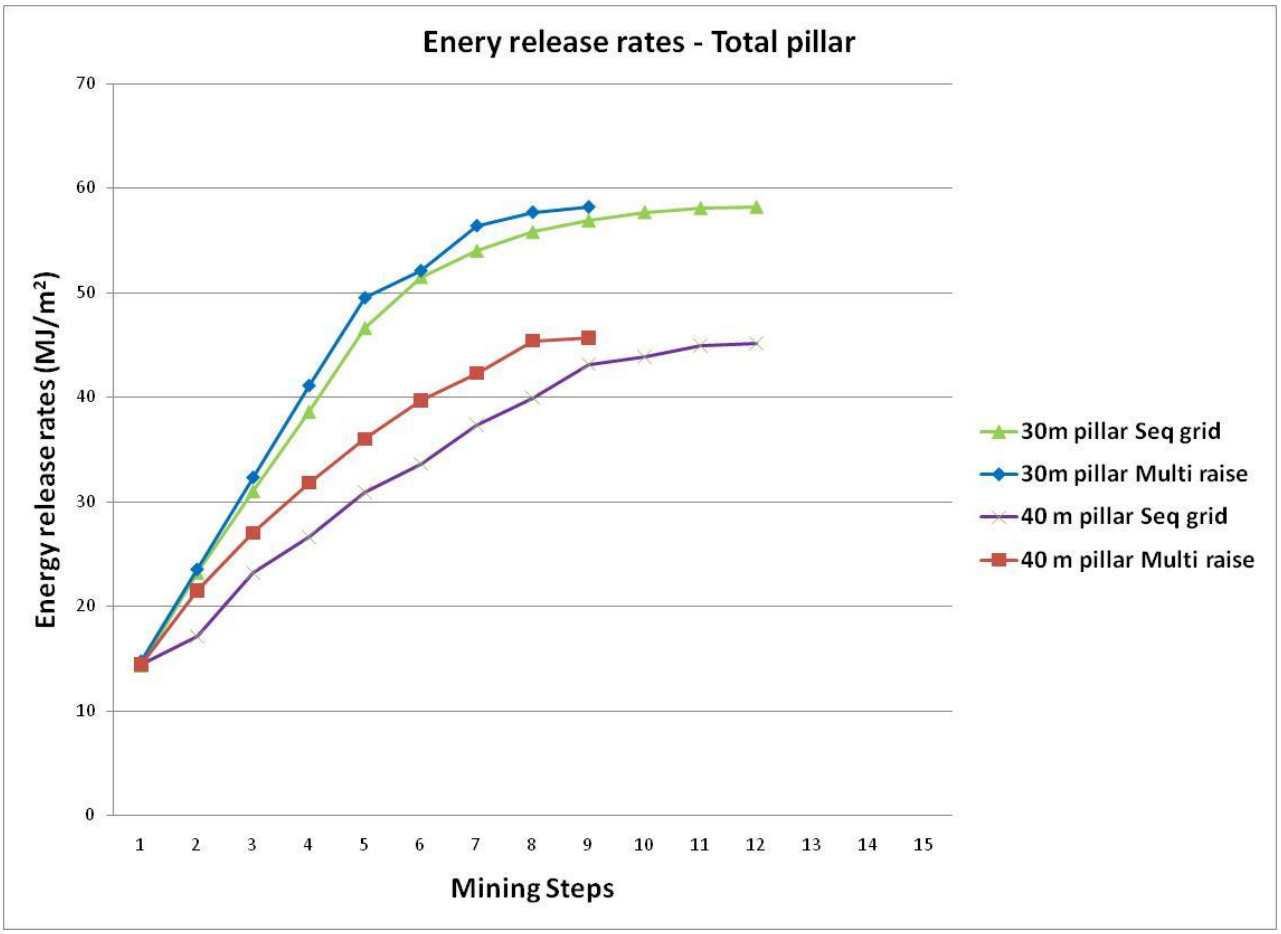

Figure 74: ERR values according to mining steps for the 40 m pillar layout (total pillar)

From the above numerical modelling results, the 40m dip pillars with 160m spans seems to obtain results significantly lower than the results obtained for the Sequential Grid and Multi-raise methods with 30 m wide pillars and 170 m spans. This can be mainly attributed to the lower extraction ratio that is achieved on the end of the mining cycle.

Chapter 8

CONCLUSIONS AND GUIDELINES FOR MULTI-RAISE DESIGN

An investigation into the rock engineering consequences of proposed changes to the Sequential Grid mining method at Kusasalethu mine was conducted by the author. A modified Multi-raise sequence was introduced at the mine as a modification to the original mining sequence. The current study has focussed on the differences between the two mining layouts with regard to the future safety and stability of the mining from both a rock engineering and seismic perspective.

In terms of the induced seismicity the two layouts were assessed using their respective seismic hazards. The results obtained from the current study reveal no significant differences between the two mining methods regarding seismic hazard parameters and in particular the relevant maximum magnitude and return period for seismic events with $M_L \geq 2.5$ although the number of seismic events with $M_L = 1.0$ shows a 33% increase for the Multi-raise mine design when compared to the Sequential Grid mine

The future seismic hazard was estimated using the recently developed concept of a Modelled magnitude. The method basically entails the projection of the equivalent stresses and displacement calculated in the modelled mining steps on to spherical regions or surfaces enclosing the respective modelled regions (IMS, 2012). The displacements, which are calculated as a result of mining, are projected to the sphere, providing the forces of an equivalent seismic moment. The resulting seismic moment is used to determine an equivalent moment magnitude for the respective mining and is labelled as a modelled magnitude for each mining step. Comparing the results obtained from the modelled magnitude method, little difference can be noticed between the two different mining methods. The only difference in the Multi-raise sequence is that the seismicity is generated much earlier in the mining steps compared with the Sequential Grid design.

Numerical modelling was conducted to compare the stress changes between the Multi-raise sequence and the original Sequential Grid sequence. To compare the two mining sequences, two numerical modelling parameters, average pillar stress (APS) and energy released rates (ERR), were compared to determine the most favourable design. The concept of an average value for the stress distribution in a pillar is referred to as the average pillar stress (APS). Although averages are generally simple to calculate given the availability of appropriate data, average values for the stress distributed within pillars is more complex, especially when working in the realm of displacement discontinuity numerical methods. Numerical models in the mining industry are used to estimate APS on a routine basis, but the fundamental properties of the methods involved are not well understood. This frequently led to erroneous estimates of average values and can lead to poor designs involving pillars. The method and procedure discussed in the dissertation can assist with minimizing problems experienced in the past with the calculation of average pillar stress (APS) used on mines to determine the stability of rock engineering pillars.

The numerical modelling of the mining layouts showed slightly higher interim Energy Release Rates (ERR) and Average Pillar Stress (APS) levels for the Multi-raise sequence during the extraction process but the final values for these parameters are nevertheless very similar to the original Sequential Grid mining method.

8.1. GUIDELINES FOR MULTI-RAISE DESIGN

It is therefore concluded that the Multi-raise mining method will not have adverse effects on the mine stability and that the only advantage will be the resulting improvement in productivity. To ensure that the method is applied correctly the following guidelines are recommended for Multi-raise mining:

- Only single sided mining is allowed
- The 70 m rule is applicable whereby panels are not allowed to mine towards each other within this distance
- Lead/lags to be kept to be less than 10 m.

- Grid mining is performed so as to mine towards the shaft first and then away from the shaft
- The number of stoping crews per raise line connection should not exceed 6 crews
- Abnormalities in terms of seismic activity and / or ground conditions must be reported.
- Increase of pillar widths to 40 m and therefore decreasing the stoping spans between the pillars with 10 m will result in decreased APS and ERR rates. This can be implemented in situations where the ground condition is deteriorating.
- Limiting the number of mining crews per raise line was also recommended as to limit the mining rate which could influence the stability of the mine design.

8.2. FURTHER WORK REQUIRED

- The rate of mining was not investigated within this dissertation and needs to be analyzed to determine any possible influence on the stability of the layout. The maximum possible event size in terms of Potency and effective volume mined has been advocated to follow the relations outlined by Mendecki (2005).
- Visible examination of the respective time series for production and the number of events with $M_L \geq 0.0$ shows a good positive cross-correlation up to March 2009. Beyond that the series appears to show a strong negative correlation. Reasons for this negative correlation are not clear but need further detailed investigation as it was considered beyond the scope of this dissertation.
- The Multi-raise design currently employed on Kusasalethu Mine needs to be continuously monitored with future mining so that any unforeseen problems related to the design can be identified early.

References

1. Aki, K and Richards, P.G, Quantitative seismology: theory and methods, University Science Books, 2002.
2. Applegate, J.D, Rock Mechanics aspects of Sequential Grid mining. Project report submitted to the University of Witwatersrand in partial fulfilment of master's degree, 1991.
3. Applegate, J.D, and Arnold, D.A, Stabilising pillar design – 76 to 85 levels. Internal report, Elandsrand gold mine, Anglogold, 1990
4. Brentley, K, Investigation of simultaneous multiple raise mining and scattered mining at Elandsrand mine, Internal report, 2006.
5. COMRO, Industry guide to methods of Ameliorating the Hazards of Rockfalls and rockbursts, CH. Of Mines, Johannesburg, 1988.
6. Cook, N.G.W, Hoek, E, Pretorius, J.P.G, Ortlepp W.D, and M.G.D, Salamon, Rock Mechanics applied to the study of rockbursts, The South African institute of mining and metallurgy, p 435-529,1966.
7. Cook, N.G.W, and Salamon, M.D.G, The use of pillars for stope support. Johannesburg, Chamber of Mines of South Africa, unpublished report, 1966.
8. Davis, Statistics and Data Analysis in Geology; Wiley & Sons Inc; New York; 3rd edition,2002
9. Deliac EP and Gay NC, The influence of stabilizing pillars on seismicity and rockbursts at ERPM, Proceedings of the 1st international Congress on Rockburst and seismicity in mines, Johannesburg, 1982.
10. Diering, D.H, Regional support at Western Deep levels limited, Association of mine manager of South Africa, Papers and Discussion, p1-74, 1987.
11. Ebrahim-Trollope, R, Gutenberg-Richter Relationship and Mine Induced Seismicity as observed at the African Rainbow Minerals Mines – Klerksdorp, RASIM5, p 501 - 508, 2001.
12. Epstein, B, and Lomnitz, C, A model for the occurrence of large earthquakes. Nature, p 954-956, 1966.
13. Francis, D.P, Coats, A.J and Gibson, D, How high can a correlation coefficient be?, Int J Cardiol**,** p 185–199, 1999.

14. Essrich, F. Review of Seismicity in Sequential Grid Mining on Elandsrand. Internal report, Reference No. 012/98, Elandsrand Mine, AngloGold West Wits Operations, 1998.
15. Essrich, F, Comparison between seismicity associated with mining of 80/32 raise line (EGM) and the 76/36 W longwall (WDL West), Internal report, Elandsrand mine, Anglogold, 1996
16. Frimmel, H.E, et al. The formation and preservation of the Witwatersrand goldfields, the largest gold province in the world. In: Hedenquist JW, Thompson J. FH, Goldfarb RJ, Richards JP, editors. Economic Geology One Hundredth Anniversary Volume. Littleton, Colorado: Society of Economic Geologists; 2005. p. 769-797.
17. Gay, N.C, Spencer, D, Van Wyk, J.J and Van der Heever, .PK, Proceedings of the 1st International Congress on Rockbursts and Seismicity in Mines, Johannesburg, 1982, SAIMM, Johannesburg, p 107 – 120, 1984.
18. Gibowicz, S.J. Variation of the frequency-magnitude relation during earthquake sequences in New Zealand. Bull., Seism., Soc Am. p517 – 528, 1973
19. Gibowicz, S.J, Bober, A, Cichowicz, A, Droste, Z, Dychtowicz, Z, Hordejuk, J, Kazimierczyk, M, and Kijko, A, Source study of the Lubin. Poland, tremor of 24 March 1977. Acta. Geophys. Pol., p 3-38, 1979.
20. Gibowicz, S.J and Kijko A, An introduction to mining seismology, Vol. 55 of International geophysics series, University of California, Academic Press, 1994.
21. Hagan, T.O, An evaluation of Systematic stabilizing pillars as a method of reducing the seismic hazard in deep and ultra-deep mines, PHD Dissertation WITS, 1987
22. Handley, M.F, De Lange, J.A.J, Essrich, F, Banning, J.A, A review of the sequential grid mining method employed at Elandsrand Gold Mine, J,S. Afr. Inst. Min. Metall., pp 1183-1194, 2000.
23. Heunis, R. The development of rockburst control strategies for South African gold mines. Afr. Insr. Min. Metal., Vol. 80,1980
24. Hill, F.G, A system of longwall stoping in a deep level mine with special reference to its bearing on the pressure burst and ventilation problems. Assoc of mine managers of the Transvaal. Papers and discussions Vol1. P 257-276 Johannesburg, 1942-1945.

25. Hoffmann, G, Correlating modelled elastic energy release with recorded seismicity in a deep tabular mine, Southern Hemisphere Rock Mechanics Symposium, 2012.
26. Jager, A.J and Ryder, J.A, A handbook on rock engineering practise for tabular hard rock mines. The safety in Mines Research Advisory Committee, SIMRAC, 1999
27. Jordan, T.H., and Richardson, E. et al., Characterization of Mining-Induced Seismicity in the Witwatersrand Basin, South Africa, Research Report, Massachusetts Institute of Technology, 2000.
28. Joughin, NC. The measurement and analyses of earth motion resulting from underground rock failure, Chamber of mine Research Report. No 73/66, 1966.
29. Kijko, A., Seismic hazard estimation for the northern part of Shaft No. 5 .Consultancy report for Vaal Reefs Exploration and Mining Company, Internal report, Anglogold, 1996.
30. Kijko,A Statistical methods in mining seismology, South African Geophysical Association, 1996.
31. Kijko, A, and Sellevoll, M.A, Estimation of earthquake hazard parameters from incomplete data files. Part 2. Incorporation of magnitude heterogeneity. Bull. Seism. Soc. Am. p120-134, 1992
32. Kijko, A, Graham, G, “Parametric - historic" procedure for probabilistic seismic hazard analysis. Part I. Estimation of maximum regional magnitude m_{max}. *Pure Appl. Geophys.*, p 413-442, 1998.
33. Klokow, J.W, Riemer, K.L, and Ferreira, R.I.L, An initial assessment of the closely spaced dip-pillar mining layout as practiced on Driefontein Gold Mine, ISRM 2003 – Technology Roadmap for Rock Mechanics; SAIMM, p655 – 663, 2003.
34. Lenhardt, W.A, and Hagan T.O, Observations and possible mechanism of pillar-associated seismicity at great depth, International deep mining conference, p1183-1194, 1990.
35. Lomnitz-Adler, J., and Lomnitz, C., A modified form of the Gutenburg-Richter magnitude-frequency relationship. Bull. Seism. Soc. Am, p1209-1204, 1979.
36. Malovichko, D, Van Aswegen, D, Clark, R, Mechanisms of large seismic events in platinum mines of the Bushveld Complex (South Africa), The Journal of the Southern African Institute of Mining and Metallurgy, June 2012.

37. Maritz, J, Groundwork's Internal Technical Note, 2010
38. McGarr, A and Wiebols GA. Influence of mine geometry and closure volume on seismicity in a deep level mine. Int J Rock.Mech, Min. Sci., and Geomech. Abstr. Vol 14, p 139–145, 1977.
39. McGarr, A, Seismic moments and volume changes, Journal of Geophysical Research, March 1976.
40. McGill, R.B, Strategies to Manage Seismicity in a Deep VCR environment on Mponeng (1995-2003), Challenges in Deep and High Stress mining, p 217-223, 2007.
41. Mendecki, A.J, Persistence of seismic rock mass response to mining, RASIM6, p97-105, 2005.
42. Mendecki, A, ed Yves Potvin and Martin Hudyma , Persistence of seismic rockmass response to mining, Sixth International Symposium on Rockburst and Seismicity in Mines Proceedings, Australian Centre For Geomechanics, pp 97-105, 2005.
43. Murie, A, The regional effect of leaving unpay blocks of ground and/or a system of regular spaced rib pillars for the scattered mining areas above 2238 level. International memorandum, Elandsrand Mine, Anglogold, 1980.
44. Napier, J.A.L, and Malan, D.F, Numerical computation of average pillar stress and implications for pillar design, The South African institute of mining and metallurgy, p837-846, 2011.
45. Nordquist, J.M, Theory of largest values applied to earthquake magnitudes, Trans. Am. Geophys. Union, p29-31, 1945.
46. Ortlepp, W.D, and Spottiswoode, S.M. The design and introduction of stabilizing pillars at Blyvooruitzicht Gold Mining Company Limited. Proceedings 12th CMMI Congress. Glen, H.W. (ed), Johannesburg, South African Institute of Mining and Metallurgy, p353 – 363, 1982.
47. Rodgers, J.L, and Nicewander, W,A, Thirteen ways to look at the correlation coefficient, The American Statistician, p59–66, February 1988.
48. Russo-Bello, F, and Murphy, S.K, Longwalling at great depth in a geologically disturbed environment – the way forward. Journal of the South African institute of mining and metallurgy, p91 -100, 2000

49. Ryder, J,A, Excess shear stress in the assessment of geological hazardous situations, Journal of the South African institute of Mining and Metallurgy, 1988.
50. Ryder, J.A and Jager, A, Textbook on rock mechanics for tabular hard rock mines. The safety in Mines Research Advisory Committee, SIMRAC, 2002.
51. Salamon, M.D.G, Elastic analysis of displacements and stresses induced by the mining of reef deposits, Symposium on Rock Mechanics and Strata Control in Mines. Johannesburg, South African Institute of Mining and Metallurgy, p 71-92, 1965.
52. Salamon, M.D.G, and Wagner, H, Role of stability pillars in the alleviation of rockburst hazards in deep mines, Proceedings 4th international Congress, International Society of Rock Mechanics, vol 2, p561-566, 1979.
53. Saunders, I, et al, Seismicity of Southern African during 2006 with special reference of the M_w7 Machaze earthquake, South African Journal of Geology, V114, p369-380, 2010.
54. Scheepers, L,J, HofMann, G, Morkel, I,G, The study of seismic response to production for a grid mining layout, Southern Hemisphere Rock Mechanics Symposium, 2012.
55. Scholz, C, The frequency-magnitude relationship of micro fracturing in rock and its relationship to earthquakes. Bull. Seism, Soc. Am., p399-415, 1968.
56. SIMRAC, GAP 303, Mine layout, geological structures and seismic hazard, Mid-Year report, Department of Minerals and Energy, Pretoria, June 1997.
57. Stankiewicz, T, Preliminary estimation of seismic hazard for Vaal Reefs No. 11 Shaft. Internal Report, Anglogold, 1998a.
58. Stankiewicz, T, 1998b. Estimation of seismic hazard associated with Reef blocks. Internal Report, Anglogold, 1998b.
59. Stankiewicz, T, Seismic Hazard Estimations for remnants in the 2K, 2F, 2P, 2G blocks Reef. Consultancy Reports, GeoHydroSeis, 2000.
60. Tanton, J,H., McCarthy, T,F, and Hagan, T,O. The introduction of stabilizing pillars to reduce rockbursts at Western Deep Levels, Limited, Proc. 1st Int. Con. on Rockbursts and Seismicity in Mines 1984, S.A.I.M.M., Johannesburg, pp. 245–252.

61. Taylor, D.W.A, Snoke, J.A, Sacks, I.S, and Takanami,I. Nonlinear frequency-magnitude relationship for the Hokkaido corner, Japan. Bull. Seism. Soc. Am., p340-353, 1990.
62. Van der Heever, P.K, Gay, N.C, Spencer, D, and Van Wyk, J.J, The Control of Geological and Mining Parameters in the Klerksdorp Gold Mining District, SAIMM, pp 107 – 120, 1984,
63. Vieira, FM.C.C, Diering, D, and Durrheim, R.J, Methods to mine the ultra-deep tabular gold-bearing reefs of the Witwatersrand Basin, South Africa. In Underground Mining Methods: Engineering Fundamentals and International Case Studies, pp. 691-704, 2001.
64. Wiles, T, Lachenicht, R and Van Aswegen, G, Integration of deterministic modelling with seismic monitoring for the assessment of rockmass response to mining: Part 1 Theory, 2001.
65. Wogan, J, The history of Gold mining in South Africa, Internet article, 2009.